

REPORT NO. NADC-78182-60

**LEVEL II**

12



DEVELOPMENT AND ANALYSIS OF A CVA AND  
A 1052 CLASS FAST FRIGATE AIR WAKE MODEL

Ronald L. Nave  
Aircraft and Crew Systems Technology Directorate  
NAVAL AIR DEVELOPMENT CENTER  
Warminster, Pennsylvania 18974

30 September 1978

FINAL REPORT  
AIRTASK NO. WF-41-400-000  
P. E. No. 62241N

APPROVED FOR PUBLIC RELEASE; DISTRIBUTION UNLIMITED

Prepared for  
NAVAL AIR SYSTEMS COMMAND  
Department of the Navy  
Washington, D.C. 20361

DDC  
RECEIVED  
JUL 25 1979  
D

AD A 071 622

DDC FILE COPY

79 07 23 187

NADC-78182-60

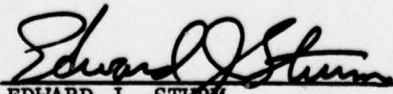
## NOTICES

**REPORT NUMBERING SYSTEM** - The numbering of technical project reports issued by the Naval Air Development Center is arranged for specific identification purposes. Each number consists of the Center acronym, the calendar year in which the number was assigned, the sequence number of the report within the specific calendar year, and the official 2-digit correspondence code of the Command Office or the Functional Directorate responsible for the report. For example: Report No. NADC-78015-20 indicates the fifteenth Center report for the year 1978, and prepared by the Systems Directorate. The numerical codes are as follows:

CODE	OFFICE OR DIRECTORATE
00	Commander, Naval Air Development Center
01	Technical Director, Naval Air Development Center
02	Comptroller
10	Directorate Command Projects
20	Systems Directorate
30	Sensors & Avionics Technology Directorate
40	Communication & Navigation Technology Directorate
50	Software Computer Directorate
60	Aircraft & Crew Systems Technology Directorate
70	Planning Assessment Resources
80	Engineering Support Group

**PRODUCT ENDORSEMENT** - The discussion or instructions concerning commercial products herein do not constitute an endorsement by the Government nor do they convey or imply the license or right to use such products.

APPROVED BY:

  
EDWARD J. STURM  
By direction

DATE:

26 Mar 79

UNCLASSIFIED

SECURITY CLASSIFICATION OF THIS PAGE (When Data Entered)

REPORT DOCUMENTATION PAGE		READ INSTRUCTIONS BEFORE COMPLETING FORM
1. REPORT NUMBER NADC-78182-60	2. GOVT ACCESSION NO.	3. RECIPIENT'S CATALOG NUMBER 9
4. TITLE (and Subtitle) Development and Analysis of a CVA and a 1052 Class Fast Frigate Air Wake Model.	5. TYPE OF REPORT & PERIOD COVERED Final Report	
7. AUTHOR(s) Ronald L. Nave	6. PERFORMING ORG. REPORT NUMBER 12	
9. PERFORMING ORGANIZATION NAME AND ADDRESS Aircraft & Crew Systems Technology Directorate Naval Air Development Center Code 6053 Warminster, PA 18974	8. CONTRACT OR GRANT NUMBER(s) AIRTASK WF-41-400-000 P.E. No. 62241N	
11. CONTROLLING OFFICE NAME AND ADDRESS Naval Air Systems Command Department of the Navy Washington, DC 20361	10. PROGRAM ELEMENT, PROJECT, TASK AREA & WORK UNIT NUMBERS 26 F414PP	
14. MONITORING AGENCY NAME & ADDRESS (if different from Controlling Office) 12102P.	12. REPORT DATE 30 September 1978	
	13. NUMBER OF PAGES 11	
	15. SECURITY CLASS. (of this report) UNCLASSIFIED	
16. DISTRIBUTION STATEMENT (of this Report) Approved for public release; distribution unlimited		
17. DISTRIBUTION STATEMENT (of the abstract entered in Block 20, if different from Report)		
18. SUPPLEMENTARY NOTES		
19. KEY WORDS (Continue on reverse side if necessary and identify by block number) Ship Air Wake Turbulence Model Digital Simulation Model FF1052 Air Wake Simulation CVA Air Wake Simulation		
20. ABSTRACT (Continue on reverse side if necessary and identify by block number) Two digital computer programs have been developed in subroutine form to simulate the ship airwake turbulence around a FF1052 Frigate and a CVA. This report documents and analyzes these two models.		

DD FORM 1 JAN 73 1473

EDITION OF 1 NOV 65 IS OBSOLETE  
S/N 0102-LF-014-6601

393 532 UNCLASSIFIED

SECURITY CLASSIFICATION OF THIS PAGE (When Data Entered)



## S U M M A R Y

This report documents two ship airwake turbulence models which have been developed to aid in the analysis and simulation of the shipboard launch and recovery dynamics of conventional and VSTOL aircraft. The two computer sub-routines represent a large deck carrier and a FF 1052 frigate air wake. The carrier model has been used extensively for automatic carrier landing simulations. The frigate airwake model has been developed more recently and has not been widely tested. The FF 1052 airwake model has been installed as part of the NAVAIRDEVCEEN VSTOL Launch and Recovery Program described in reference (a). The model has been analytically validated against wind tunnel data, but it has not been tested in a piloted simulator.

These two models are being documented in the hope that they may form the basis for a standardized method of simulating turbulence for shipboard launch and recovery analysis.

Accession For	
NTIS GRA&I	<input checked="checked" type="checkbox"/>
DDC TAB	<input type="checkbox"/>
Unannounced	<input type="checkbox"/>
Justification	
By _____	
Distribution/ _____	
Availability Codes	
Dist	Avail and/or special
A	

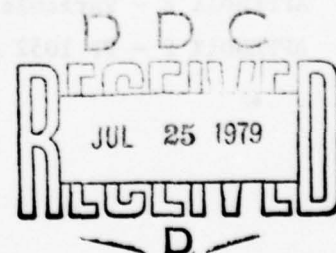




## TABLE OF CONTENTS

	<u>Page</u>
SUMMARY .....	1
LIST OF TABLES .....	3
LIST OF FIGURES .....	4
INTRODUCTION .....	6
DESCRIPTION OF THE CARRIER AIRWAKE MODEL .....	8
DESCRIPTION OF THE FF 1052 TURBULENCE MODEL .....	12
ANALYSIS OF WIND TUNNEL DATA .....	18
DYNAMIC NATURE OF THE MEASURED AND SIMULATED AIRWAKE TURBULENCE .....	20
CORRELATION ANALYSIS .....	49
SENSITIVITY ANALYSIS OF THE EFFECTS OF THE ASSUMED FORM OF THE TURBULENCE SPECTRUM .....	52
TIME HISTORY COMPARISON .....	54
RESULTS AND CONCLUSIONS .....	55
RECOMMENDATIONS .....	59
LIST OF SYMBOLS .....	61
REFERENCES .....	62
APPENDIX A - Listing of CVA Turbulence Model .....	A-1
APPENDIX B - Definition of Variables Used in CVA Program .....	B-1
APPENDIX C - Flow Chart for CVA Model .....	C-1
APPENDIX D - Listing of FF 1052 Turbulence Subroutine .....	D-1
APPENDIX E - Variable Definitions for FF 1052 Program .....	E-1
APPENDIX F - FF 1052 Algorithm Flow Chart .....	F-1

## LIST OF TABLES

<u>Table No.</u>	<u>Title</u>	<u>Page</u>
I	Selected Wind Tunnel Test Points Used in Spectral Analysis .....	21
II	Statistics of Frequency Value Corresponding to Maximum of Spectra Grouped by Velocity and Velocity Component .....	22
III	Statistics of Peak Spectral Velocity Grouped by Velocity Only .....	22
IV	Turbulence Frequency Versus Airspeed .....	23
V	Filter Break Frequencies at $X = 0$ .....	35
VI	Filter Break Frequencies at $X = 58$ M. (190 Ft.) .....	40
VII	Test Versus Simulation Equivalent Frequency .....	48
VIII	Test Versus Simulation Average Frequency .....	48
IX	Test Versus Adjusted Simulation Frequency .....	49
X	Correlation Summary .....	51
XI	RMS Pitch Versus Gust Frequency .....	54

## LIST OF FIGURES

<u>Figure No.</u>	<u>Title</u>	<u>Page</u>
1	Pitch Attitude and Angle of Attack During STO Launch .....	7
2	CVA Ship Burble Steady Wind Ratios .....	11
3	U Component Burble Time Constant and Variance .....	13
4	Sample Burble Components, $V_0 = V_S = 18$ M./Sec. (60 Ft/Sec.) .....	14
5	Sample of CVA Simulated Free Air Turbulence .....	15
6	FF 1052 Ship Airwake Model Geometry .....	17
7	Nondimensionalized Turbulence Parameters Versus Range .....	19
8	Measured Gust Spectra, $V = 9$ M./Sec., X, Y, and Z Components .....	24
9	Measured Gust Spectra, $V = 16$ M./Sec., X, Y, Z Components .....	25
10	Measured Gust Spectra, $V = 23$ M./Sec., X, Y, Z Components .....	26
11	Peak Spectral Frequency Versus Airspeed .....	27
12	Simulated Turbulence Spectrum, $V = 23$ M./Sec. (76 Ft/Sec.), X Velocity Component .....	29
13	Simulated Turbulence Spectrum, Increased Filter Frequency, Z Velocity Component .....	30
14	Simulated Turbulence, 0.7 Damping, Z Velocity Component ....	31
15	Simulated Turbulence Spectrum, 0.1 Damping, Z Velocity Component .....	32
16	Simulated Turbulence Spectrum, First Order Numerator .....	34
17	Normalized Spectra for $V = 10$ M./Sec., $X = 0$ (Measured), X, Y, Z Components .....	36
18	Normalized Spectra for $V = 10$ M./Sec., $X = 76$ M. (Measured), X, Y, Z Components .....	37
19	Normalized Spectra for $V = 23$ M./Sec., $X = 0, 11$ M. (Measured), X, Y, Z Components .....	38
20	Normalized Spectra for $V = 23$ M./Sec., $X = 38$ M., 76 M. (Measured), X, Y, Z Components .....	39
21	Comparison of Test and Simulated Turbulence Spectra .....	41
22	Normalized VZ - Velocity Distribution - Composite of 16 Test Points, $V_\infty = 23$ M./Sec., $\psi = 50^\circ$ , $\phi = 0$ , $X = 0, 27$ M. ....	42



## LIST OF FIGURES (Continued)

<u>Figure No.</u>	<u>Title</u>	<u>Page</u>
23	Normalized VY - Velocity Distribution - Composite of 16 Test Points, $V_{\infty} = 23$ M./Sec., $\psi = 50^{\circ}$ , $\phi = 0$ , $X = 0$ , 27 M. ....	43
24	Normalized VX - Velocity Distribution - Composite Average of 16 Test Points, $V_{\infty} = 23$ M./Sec., $\psi = 50^{\circ}$ , $\phi = 0$ , $X = 0$ , 27 M. ....	44
25	Normalized VX - Distribution - Composite Average - 4 x 1024 Points - Simulated Data, $V_{\infty} = 23$ M./Sec., $\phi = 0$ , $\psi = 50^{\circ}$ ....	45
26	Normalized VY - Distribution - Composite Average - 4 x 1024 Points - Simulated Data, $V_{\infty} = 23$ M./Sec., $\phi = 0$ , $\psi = 50^{\circ}$ ....	46
27	Normalized VZ - Distribution - Composite Average - 4 x 1024 Points - Simulated Data, $V_{\infty} = 23$ M./Sec., $\phi = 0$ , $\psi = 50^{\circ}$ ....	47
28	Simulated Spectra With Adjusted Time Constants, X, Y, Z Components ....	50
29	Closed Loop Gust Response Transfer Function ....	53
30	X - Component Simulated and Measured Turbulence ....	56
31	Y - Component Simulated and Measured Turbulence ....	57
32	Z - Component Simulated and Measured Turbulence ....	58

## I N T R O D U C T I O N

Two turbulence model algorithms have been developed for use in the design and analysis of conventional and vertical take-off aircraft. These are an attack carrier model (CVA) and a FF 1052 frigate model. The CVA model has been used since 1971 in the simulation of manual and automatic landings aboard large deck carriers. This model has been used at the NASA Ames Research Simulation Facility in piloted simulations of the F-14, A-7, and EA-6B aircraft. References (b) and (c) describe the data and equations used to develop the model. Free air turbulence, steady, and unsteady burble components are combined to produce the complete CVA model. To make the algorithm more suitable for VSTOL aircraft, several changes have been made from the form described in reference (c). These are as follows:

1. The ship airwake velocity components are programmed to exponentially decrease in magnitude beyond specified bounds of altitude and lateral position.
2. The vertical component of the steady air wake has been changed to include an upwash near the bow. This was inferred from time histories of AV8A launches aboard the U.S.S. Roosevelt. (See figure 1.)
3. An option to provide discrete gust sinusoids in place of the ship air wake model has been added. These inputs follow the form described in reference (f).

The model is limited to cases where the wind is aligned with the landing deck. Wind velocity is specified by setting the ship speed variable, VS.

The second model has been developed exclusively for VSTOL aircraft and is intended to represent wind conditions near an FF 1052 frigate.

The turbulence algorithm was developed from data derived from the wind tunnel test of a 1/50 scale FF 1052 ship model. These data are contained in reference (d). The structure for the algorithm was based on work performed by the Vought Corporation and described in reference (e). However, the model described herein has been modified from the original format as a result of additional analysis of the data contained in reference (d). The model described herein is a somewhat refined version of the Vought model.

This model was programmed on the NAVAIRDEVCON CDC 6600 computer. The Fortran listings included in this report represent the present status of the two models.

The subroutines have been tested in batch mode runs and are considered to be reasonably accurate. However, the author takes responsibility for any deficiencies that may still remain in the code.

The FF 1052 air wake model was examined by computing time histories, power spectra, and probability distributions and then comparing these with the wind tunnel velocity time histories.

This report describes all work done to validate and adjust the FF1052 model to agree with wind tunnel data. Both the CVA model and the FF1052 model are offered for inspection, use, and criticism.

NADC-78182-60

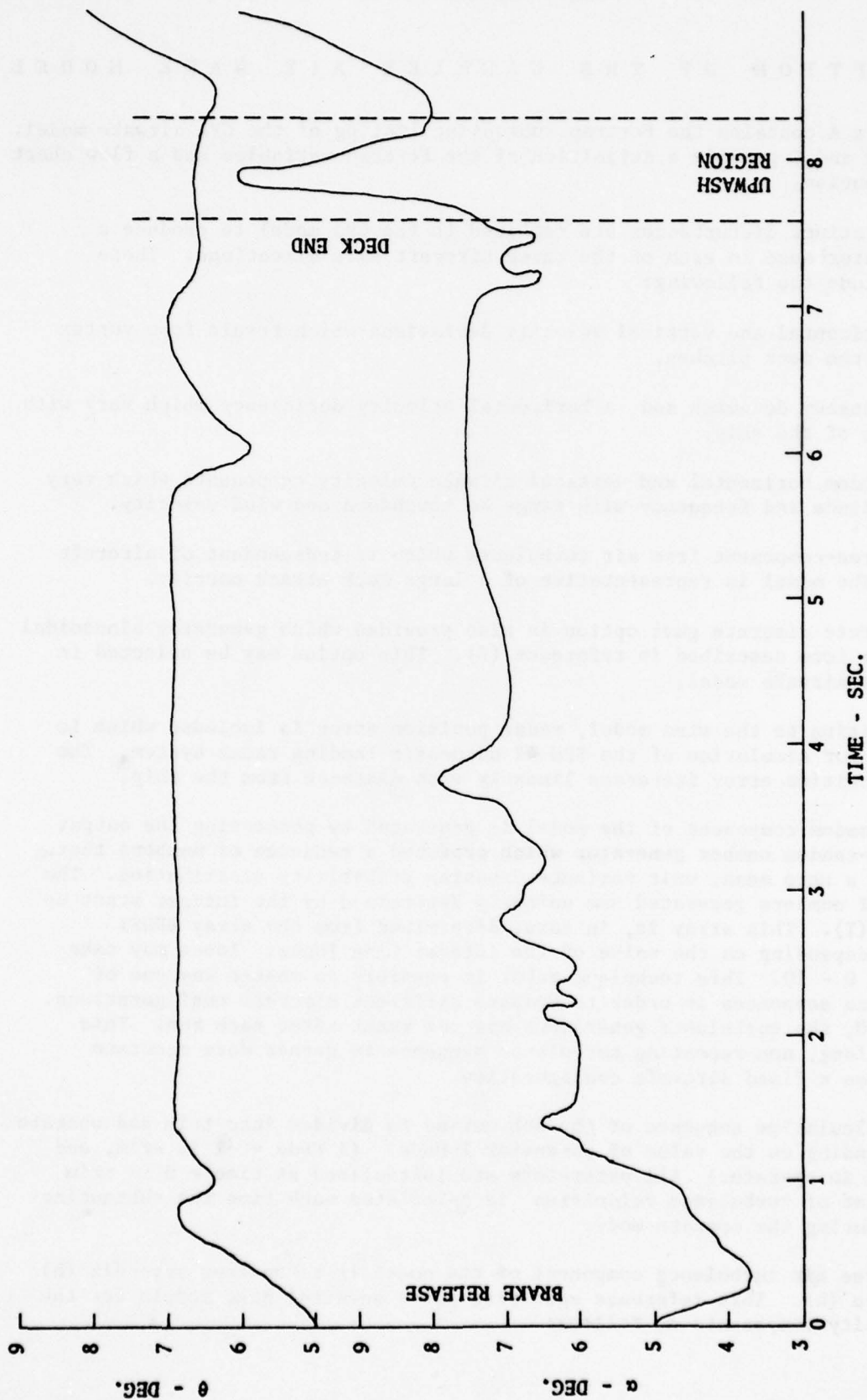


Figure 1 - Pitch Attitude and Angle of Attack During STO Launch



## DESCRIPTION OF THE CARRIER AIR WAKE MODEL

Appendix A contains the Fortran subroutine listing of the CVA airwake model. Appendices B and C provide a definition of the Fortran variables and a flow chart of the subroutine.

Four distinct disturbances are combined in the CVA model to produce a velocity disturbance in each of the three aircraft axis directions. These sources include the following:

1. Horizontal and vertical velocity deviations which result from vortex shedding as the deck pitches.
2. A steady downwash and a horizontal velocity deficiency which vary with distance aft of the ship.
3. Random horizontal and vertical airwake velocity components which vary in RMS amplitude and frequency with range to touchdown and wind velocity.
4. Three-component free air turbulence which is independent of aircraft position. The model is representative of a large deck attack carrier.

A separate discrete gust option is also provided which generates sinusoidal gusts of the form described in reference (f). This option may be selected in place of the airwake model.

In addition to the wind model, radar position error is included which is appropriate for simulation of the SPN-42 automatic landing radar system. The simulated position error increases linearly with distance from the ship.

Each random component of the model is generated by processing the output of a pseudo-random number generator which produces a sequence of numbers that approximate a zero mean, unit variance Gaussian probability distribution. The sequences of numbers generated are uniquely determined by the integer start up array IRDST(I). This array is, in turn, determined from the array IRDSI (I, Ionce) depending on the value of the integer flag Ionce. Ionce may take values from 0 - 10. This technique makes it possible to repeat any one of 10 turbulence sequences in order to compare different aircraft configurations. If Ionce = 0, the turbulence generators are not reset after each run. This produces a long, non-repeating turbulence sequence to gather more accurate statistics on a fixed aircraft configuration.

The calculation sequence of the subroutine is divided into trim and operate modes depending on the value of parameter I Mode. (I Mode = -1 in trim, and I Mode = +1 in operate.) All parameters are initialized at time = 0 in trim and a new set of turbulence velocities is calculated each time the subroutine is called during the operate mode.

The free air turbulence component of the model is taken from appendix (b) of reference (h). This reference specifies power spectral gust models for the three velocity components as follows:

$$\phi \frac{\Delta u}{v_0} = \frac{200/v_0^3}{\left(\frac{s}{v_0/100} + 1\right) \left(\frac{-s}{v_0/100} + 1\right)} \frac{(\text{ft/sec})^2}{(\text{rad/sec})}$$

$$\phi \frac{\Delta v}{v_0} = \frac{\left(\frac{5900}{v_0^3}\right) \left(\frac{s}{v_0/400} + 1\right) \left(\frac{-s}{v_0/400} + 1\right)}{\left(\frac{s}{v_0/1000} + 1\right) \left(\frac{-s}{v_0/1000} + 1\right) \left(\frac{s}{3v_0/400} + 1\right) \left(\frac{-s}{3v_0/400} + 1\right)} \frac{(\text{ft/sec})^2}{(\text{rad/sec})}$$

$$\phi \frac{\Delta w}{v_0} = \frac{71.6/v_0^3}{\left(\frac{s}{v_0/100} + 1\right) \left(\frac{-s}{v_0/100} + 1\right)} \frac{(\text{ft/sec})^2}{(\text{rad/sec})}$$

The corresponding root-mean-square gust amplitudes are:

$$u_G = .76 \text{ M./sec (2.5 ft/sec)}$$

$$w_G = .457 \text{ M./sec (1.5 ft/sec)}$$

$$v_G = .728 \text{ M./sec (2.39 ft/sec)}$$

The frequency parameters of the free air turbulence filters are determined by the trim airspeed  $v_0$ . Since the algorithm was developed for conventional flight simulation, the equations do not permit the direct substitution of zero airspeed for a hover case. For low trim speeds, the parameter is arbitrarily set to 18.29 M./sec (60 ft/sec). This value was selected as a reasonable estimate of the maximum relative wind over a moving ship.

The turbulence routine options are determined by selecting integer flag parameters as either 0 or 1. The normal values of these flags are as follows:

$$I_{wind} = 1$$

$$I_{Lburb} = 1$$

$$I_{Lturb} = 1$$

$$I_{Bfrz} = 0$$

$$I_{disct} = 0$$

$$I_{ubt} = 0$$

Ivbt = 0

Iwbt = 0

This produces a complete ship airwake model for approach simulation. The complementary values produce these effects:

Iwind = 0 Return all zero turbulence values.

ILburb = 0 Select alternate downwash function.

ILturb = 0 Set all free air turbulence components to zero.

IBfrz = 1 Fix turbulence range variable to  $x_d = x_{frz}$ .

Iubt = 1 Set u component of airwake burble to zero.

Ivbt = 1 Set v component of airwake burble to zero.

Iwbt = 1 Set w component of airwake burble to zero.

IDisct = 1 Select discrete gust options in place of carrier airwake model.

The ship dependent portion of the airwake was developed primarily from water tunnel tests of CVA ship models. The steady components consist of tabulated values of horizontal and vertical velocity functions ( $\Delta u/v_s$  and  $\Delta w/v_s$ ) versus range. These functions are shown in figure 2. The downwash and reduction in relative wind is determined by multiplying the tabulated functions by ship speed  $v_s$ . The model assumes that all the wind is generated by the ship and that the velocity is aligned with the landing deck.

Periodic wind components with magnitudes proportional to ship pitch are also included. These sinusoidal vertical and horizontal components propagate aft from the ship at 85 percent of the ship speed and decay in amplitude with range.

The apparent frequency at which the velocity varies is determined by the aircraft closing speed according to formula

$$\text{Magnitude} = \cosine \left[ \omega_p \left( 1 + \frac{\Delta v}{0.85 \cdot v_s} \right) \cdot t + \frac{x_d}{0.85 \cdot v_s} + \phi - 1.57 \right]$$

where  $\omega_p$  = ship frequency,  $\Delta v$  = aircraft closing rate,  $v_s$  = ship speed,  $x_d$  = distance to ship cg, and  $\phi$  = phase.

The magnitude of the sinusoid decreases linearly with distance aft of the ship. The burble is set to zero outside of established limits fore and aft of the ship. Additional limits on magnitude are established by altitude and lateral position of the aircraft. The magnitude is assumed to decrease exponentially at distances greater than 100 feet to the left or right of the ship and at altitudes greater than 50 feet above the deck. Reference (i) indicates that the burble is largely restricted to this region.



NADC-78182-60

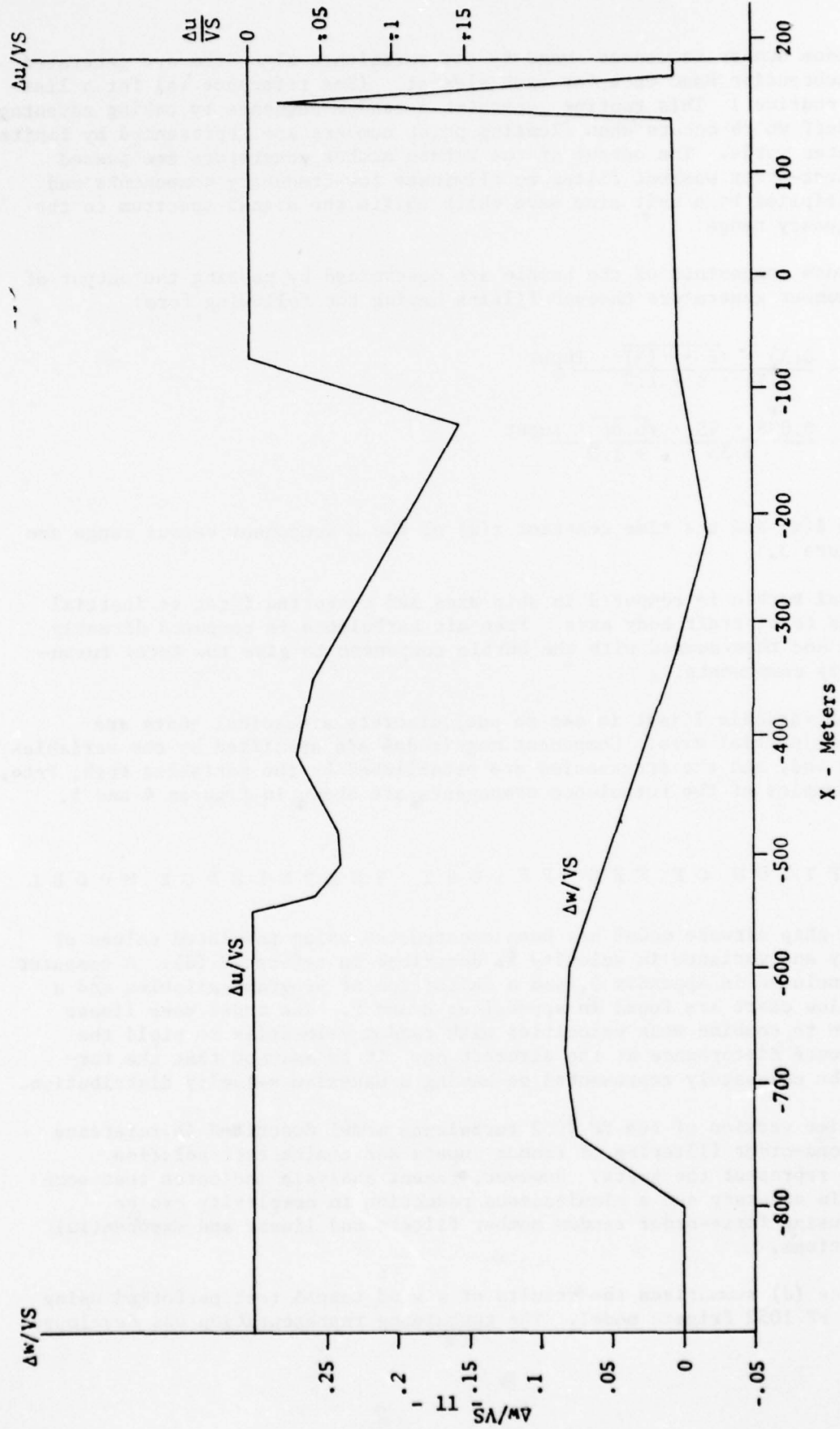


Figure 2 - CVA Ship Burble Steady Wind Ratios

The random number sequences used by the turbulence algorithm are generated by calling subroutine Rand once for each element. (See reference (a) for a listing of this routine.) This routine generates a random sequence by taking advantage of the roundoff which occurs when floating point numbers are represented by finite length computer words. The output of the random number generators are passed through a first-order washout filter to eliminate low-frequency components and are then multiplied by a unit sine wave which shifts the signal spectrum to the desired frequency range.

The random components of the burble are determined by passing the output of the random number generators through filters having the following form:

$$ub2(s) = \frac{\delta(X) \cdot \sqrt{2 \cdot \tau(X)} \cdot \text{Input}}{\tau(X) \cdot s + 1.0}$$

$$wb2(s) = \frac{0.035 \cdot VS \cdot \sqrt{6.66} \cdot \text{Input}}{3.33 \cdot s + 1.0}$$

The variance  $\delta(x)$  and the time constant  $\tau(x)$  of the u component versus range are shown on figure 3.

The total burble is computed in ship axes and converted first to inertial axes and then to aircraft body axes. Free air turbulence is computed directly in body axes and then summed with the burble component to give the total turbulence velocity components.

When the variable Idisct is set to one, discrete sinusoidal gusts are calculated in inertial axes. Component magnitudes are specified by the variables Vmn, Vme and Vmd, and the frequencies are established by the variables Frth, Frte, and Frtd. Samples of the turbulence components are shown in figures 4 and 5.

#### DESCRIPTION OF THE FF1052 TURBULENCE MODEL

A small ship airwake model has been constructed using tabulated values of mean velocity and variance in velocity as described in reference (d). A computer listing is included in appendix D, and a definition of program variables and a subroutine flow chart are found in appendices E and F. The model uses linear superposition to combine mean velocities with random velocities to yield the total turbulence disturbance at the aircraft cg. It is assumed that the turbulence may be adequately represented as having a Gaussian velocity distribution.

An earlier version of the FF 1052 turbulence model described in reference (e) used second-order filtering of random inputs and cosine extrapolation functions to represent the gusts. However, recent analysis indicates that some improvement in accuracy and a simultaneous reduction in complexity can be achieved by using first-order random number filters and linear and exponential shaping functions.

Reference (d) summarizes the results of a wind tunnel test performed using a 1/50 scale FF 1052 frigate model. The turbulence representation was developed

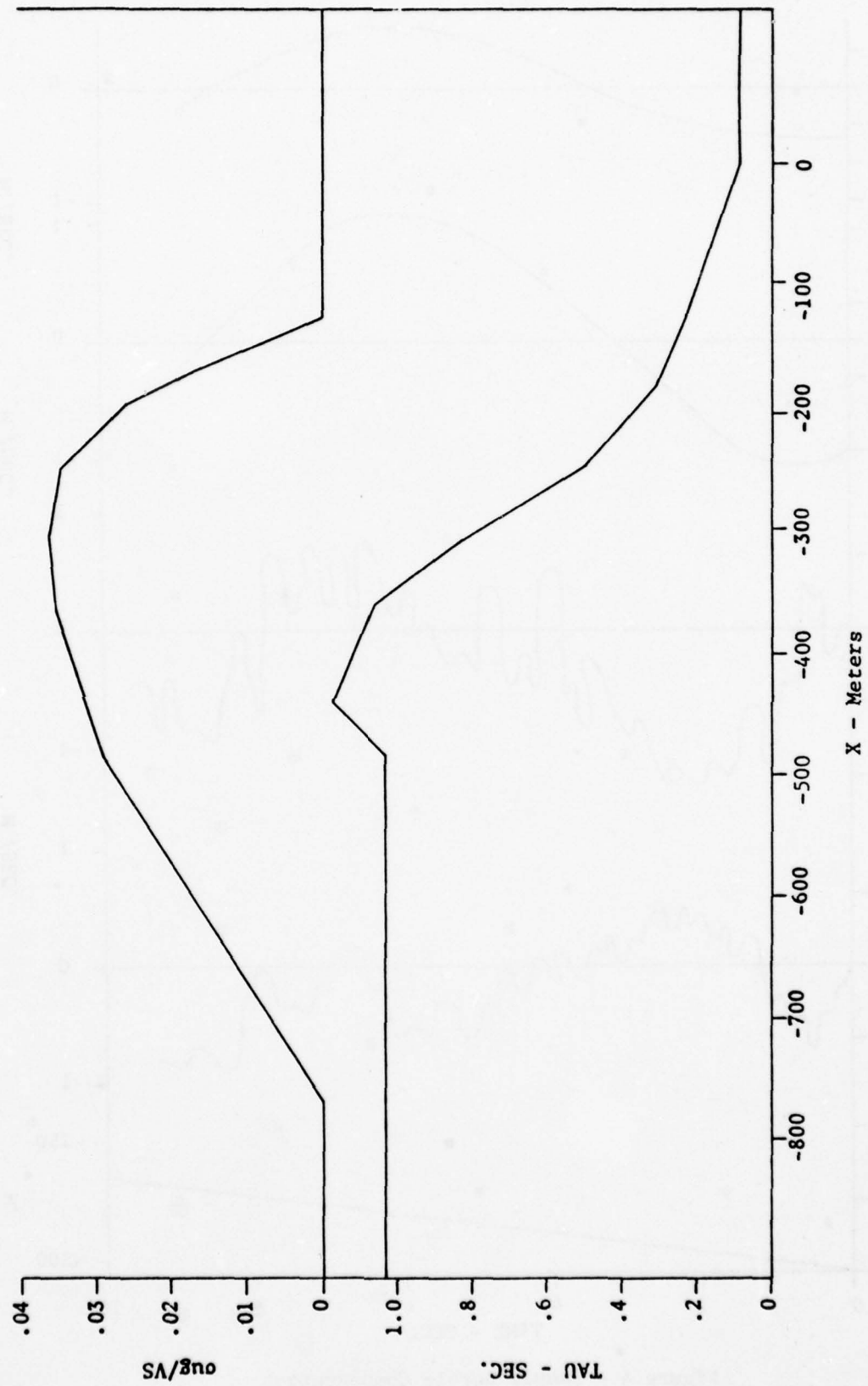


Figure 3 - U Component Burble Time Constant and Variance



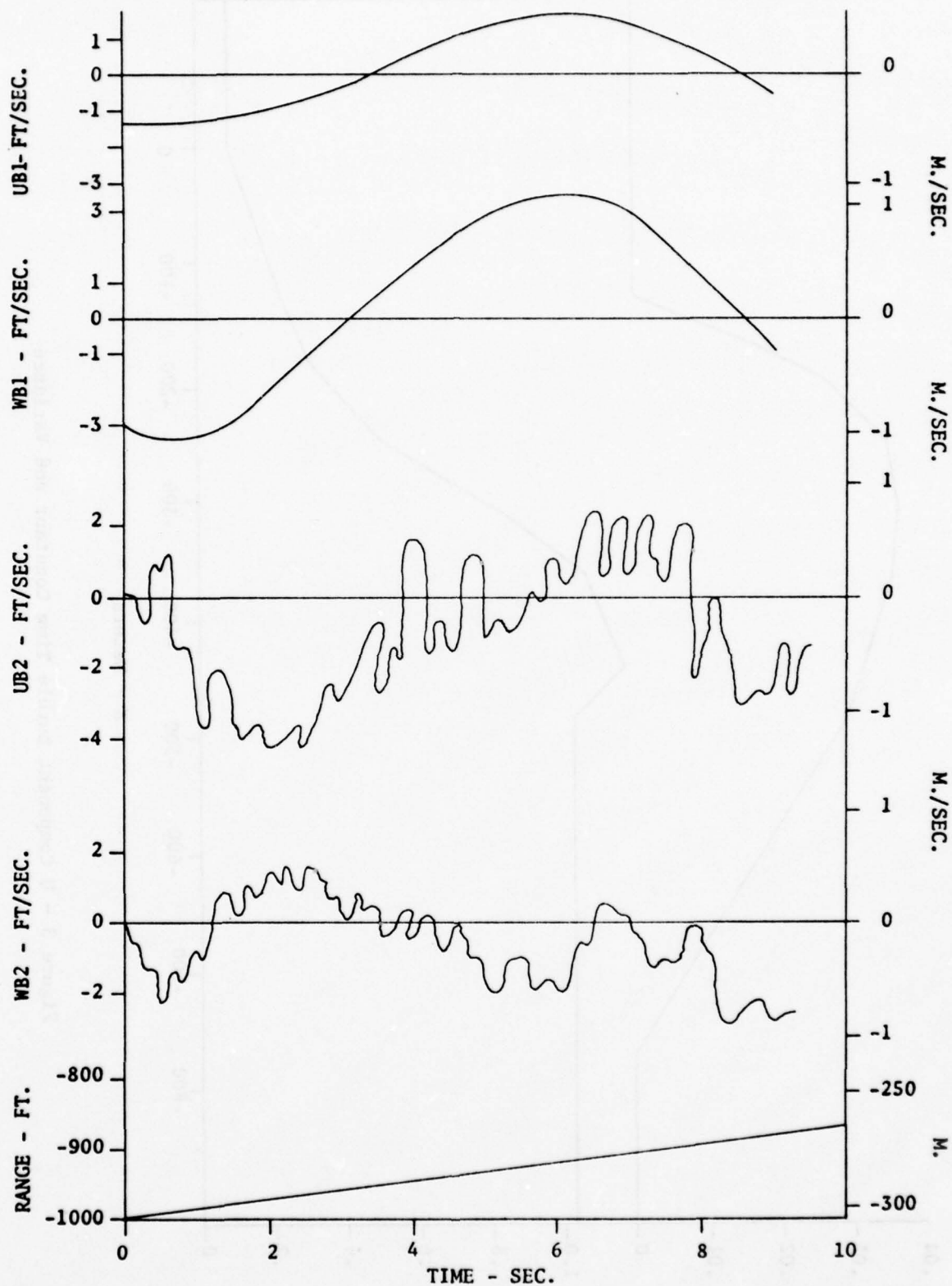


Figure 4 - Sample Burble Components  
 VO = VS = 18 M./Sec. (60 Ft./Sec.)

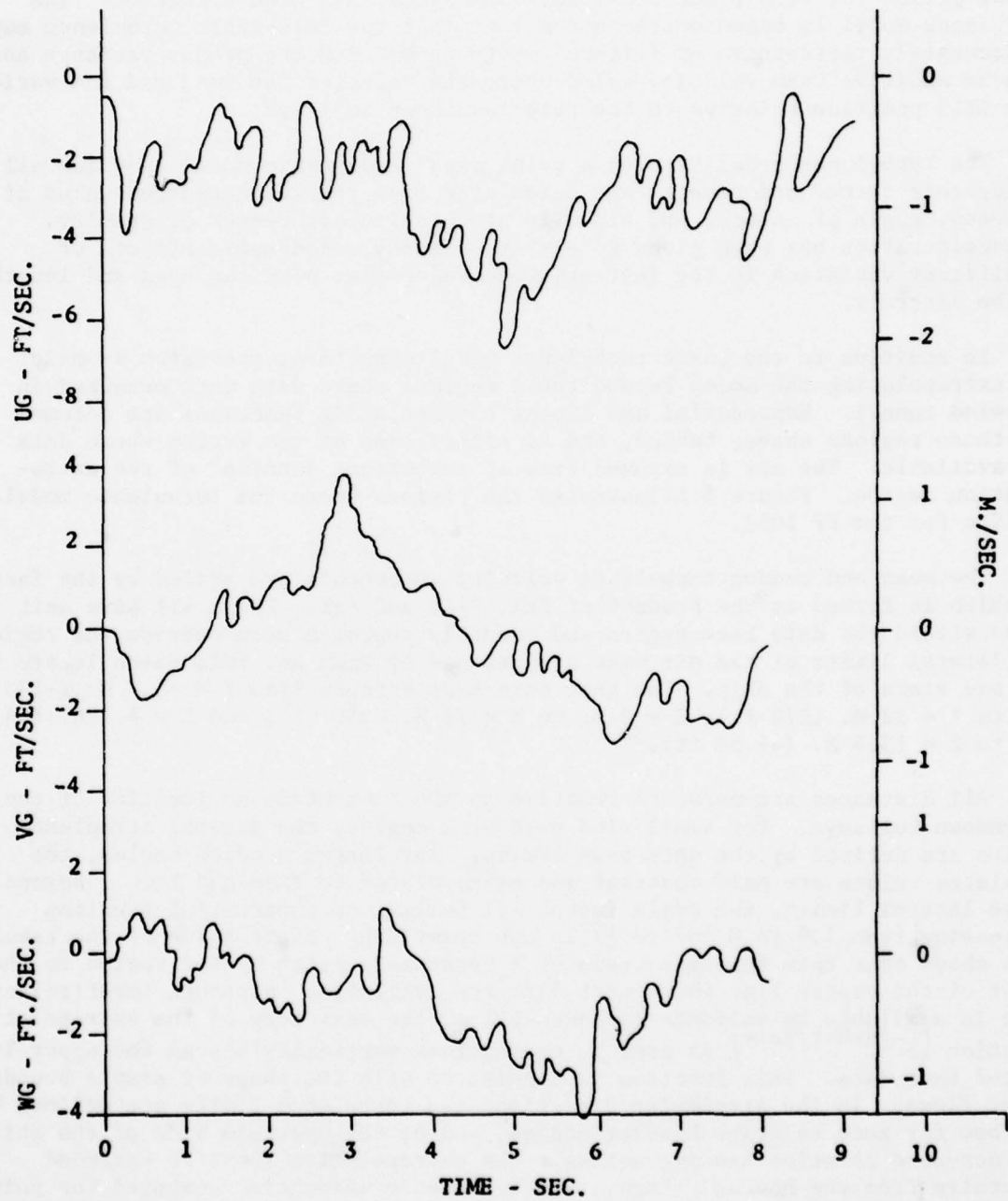


Figure 5 - Sample of CVA Simulated Free Air Turbulence

from statistical summaries of the measured turbulence velocities which define the mean and variance of the three velocity components recorded by an array of hot wire anemometer probes placed downstream of the ship model. The mean and variance were computed from a series of 262 measurements made over a 1.6-second period for each probe location, wind speed, and wind direction. The turbulence model is based on the assumption that the full-scale turbulence may be accurately represented as filtered white noise with the proper variance and with an additive mean velocity value where the value of the mean and the variance vary with position relative to the ship touchdown bullseye.

The turbulence model assumes a point mass aerodynamic model in which all aerodynamic forces and moments are calculated from the instantaneous value of airspeed, angle of attack, and sideslip at the aircraft center of gravity. No consideration has been given to either unsteady aerodynamic effects or significant variation in the instantaneous velocities over the span and length of the aircraft.

In addition to the basic turbulence model structure, provision is made for extrapolating the model beyond those regions where data were measured in the wind tunnel. Exponential and linear extrapolation functions are assumed for those regions above, behind, and to either side of the region where data are available. The air is assumed free of turbulence outside of the extrapolation region. Figure 6 illustrates the regions where the turbulence model applies for the FF 1052.

The mean and random turbulence velocity components are scaled by the factor  $F_1$  which is formed as the product of  $F_{x1}$ ,  $F_{y1}$ , and  $F_{z1}$ . These all have unit value within the data base region and smoothly approach zero outside the region. The lateral limits of the air wake are defined by  $Y_{max}$  and  $Y_{min}$  which locate the bow and stern of the ship. The test data base extends from  $Y = -5.7$  M. (-18.75 ft) to  $Y = 52$  M. (170 ft),  $X = 0$  M. to  $X = 76$  M. (250 ft), and  $Z = 4.4$  M. (14.58 ft) to  $Z = 13.6$  M. (44.58 ft).

All distances are measured relative to the instantaneous location of the touchdown bullseye. For small wind over deck angles, the lateral turbulence limits are defined by the data base limits. For larger heading angles, the tabulated values are held constant and extrapolated to  $Y_{max}$  and  $Y_{min}$ . Beyond these lateral limits, the scale factor  $F_{y1}$  follows an exponential function decreasing from 1.0 to 0.367 ( $e^{-1}$ ) in one beamwidth. Examination of the tabulated data shows that this function produces a reasonable match in the region to the right of the center line where most data are available. Although insufficient data is available to validate the assumption, the same form of the extrapolating function ( $e^{-(H-H_0)/\text{Beam}}$ ) is used to extrapolate vertically beyond the upper limit of the test data. This function is consistent with the shape of simple boundary layer flows. In the streamwise direction, the turbulence limits are defined by the bow for zero relative heading angles, and by the upstream side of the ship for non-zero relative heading angles. The extrapolation limit is extended laterally from the bow and stern. All turbulence velocities computed for points in front of this line are diminished by the  $X$  extrapolation function  $F_{x1}$  which decays exponentially. A linearly scaled extrapolation function is used for  $F_{x1}$  aft of the data base limit of 76 M. (250 feet).



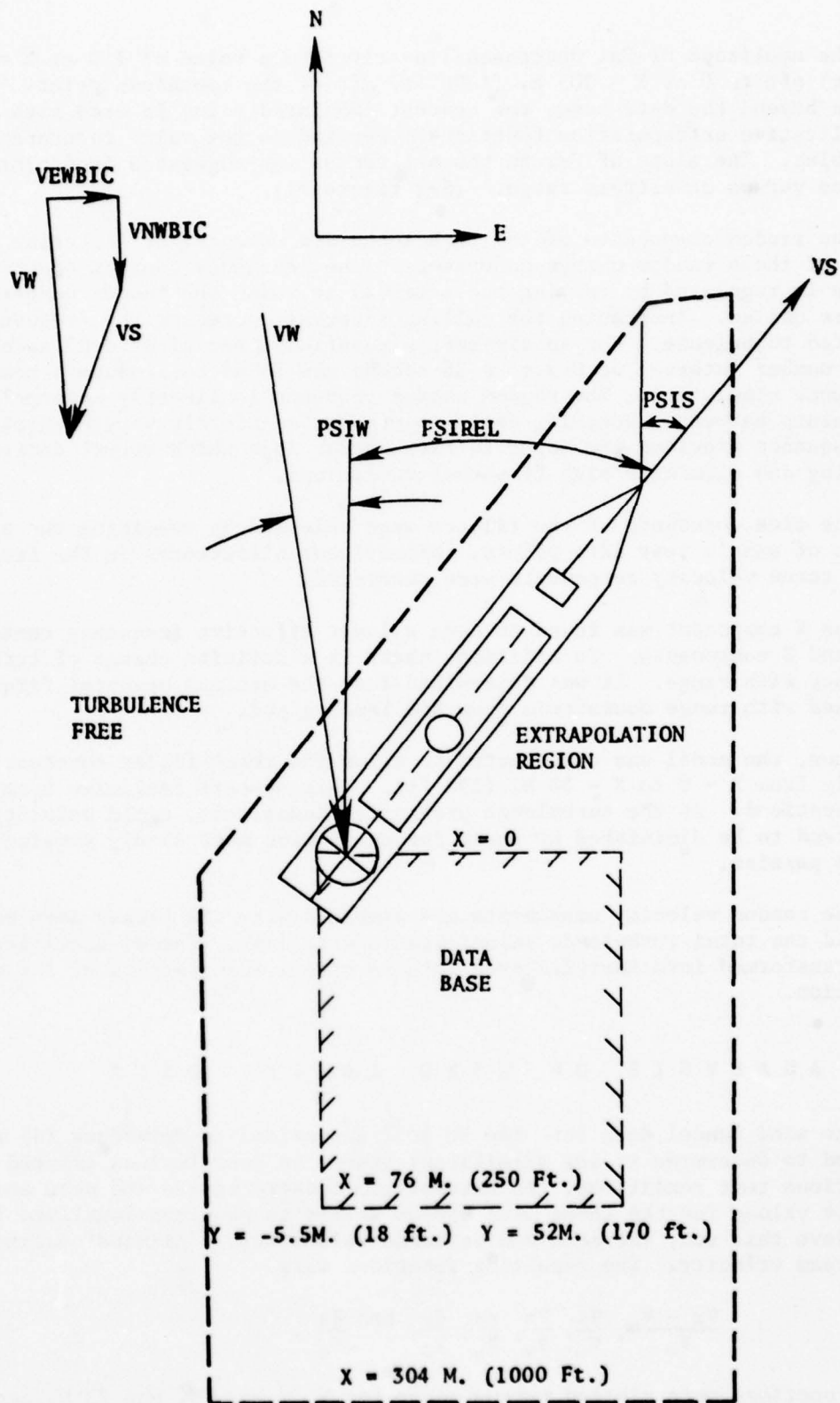


Figure 6 - FF 1052 Ship Airwake Model Geometry

The amplitude of  $F_{x1}$  decreases linearly from a value of 1.0 at  $X = 76$  M. (250 ft) aft to 0 at  $X = 305$  M. (1000 ft) aft of the touchdown point. In the regions beyond the data base, the nearest tabulated value is used with the multiplicative extrapolation function  $F1$  applied to the value returned from the tables. The slope of  $F_{x1}$  in the aft region was suggested from plots of variance versus downstream range. (See figure 7.)

The random components of the turbulence are produced by filtering the output of these random number generators. The frequency content of the turbulence is regulated by varying the interval at which the random number generators are called. Increasing the calling interval decreases the frequency of the simulated turbulence. For an aircraft simulation interval of 0.05 second, a random number interval of 0.3 to 0.35 second was found to produce a reasonable turbulence simulation. The random number sequence is linearly interpolated for time values between succeeding calls to produce a smoothly varying number sequence. This sequence provides the input to first-order lags which effect additional filtering and eliminate high frequency variations.

The time constants of the filters were selected by examining the power spectra of sample test data points. Significant differences in the frequencies of the three velocity components were uncovered.

The X component was found to have a lower effective frequency content than the Y and Z components. In addition, there is a definite change of turbulence frequency with range. It was determined that the maximum spectral frequency decreased with range downstream from the landing pad.

Thus, the model was constructed to allow the three filter constants to vary linearly from  $X = 0$  to  $X = 58$  M. (190 ft). This appears realistic from physical considerations. As the turbulence propagates downstream, rapid velocity fluctuations tend to be diminished by shear forces whereas more slowly varying velocities tend to persist.

The random velocity components are combined with the steady mean components to yield the total turbulence velocities in wind axes. These velocities are then transformed into inertial axes for use by the main portion of the aircraft simulation.

#### ANALYSIS OF WIND TUNNEL DATA

The wind tunnel data for the FF 1052 summarized in reference (d) were analyzed to determine if any significant trends or correlations existed among the various test conditions. An attempt was made to reduce the mean and variance values for the three wind speeds tested to nondimensionalized functions. To achieve this end, the mean and variance values were nondimensionalized by the freestream velocity. The resulting functions were

$$\frac{V_x - V_\infty}{V_\infty}, \frac{V_y}{V_\infty}, \frac{V_z}{V_\infty}, \frac{\delta x}{V_\infty}, \frac{\delta y}{V_\infty}, \text{ and } \frac{\delta z}{V_\infty}.$$

These functions were plotted versus range for  $V_\infty = 10, 18, \text{ and } 23$  M./sec.

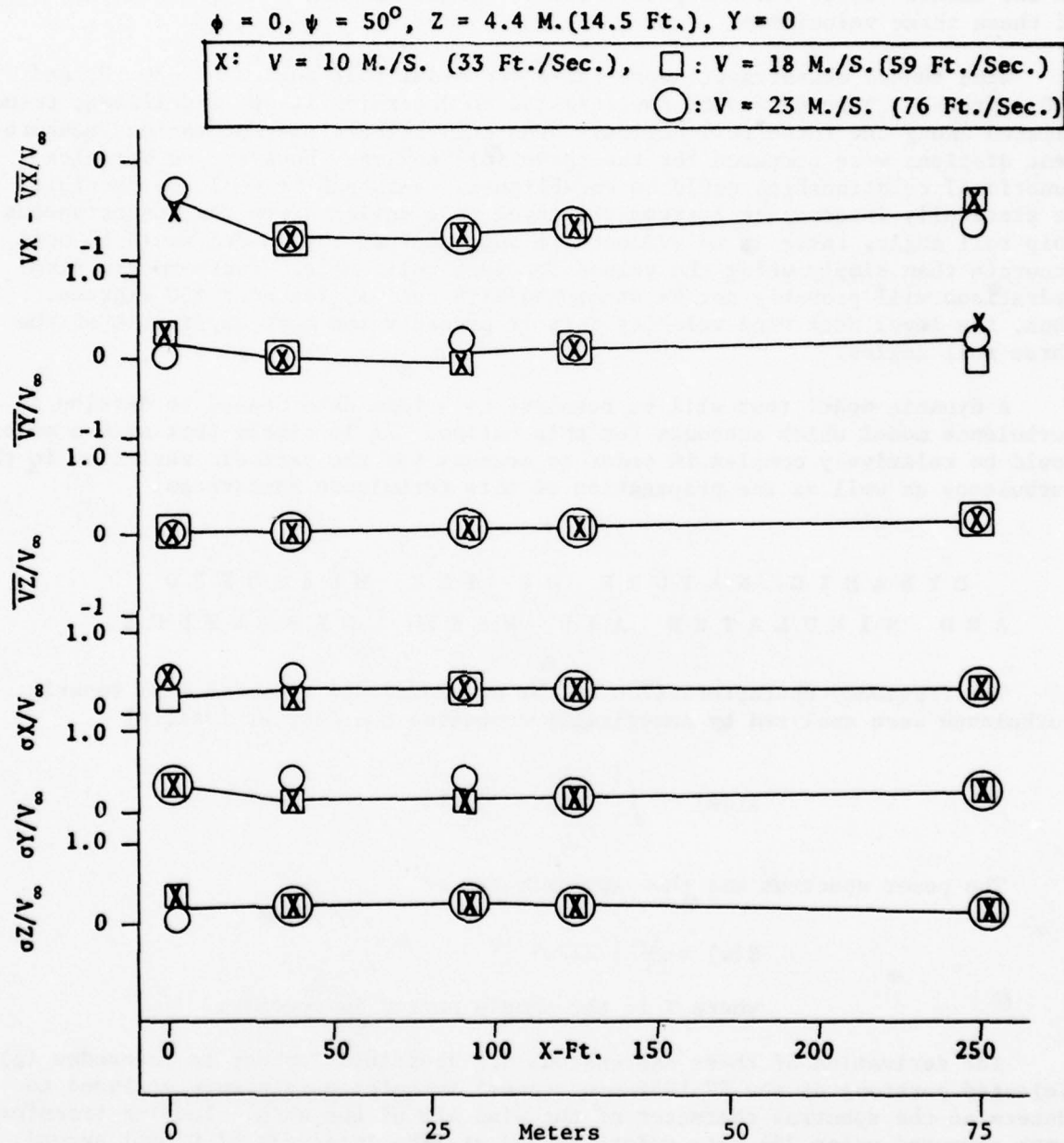


Figure 7 - Nondimensionalized Turbulence Parameters Versus Range



Figure 7 illustrates these functions. It can be seen that the nondimensionalized functions for the three velocities agree rather well. This suggests that a generalized model could be used which would be valid for all relative wind velocities. However, the present model is restricted to the three freestream velocities used in the tunnel tests, and a separate set of nonlinear tables is required for each of these three velocities.

Wind tunnel measurements were taken for model roll angles of -30, 0, and +30 degrees. These data were investigated to determine if any significant trends existed among the three roll angles. Mean and variance size at various measurement stations were compared for the three roll angles. However, no definite functional relationships could be established. Although it would be possible to statically interpolate between the three roll angles given the instantaneous ship roll angle, there is no evidence to suggest that this model would be more accurate than simply using the values for zero roll angle. Furthermore, air operations will probably not be attempted with roll angles near  $\pm 30$  degrees. Thus, the level deck wind velocity data is probably the most applicable of the three roll angles.

A dynamic model test will be required to obtain data needed to develop a turbulence model which accounts for ship motion. It is likely that such a model would be relatively complex in order to account for the periodic variation in the turbulence as well as the propagation of this turbulence downstream.

#### DYNAMIC NATURE OF THE MEASURED AND SIMULATED AIR WAKE TURBULENCE

The frequency characteristics of the simulated and measured wind tunnel turbulence were analyzed by numerically computing the Fourier integral

$$X(j\omega) = \int_0^T X(t) e^{-j\omega t} dt.$$

The power spectrum was then approximated as

$$S(\omega) \approx \frac{1}{2T} |X(j\omega)|^2$$

where T is the sample period in seconds.

The derivation of these expressions are described further in reference (g). Selected portions of the FF 1052 wind tunnel turbulence data were analyzed to determine the spectral character of the wind aft of the ship. Fourier transforms were computed using 256 data points spaced at time intervals of 0.0061 second. A fast Fourier transform routine was used to compute the spectra from 0 to 515 rad/sec. model scale. The transform was calculated with

$$\Delta\omega = \frac{2 \cdot \pi}{N_{\text{samples}}} \text{ rad./sec. and}$$

$$\text{maximum frequency} = \frac{\pi}{\Delta T} = 515 \text{ rad./sec.}$$

TABLE I  
Selected Wind Tunnel Test Points Used in Spectral Analysis

<u>Yaw (deg.)</u>	<u>Roll (deg.)</u>	<u>Speed (M/S)</u>	<u>X (Meters)</u>	<u>Y (Meters)</u>	<u>Z (Meters)</u>
30	0	9	0	0	4.2
50		9	0	0	4.2
50		9	0	0	7.6
0		16	0	5.5	4.2
0		16	0	0	4.2
0		16	0	0	7.6
30		16	0	5.5	4.2
30		16	0	0	4.2
30		16	0	0	7.6
50		16	0	0	4.2
50		16	0	0	7.6
0		22	0	5.5	4.2
30		22	0	0	4.2
30		9	11	0	4.2
30		9	11	0	7.6
50		9	11	0	4.2
50		9	11	0	7.6
30		16	11	0	7.6
30		23	11	0	4.2
30		10	27	0	4.2
30	0	18	27	0	4.2

TABLE II

Statistics of Frequency Value Corresponding to Maximum  
of Spectra Grouped by Velocity and Velocity Component

<u>Freestream Velocity</u>			<u>Frequency - Rad/Sec.</u>			
<u>M./S.</u>	<u>(ft/sec)</u>	<u>Component</u>	<u>Average</u>	<u>Maximum</u>	<u>Minimum</u>	<u>RMS</u>
9.1	30	X	60	110	30	30
9.1	30	Y	76	110	10	34
9.1	30	Z	90	150	30	43
16.46	54	X	95	190	10	52
16.46	54	Y	108	260	10	99
16.46	54	Z	140	290	30	90
21.9	72	X	90	170	30	58
21.9	72	Y	130	170	70	43
21.9	72	Z	290	410	150	107

TABLE III

Statistics of Peak Spectral Velocity Grouped by Velocity Only

<u>Velocity</u>		<u>Peak Spectral Frequency - Rad/Sec.</u>			
<u>M./S.</u>	<u>(Ft./Sec.)</u>	<u>Average</u>	<u>Maximum</u>	<u>Minimum</u>	<u>RMS</u>
9.1	(30)	75	150	30	45
16.46	(54)	114	290	15	80
21.9	(72)	170	410	30	114



Because the number of samples was relatively small, the power spectra were generally very erratic. The data were thus smoothed by averaging over groups of six succeeding frequency points. Figures 8 to 10 illustrate samples of the smoothed spectral data. The sample cases shown in table I were examined with regard to spectral content.

These data were analyzed to determine if any significant trends existed with respect to the spectral distributions. The frequency at which the spectrum attained its maximum value was computed for each case and the data were sorted according to freestream velocity and velocity component. The maximum, minimum, average, and RMS value of the frequency at which the peak of the spectrum occurs is tabulated in table II.

Grouping the data by freestream velocity only, the frequency statistics can be summarized as shown in table III.

Figure 11 summarizes the frequency trend as a function of test condition velocity. A least squares fit of the three gross averaged frequencies yields the relation

$$\omega_{\text{test}}^{\text{max}} = 3.837 + 2.2274 \cdot V - \text{rad/sec.}$$

Strouhal scaling based on model length is used to obtain the equivalent full-scale frequency as

$$\omega_{\text{full scale}}^{\text{max}} = 0.07674 + 0.04548 \cdot V - \text{rad/sec.}$$

For the test velocities, this becomes

TABLE IV  
Turbulence Frequency Versus Airspeed

$\omega$ - Full Scale	V - Ft./Sec.
1.440	30
2.76	59
3.53	76

This differs from the second-order filter model frequency of 1.9 rad./sec. at  $V = 18$  M./S. (59 ft./sec.) as described in reference (d). If additional wind tunnel data is unavailable, the FF 1052 model may be applied to larger or smaller ships having similar geometry or the same ship at different velocities by applying Strouhal scaling, where

$$SN = \frac{f \cdot h}{V}$$

SN = Strouhal number  
f = Turbulence frequency  
h = Ship beam  
V = Flow velocity

$X = 0, Y = 0, Z = 7.6 \text{ M.}, \psi = 50$   
 $\phi = 0, V = 9 \text{ M./S.}$

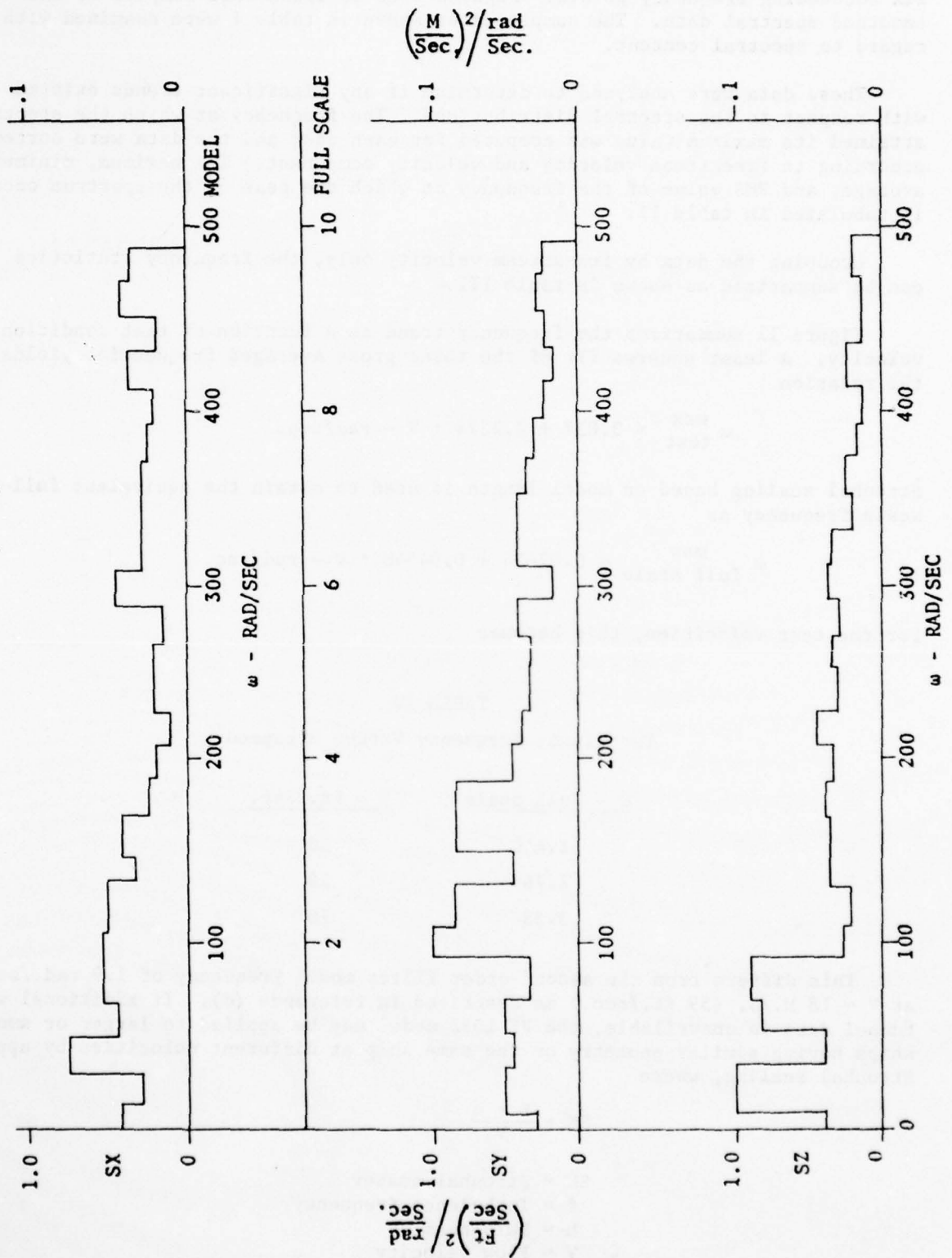
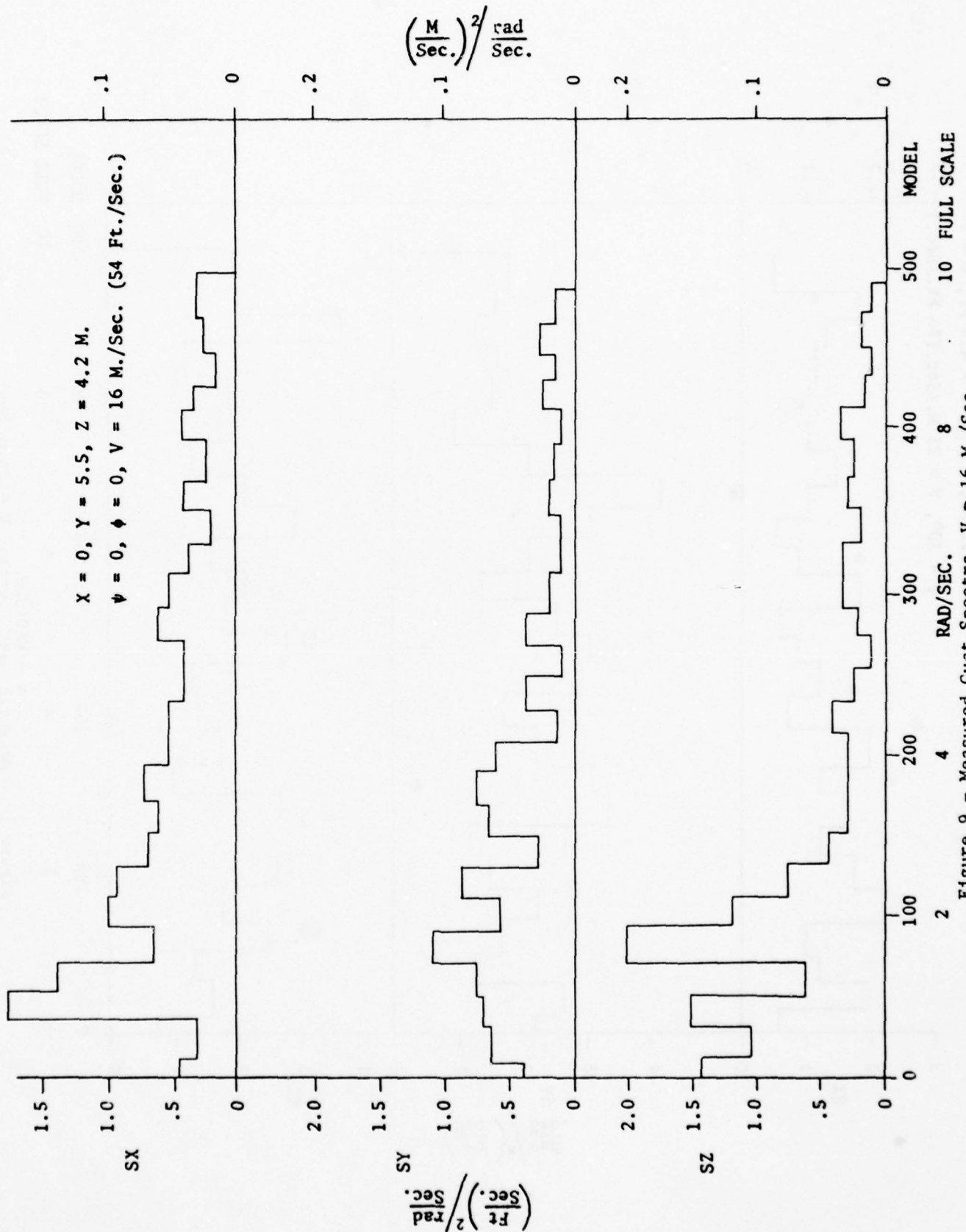


Figure 8 - Measured Gust Spectra,  $V = 9 \text{ M./Sec.}$ ,  
 X, Y, and Z Components



2 Figure 9 - Measured Gust Spectra,  $V = 16 \text{ M./Sec.}$ ,  
X, Y, Z Components



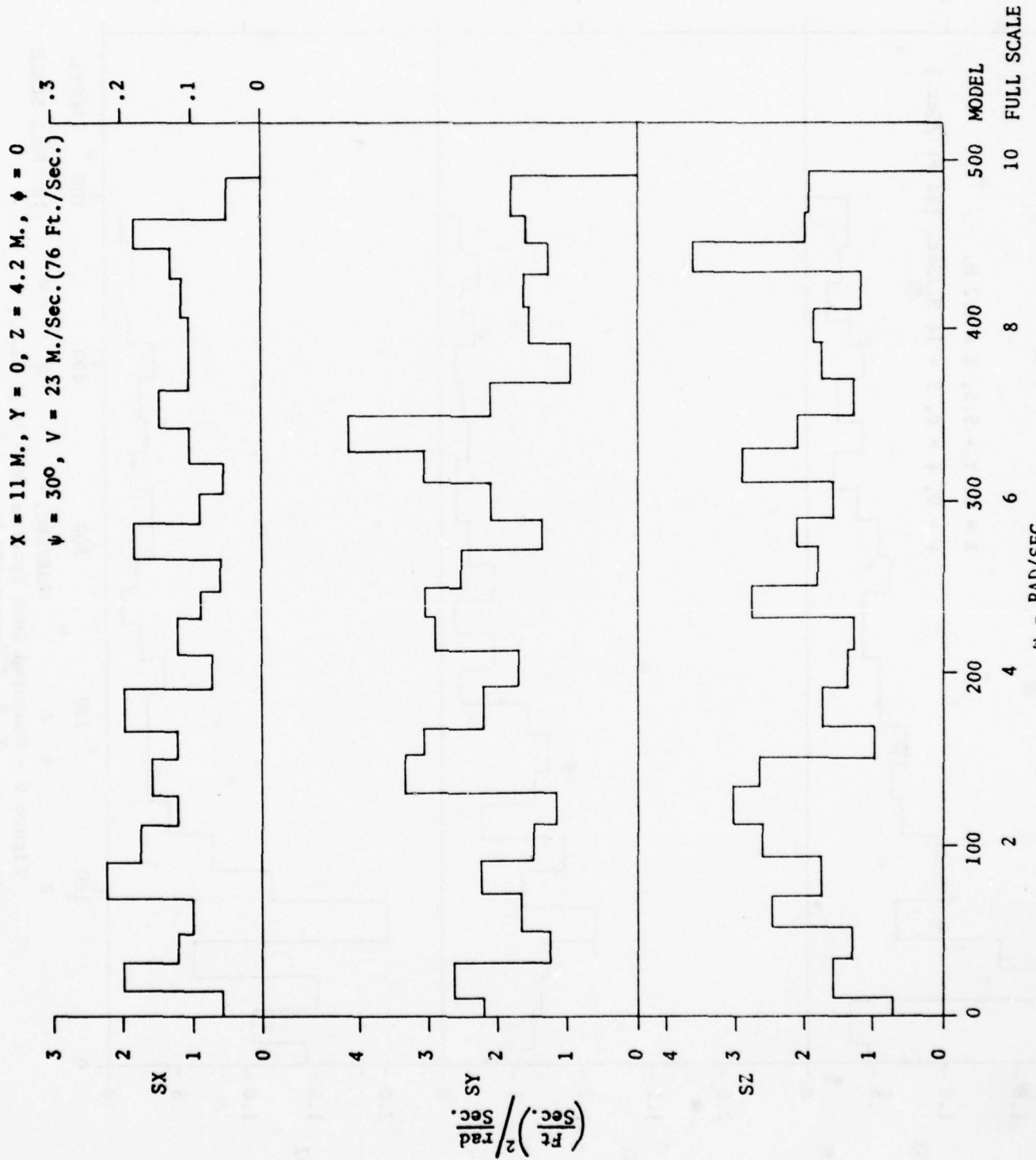


Figure 10 - Measured Gust Spectra,  $V = 23 \text{ M./Sec.}$ ,  $X, Y, Z \text{ Components}$

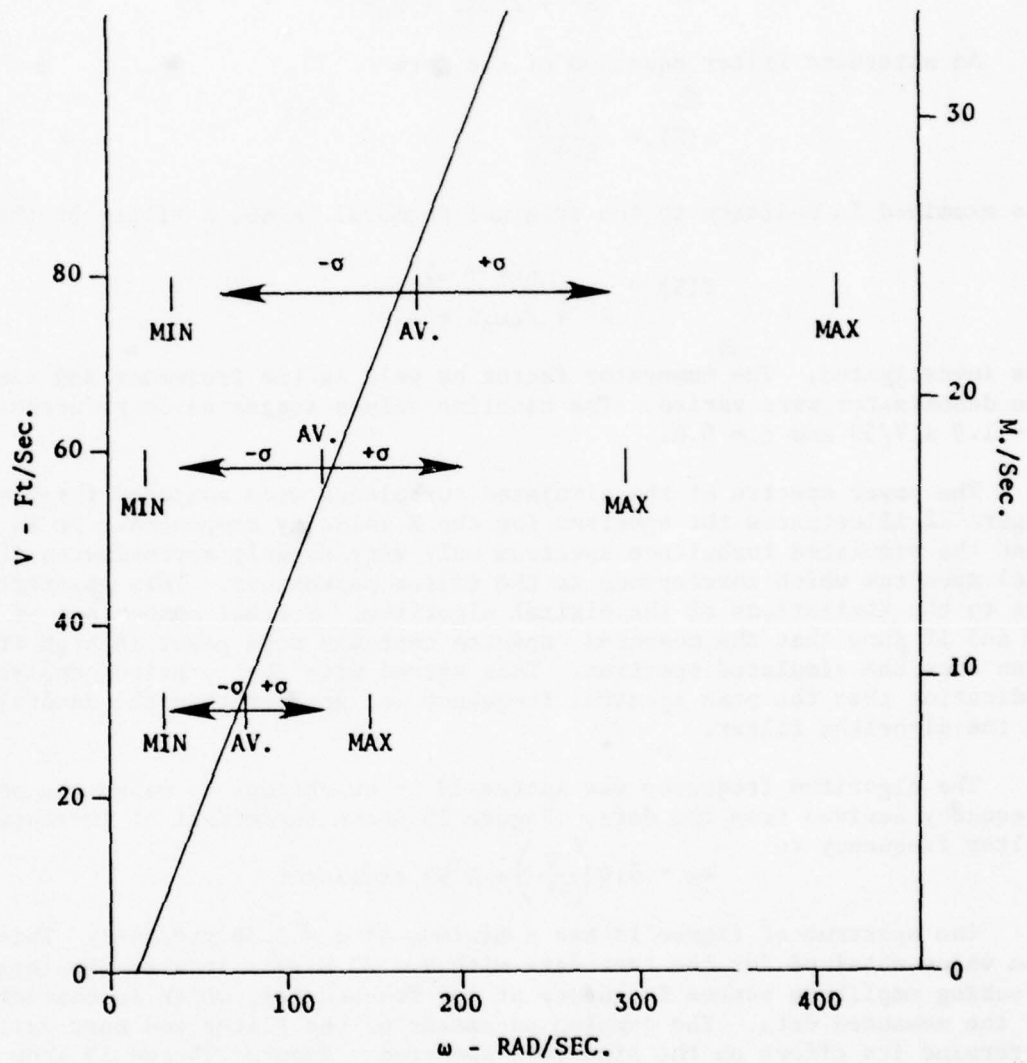


Figure 11 - Peak Spectral Frequency Versus Airspeed

The turbulence model was next examined to see how the properties of the simulated turbulence compared with the measured turbulence. The algorithm filter parameters were varied to determine if an improved match could be obtained between the simulated and test data turbulence. The basic filter equation proposed by reference (d) is

$$F(S) = \frac{\delta(x, y, z) \cdot \sqrt{4\zeta\omega_n^3}}{S^2 + 2\zeta\omega_n S + \omega_n^2}$$

An alternate filter equation of the form

$$F(S) = \frac{\delta \cdot \sqrt{\omega}}{S + \omega}$$

was examined in addition to the original formula. Also, a filter of the form

$$F(S) = \frac{K(S + a)}{S^2 + 2\zeta\omega_n S + \omega_n^2}$$

was investigated. The numerator factor as well as the frequency and damping of the denominator were varied. The baseline values suggested in reference (d) were  $\omega = 1.9 \times V/59$  and  $\zeta = 0.4$ .

The power spectra of the simulated turbulence were computed for  $V = 23$  M./S. Figure 12 illustrates the spectrum for the X velocity component. It is apparent that the simulated turbulence spectrum only very roughly approximates the theoretical spectrum which corresponds to the filter parameters. This apparently occurs due to the limitations of the digital algorithm. Further comparison of figures 10 and 12 show that the measured spectra contains more power at high frequencies than does the simulated spectrum. This agreed with the previous analysis indicating that the peak spectral frequency was greater than the natural frequency of the algorithm filter.

The algorithm frequency was increased in an attempt to match the peak frequency derived from the data. Figure 13 shows the effect of increasing the filter frequency to

$$\omega_z = 4.6 \left( \frac{V}{59} \right) = 5.93 \text{ rad./sec.}$$

The spectrum of figure 13 has a maximum at  $\omega = 2.36$  rad./sec. This matches the value obtained for the test data with  $V = 23$  M./S. It also displays an increasing amplitude versus frequency at low frequencies, which is characteristic of the measured data. The damping parameter of the filter was next varied to determine its effect on the simulated spectrum. Figures 14 and 15 show spectra with  $\omega = 5.9$  and  $\zeta = 0.1$  and  $0.7$ .

Compared to the case with  $\zeta = .4$ , the configuration with  $\zeta = 0.7$  had its peak amplitude at a lower frequency and lower amplitude at high frequencies. The  $\zeta = 0.1$  case showed a large peak amplitude near the damped natural frequency and a rapid amplitude roll off at lower and higher frequencies. Thus, neither configuration appears to improve the correspondence with test data over that achieved with the original value of  $\zeta = 0.4$ .

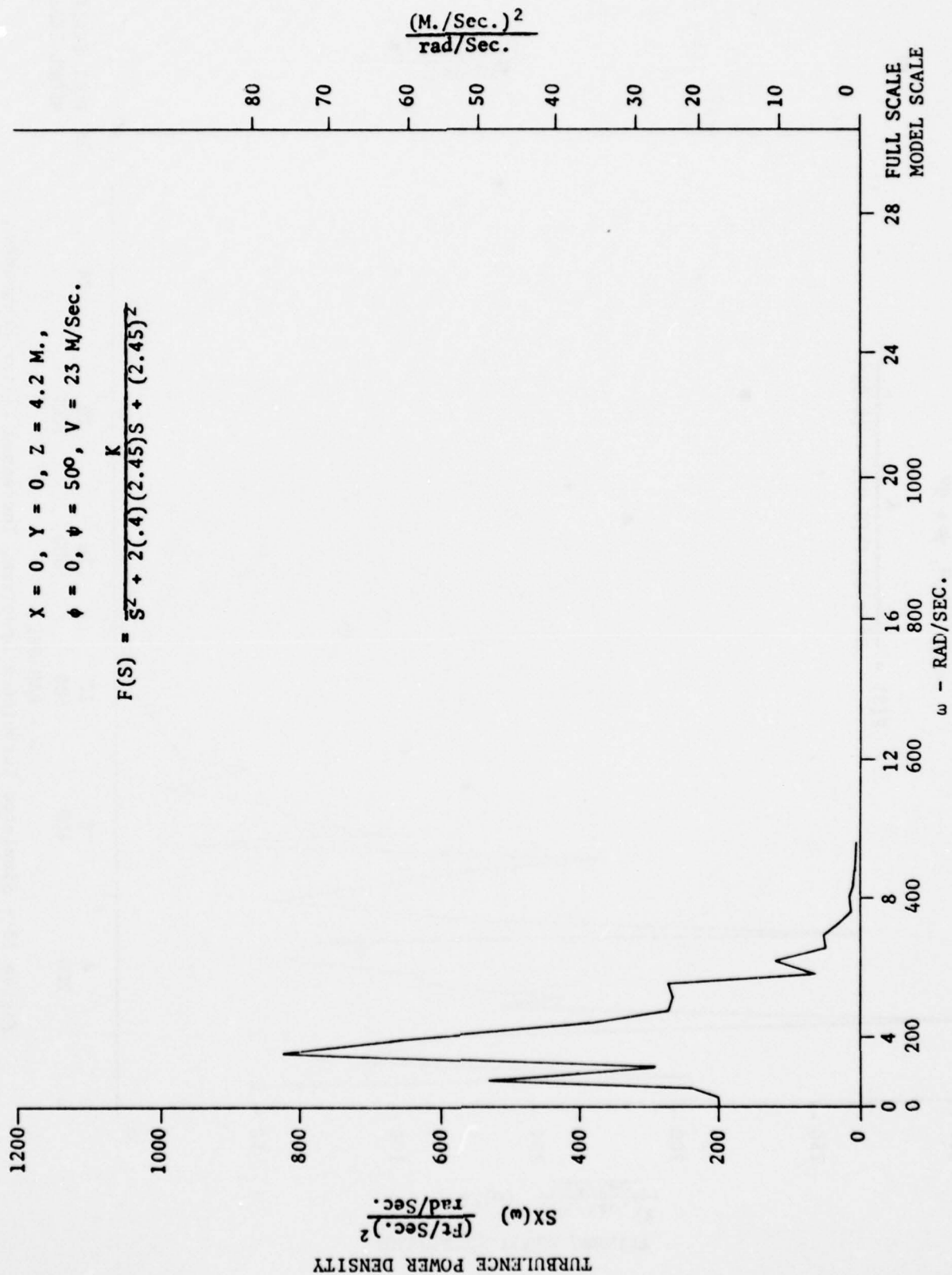


Figure 12 - Simulated Turbulence Spectrum,  $V = 23 \text{ M./Sec. (76 Ft/Sec.)}$ ,  
X Velocity Component



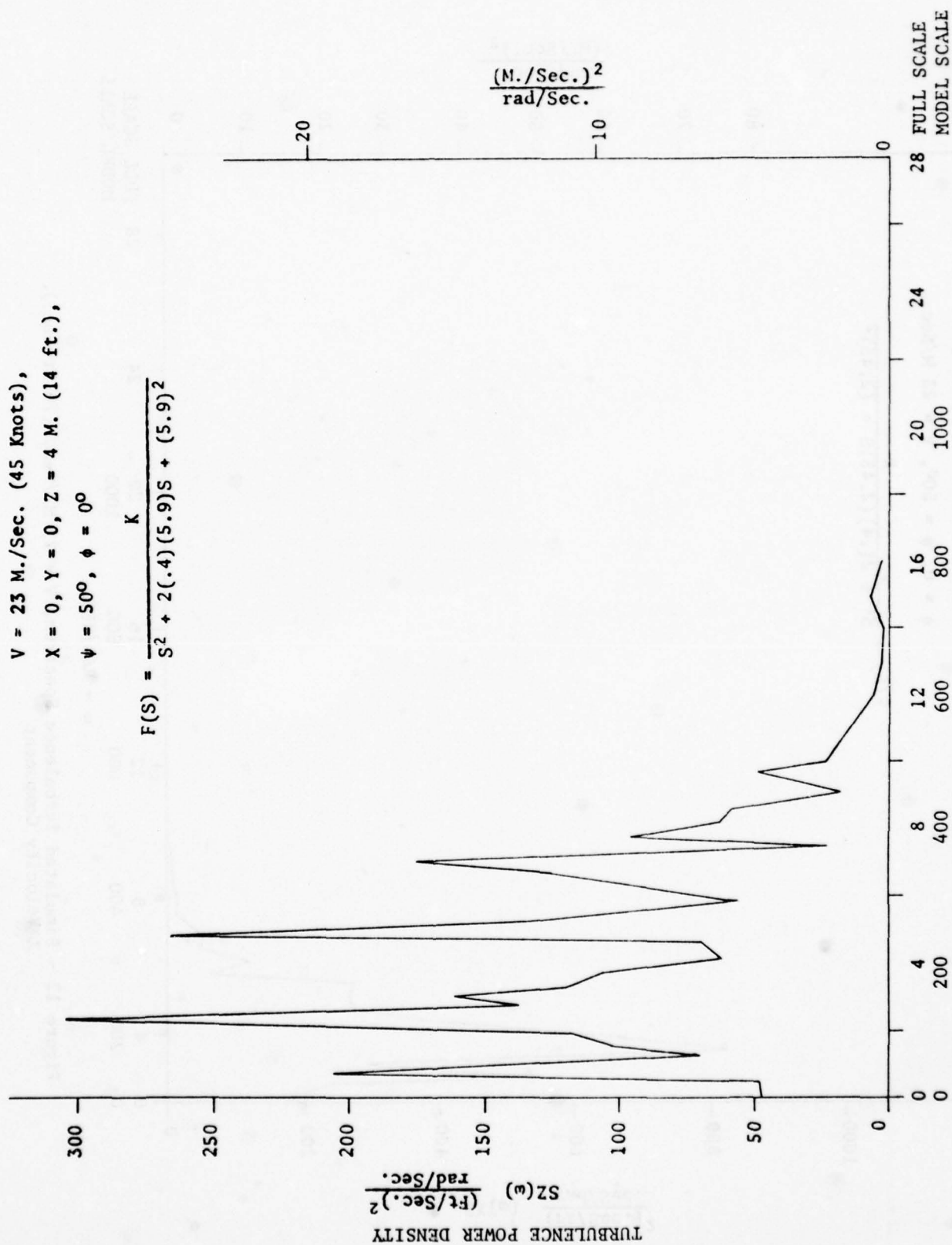


Figure 13 - Simulated Turbulence Spectrum, Increased Filter Frequency,  
Z Velocity Component

$SZ(\omega)$   
 $\frac{(\text{Ft./Sec.})^2}{\text{rad/Sec.}}$

500

400

TURBULENCE POWER DENSITY

- 11 -

$V = 23 \text{ M./Sec. (45 Knots),}$   
 $X = 0, Y = 0, Z = 4 \text{ M. (14 Ft),}$   
 $\psi = 0 \quad \phi = 0$

$$F(S) = \frac{K}{S^2 + 2(.7)(5.9)S + (5.9)^2}$$

$\frac{(\text{M./Sec.})^2}{\text{rad/Sec.}}$

NADC-78182-60

30

20

10

9

8

7

6

5

4

3

2

1

0

$\omega$  - RAD/SEC. - FULL SCALE

Figure 14 - Simulated Turbulence, 0.7 Damping,  
 Z Velocity Component

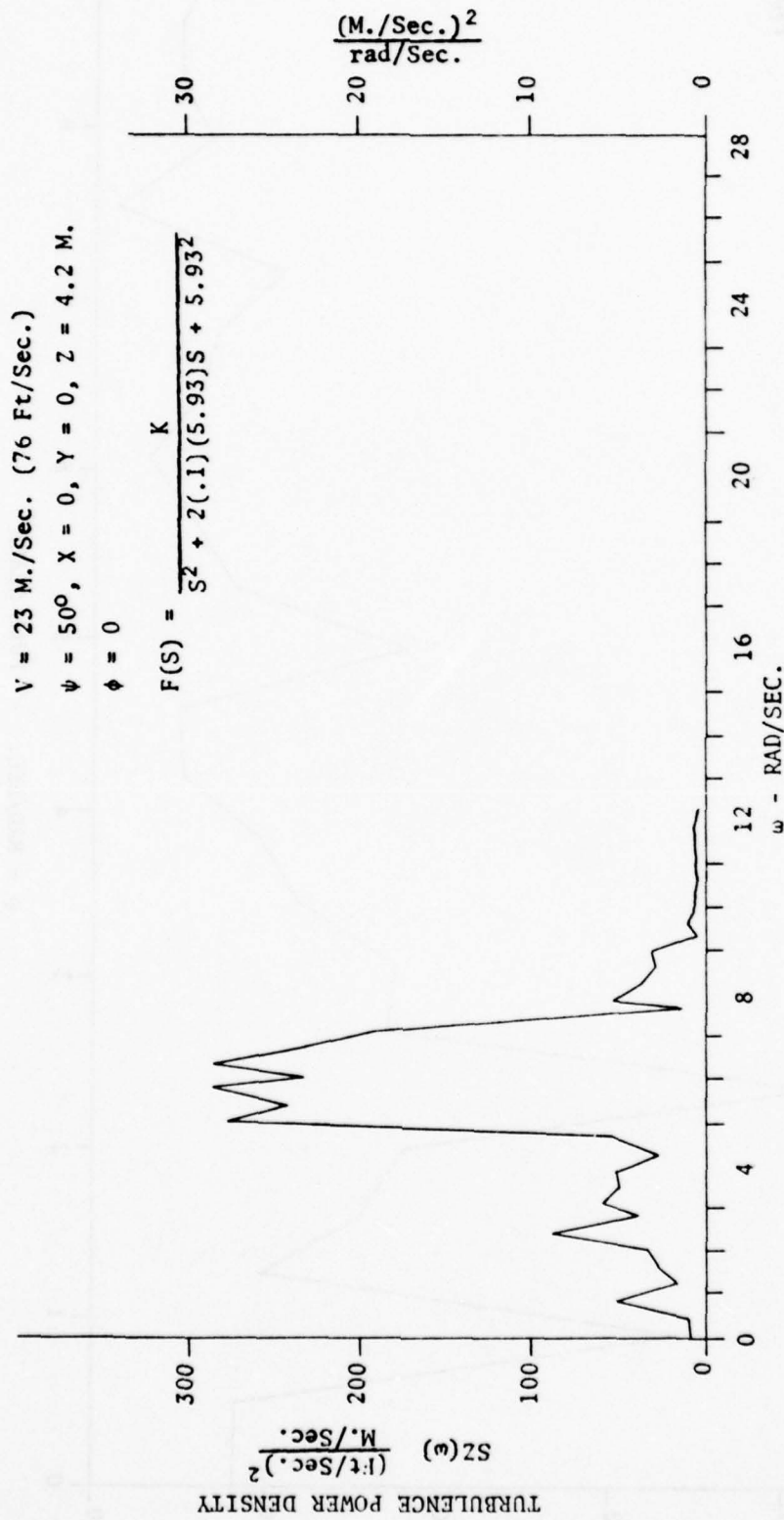


Figure 15 - Simulated Turbulence Spectrum, 0.1 Damping,  
Z Velocity Component

One additional filter configuration was examined in which a first-order numerator term was introduced with a break point at the denominator natural frequency. The resultant filter had the form

$$F(S) = \frac{K (S + \omega)}{S^2 + 2 (0.4) \omega S + \omega^2}$$

A representative spectrum for this configuration is shown on figure 16. This configuration shows a more pronounced peak and a less rapid dropoff at high frequency than does figure 12. However, it does not appear to match the measured data as well as the configuration shown on figure 13.

Comparison of the various power spectra is found to be a less than conclusive method of establishing the proper form for a turbulence simulation. The measured data was limited to 256 point samples. Because of the extremely random nature of the turbulence, the short data sample appears inadequate to exactly define the power spectra. Even the artificially generated turbulence is found to have rather irregular spectra although the equations used in the algorithm should theoretically produce a smooth spectra. This may be caused by either the finite samples examined or by the approximations of the digital algorithm.

Because of difficulty in defining an exact mathematical relation for the spectra of either the measured turbulence or the simulated turbulence, the modeling effort was limited to matching the mean value, the variance, the frequency at which the power spectra attained its maximum value, and the overall slope of the spectrum above and below the peak frequency. Only the mean and variance can be matched in an exact manner by adjusting the mean functions and the random filter gains. The remaining characteristics must be established on a trial basis.

All of the second-order simulation models showed a more pronounced peak and a more rapid high frequency dropoff than did the test data. As a result, it was concluded that a first-order model might be more appropriate. The principal disadvantage of the first-order filter is that the output velocities tend to be more jerky and less smooth than those produced with a second-order filter. The problem was recognized as being caused by the way in which the random number sequences were generated. When a random number sequence is generated at each aircraft integration interval (typically 0.05 second), the bandwidth of the random noise sequence is high. The magnitude of a purely random sequence is essentially uncorrelated from one point to the next. In fact, turbulent velocity variations occur over finite times, and real measured data shows correlation over a very short time duration.

The apparent solution to this problem was to generate the random number sequence less frequently than the aircraft equations of motion were integrated. By interpolating linearly between succeeding random numbers, a smoothed input was generated which had limited bandwidth. By specifying the ratio of aircraft equation update interval to random number update interval, the power spectral content of the simulated turbulence could be more readily adjusted to match the test data.



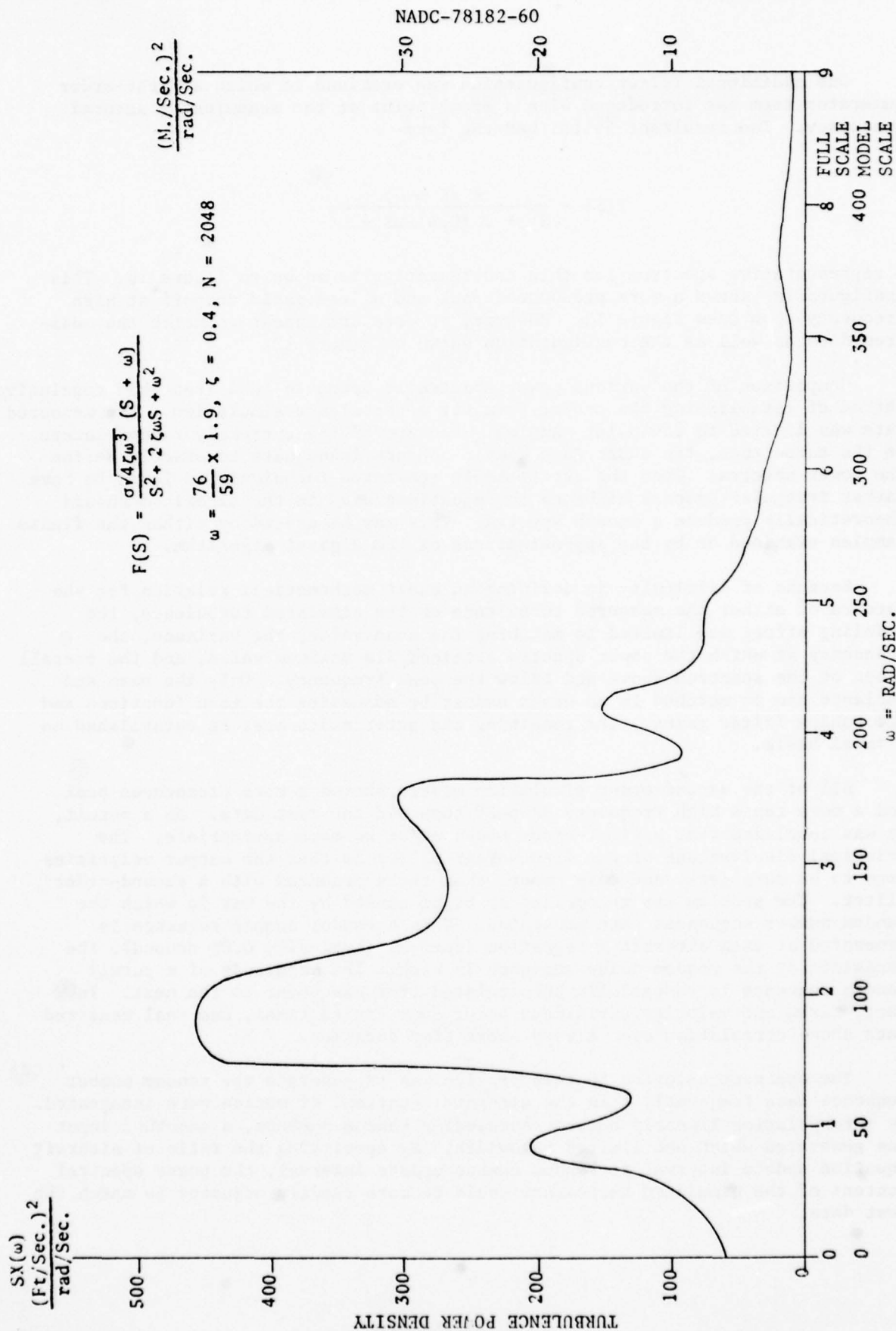


Figure 16 - Simulated Turbulence Spectrum, First Order Numerator

The smoothed random number sequence can be further processed to yield a reasonable simulation of the measured turbulence data by passing the number sequence through a properly designed first-order filter.

Because of the erratic nature of the measured data, it was decided to examine groups of points at various downstream ranges. Individual power spectra were normalized by dividing by their peak amplitudes. Then, these spectra were averaged on a component by component basis. The data selected included all cases for which  $\phi = 0$ ,  $\psi = 50$  deg,  $V = 23$  M./Sec. The same process was performed for all data for which  $\phi = 0$ ,  $\psi = 50$  deg., and  $V = 9$  M./Sec.

All points at a given downstream range were lumped together regardless of lateral position or height. Figures 17 to 20 show the effects of downstream station and freestream velocity on the character of the normalized spectra for the X, Y, and Z velocity components.

All four figures show a more pronounced dropoff of spectral amplitude with frequency for the X component than for the Y or Z components. Further, figures 17 and 18 show an overall lower frequency break point than do figures 19 and 20. This illustrates the fact that the turbulence frequency decreases as the distance downstream from the ship increases.

A least square straight line curve fit was first applied to the averaged test spectra. Then the break frequency of the first-order filter was assigned a value corresponding to the point at which the straight line reached a value of 0.5 times its value at zero frequency. This was chosen because the magnitude of

$$\left| \frac{1}{\frac{S}{\omega} + 1} \right|^2$$

reaches 0.5 at  $S = \omega$ . The curve fit analysis was applied to the cases for  $V = 23$  M./Sec. (76 ft/Sec.).

Based on the assumption that Strouhal scaling could be applied, the filter frequency was made proportional to freestream velocity. The selected frequency was ratioed to the value obtained for the  $V = 23$  M./S case by multiplying by  $V/76$ . The selected turbulence algorithm was then run repeatedly to obtain a good estimate of the spectral properties of the model. These spectra were averaged component by component and compared with the test spectra.

The filter break frequencies selected for  $V = 23$  M./S., and  $X = 0$  were as follows:

TABLE V	
Filter Break Frequencies at $X = 0$	
<u>Component</u>	<u>Break Frequency (rad./sec.)</u>
X	8.17
Y	10.41
Z	10.0

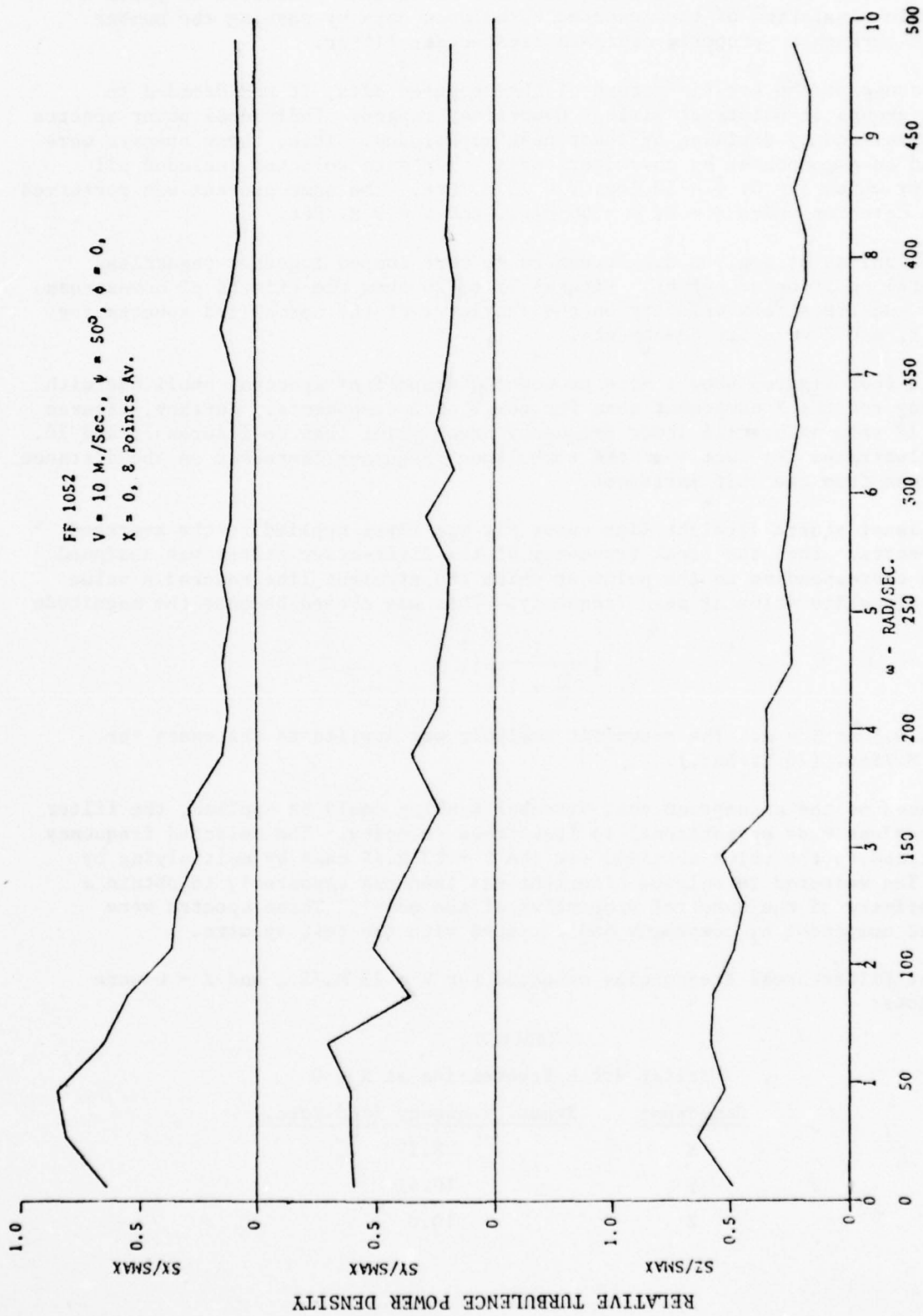


Figure 17 - Normalized Spectra for  $V = 10 \text{ M./Sec.}, X = 0$  (Measured),  
 $X, Y,$  and  $Z$  Components

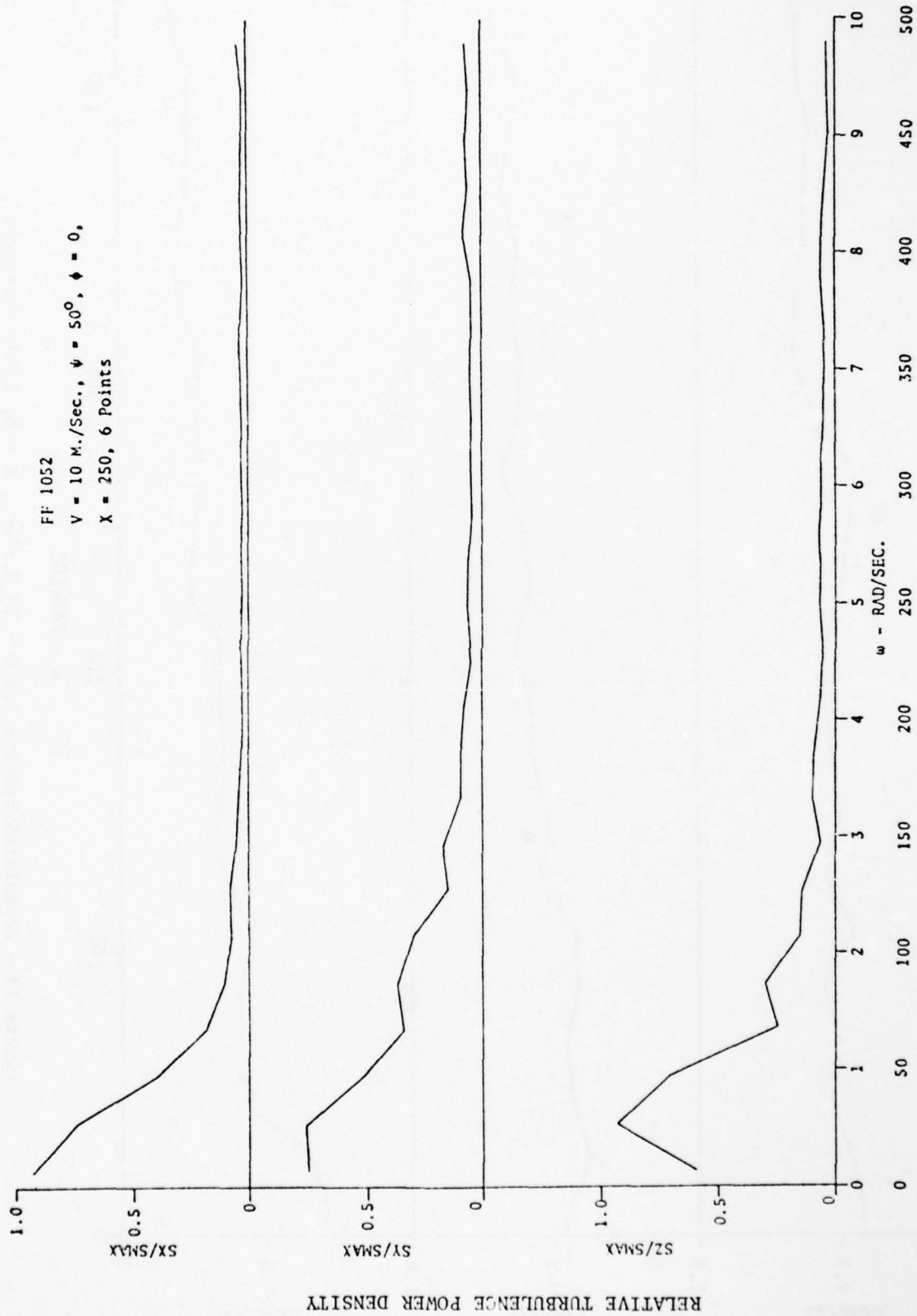


Figure 18 - Normalized Spectra for  $V = 10 \text{ M./Sec.}, X = 76 \text{ M. (Measured)}$ ,  
 $X, Y,$  and  $Z$  Components



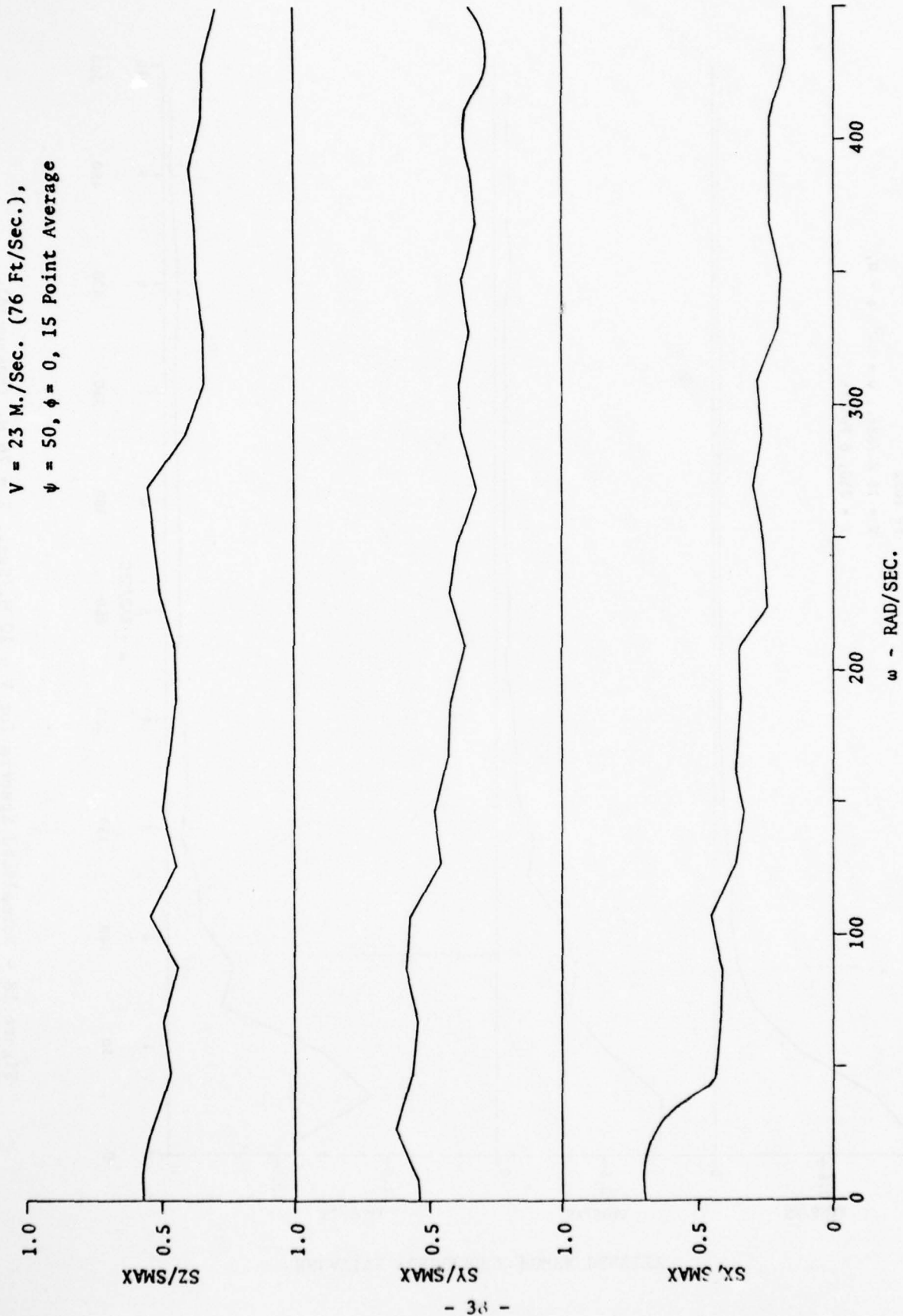


Figure 19 - Normalized Spectra for  $V = 23 \text{ M./Sec.}$ ,  $X = 0, 11 \text{ M. (Measured)}$ ,  $X, Y$ , and  $Z$  Components

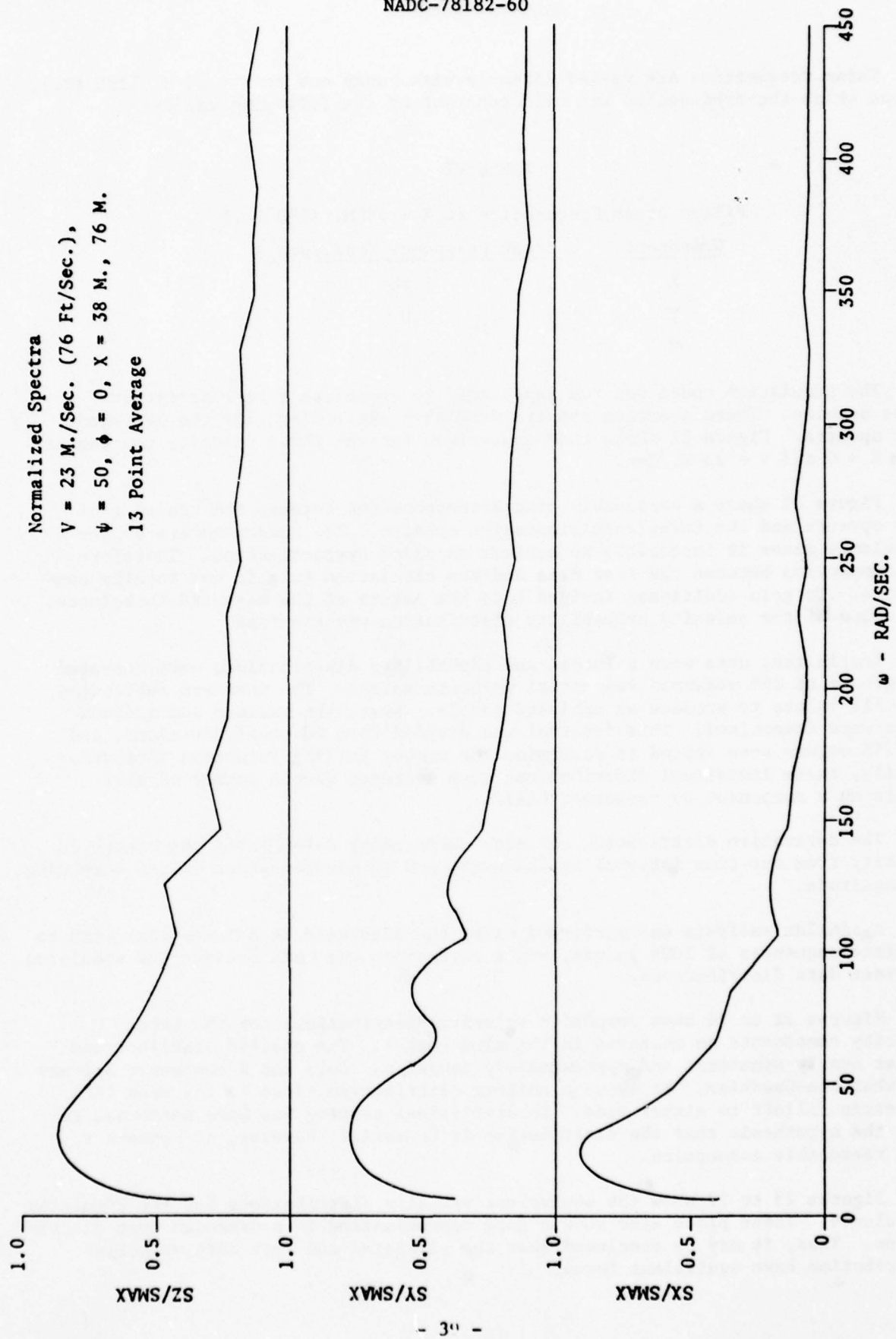


Figure 20 - Normalized Spectra for  $V = 23 \text{ M./Sec.}$ ,  $X = 38 \text{ M.}$ ,  $76 \text{ M.}$  (Measured),  
 $X$ ,  $Y$ , and  $Z$  Components

These frequencies are varied linearly with range out to  $X = 58$  M. (190 ft.), beyond which the frequencies are held constant at the following values:

TABLE VI

Filter Break Frequencies at  $X = 58$  M. (190 ft.)

<u>Component</u>	<u>Break Frequency (rad./sec.)</u>
X	1.58
Y	3.0
Z	2.88

The simulation model was run repeatedly to establish a representative power spectra. These averaged spectra were then plotted against the averaged test spectra. Figure 21 shows this comparison for the three velocity components with  $X = 0$  and  $V = 23$  M./Sec.

Figure 21 shows a reasonably good correspondence between the scaled test data spectra and the turbulence simulation spectra. The random nature of the turbulence makes it impossible to achieve an exact spectral match. Therefore, the comparison between the test data and the simulation data is not totally conclusive. To gain additional insight into the nature of the measured turbulence, the shape of the velocity probability distribution was examined.

Sample test data were selected and probability distributions were computed for groups of 256 measured sequential velocity values. The mean was subtracted from all values to produce an unbiased sample. Next, the maximum and minimum value were determined. This interval was divided into 20 equal divisions, and the 256 values were sorted to determine the number falling into each interval. Finally, these individual distributions were averaged over a number of test points on a component by component basis.

The derivative distribution was also computed by determining the change in velocity from one time interval to the next, and by sorting these values according to magnitude.

A similar analysis was performed using the simulated turbulence algorithm to generate sequences of 1024 points, and a comparison was made between the simulated and test data distributions.

Figures 22 to 24 show composite velocity distributions for the three velocity components as measured in the wind tunnel. The plotted distributions appear nearly symmetric and approximately Gaussian. Only the X component appears somewhat non-Gaussian. It shows a uniform distribution close to the mean with symmetric falloff to either side. No statistical testing has been performed to test the hypothesis that the distribution is Gaussian. However, it appears to be a reasonable assumption.

Figures 25 to 27 show the equivalent velocity distributions for the simulated turbulence. These plots also show a good approximation to a Gaussian type distribution. Thus, it may be concluded that the simulated and test data velocity distribution have equivalent forms.

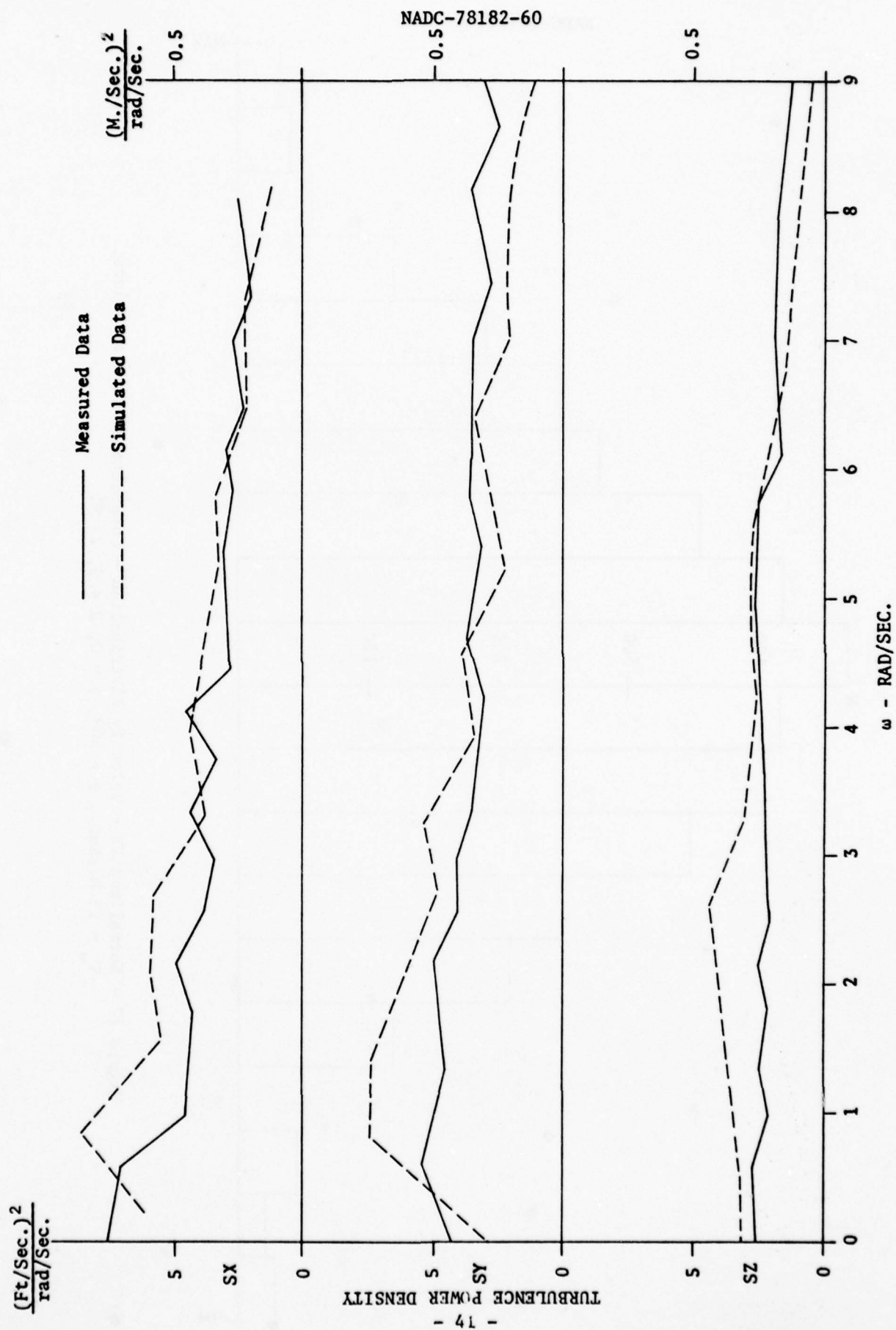


Figure 21 - Comparison of Test and Simulated Turbulence Spectra



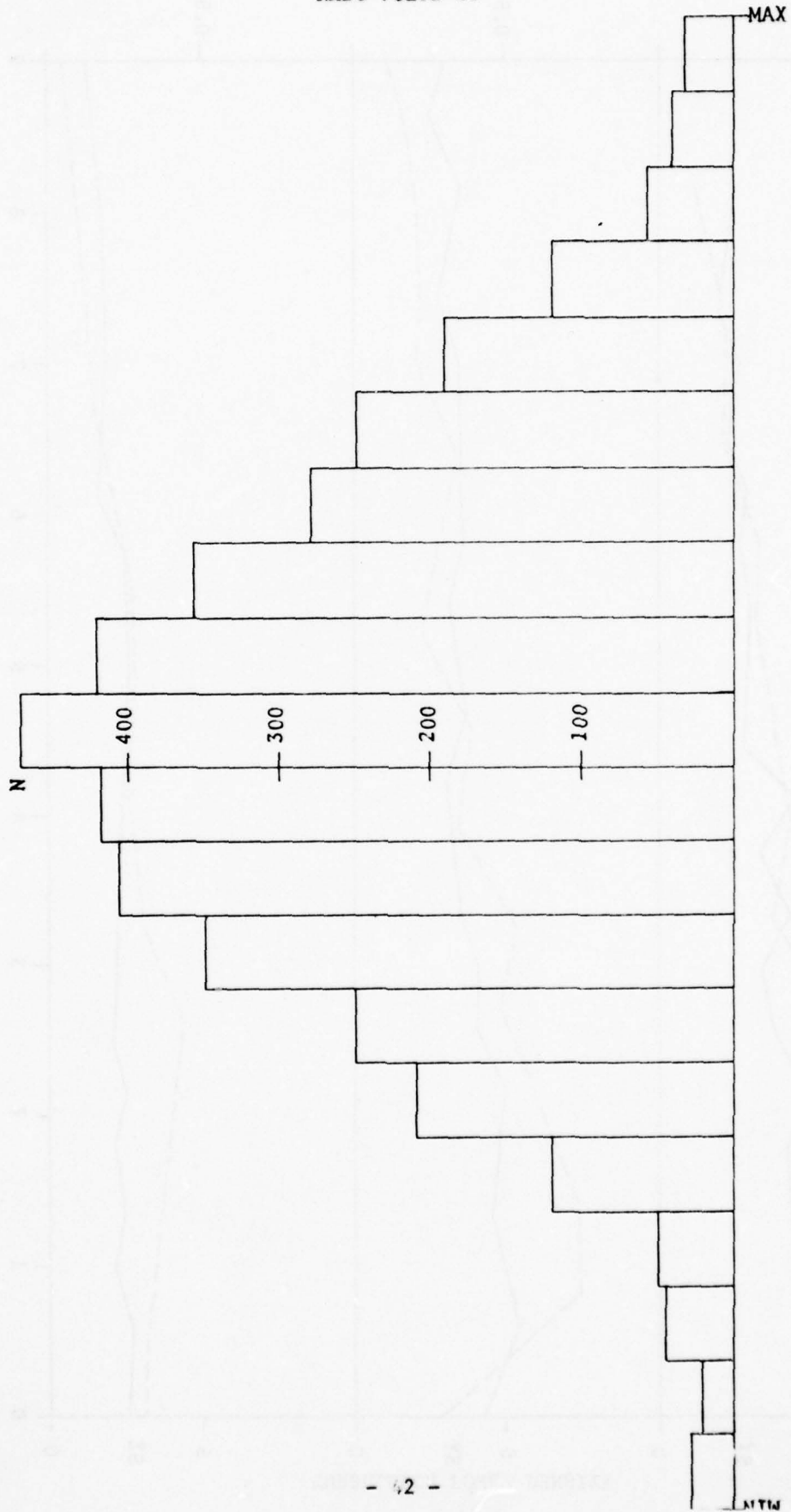


Figure 22 - Normalized VZ - Velocity Distribution - Composite of 16 Test Points,  
 $V_{\infty} = 23 \text{ M./Sec.}, \psi = 50^{\circ}, \phi = 0, X = 0, 27 \text{ M.}$

NADC-78182-60



Figure 23 - Normalized VY - Velocity Distribution - Composite of 16 Test Points,  
 $V_{\infty} = 23 \text{ M./Sec.}, \psi = 50^{\circ}, \phi = 0, X = 0, 27 \text{ M.}$

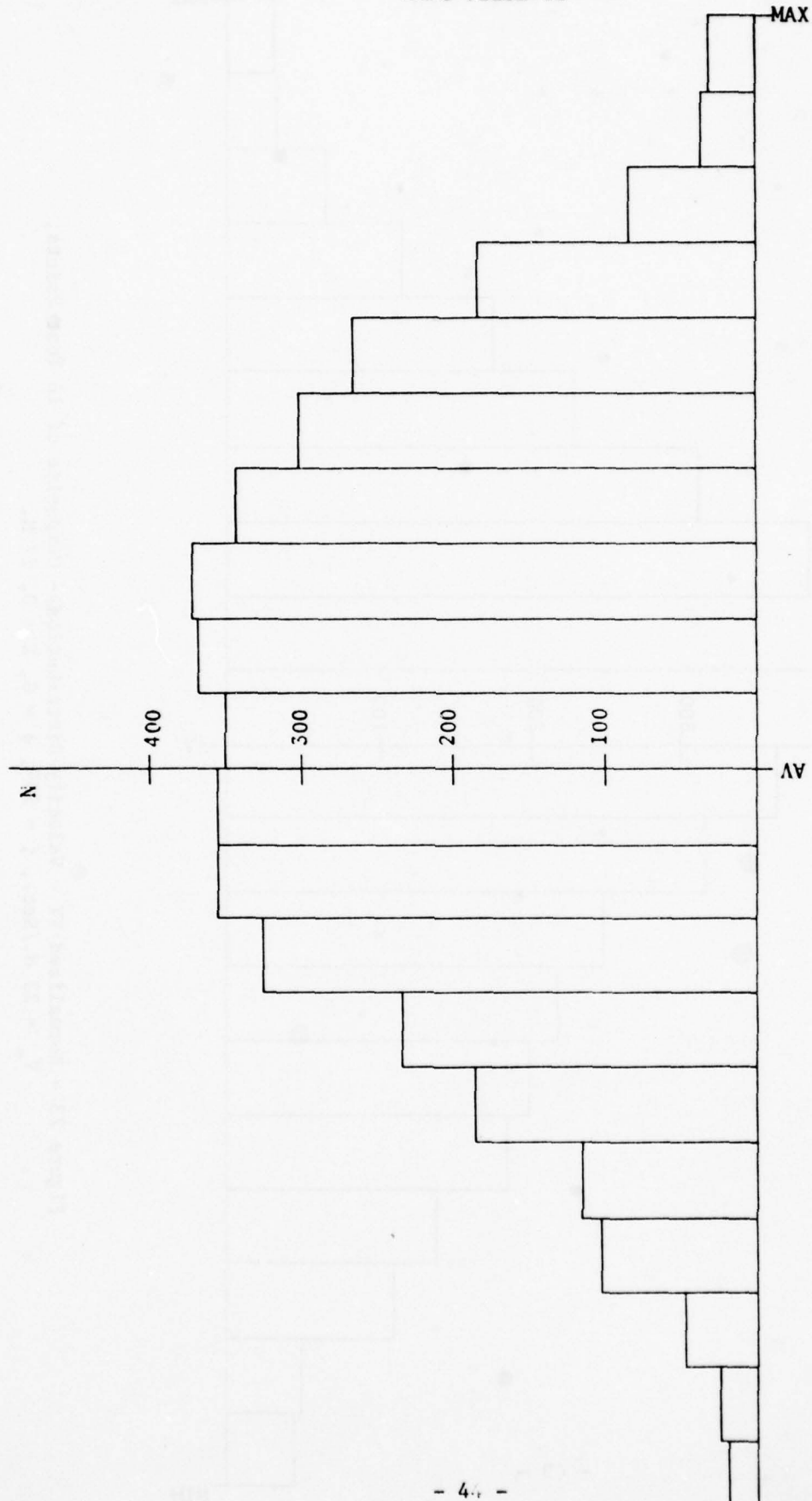


Figure 24 - Normalized VX - Velocity Distribution - Composite Average of 16 Test Points  
 $V_{\infty} = 23 \text{ M./Sec.}, \psi = 50^{\circ}, \phi = 0, X = 0, 27 \text{ M.}$

NADC-78182-60

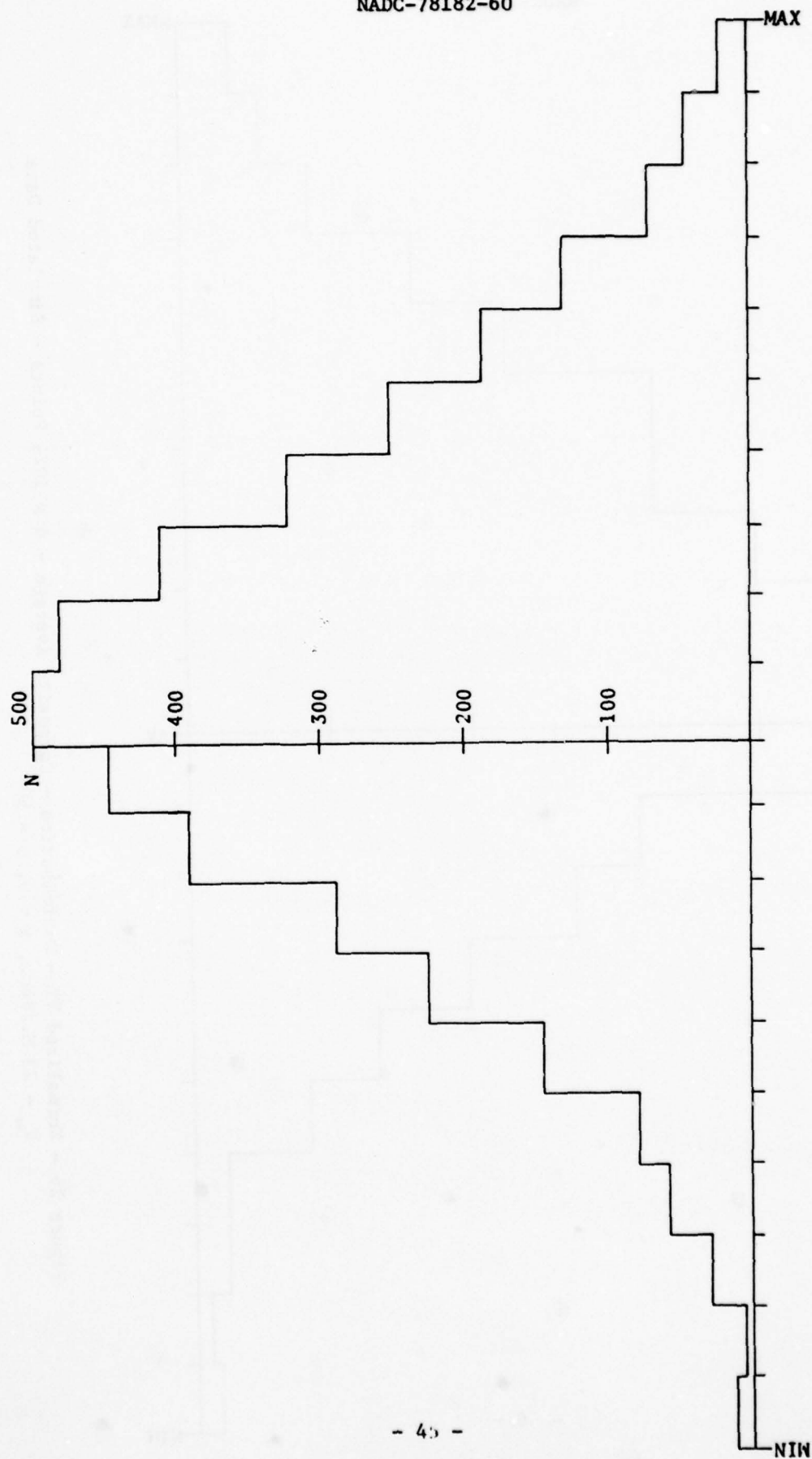


Figure 25 - Normalized VX - Distribution - Composite Average - 4 x 1024 Points - Simulated Data  
 $V_{\infty} = 23 \text{ M./Sec.}, \phi = 0, \psi = 50^{\circ}$



NADC-78182-60

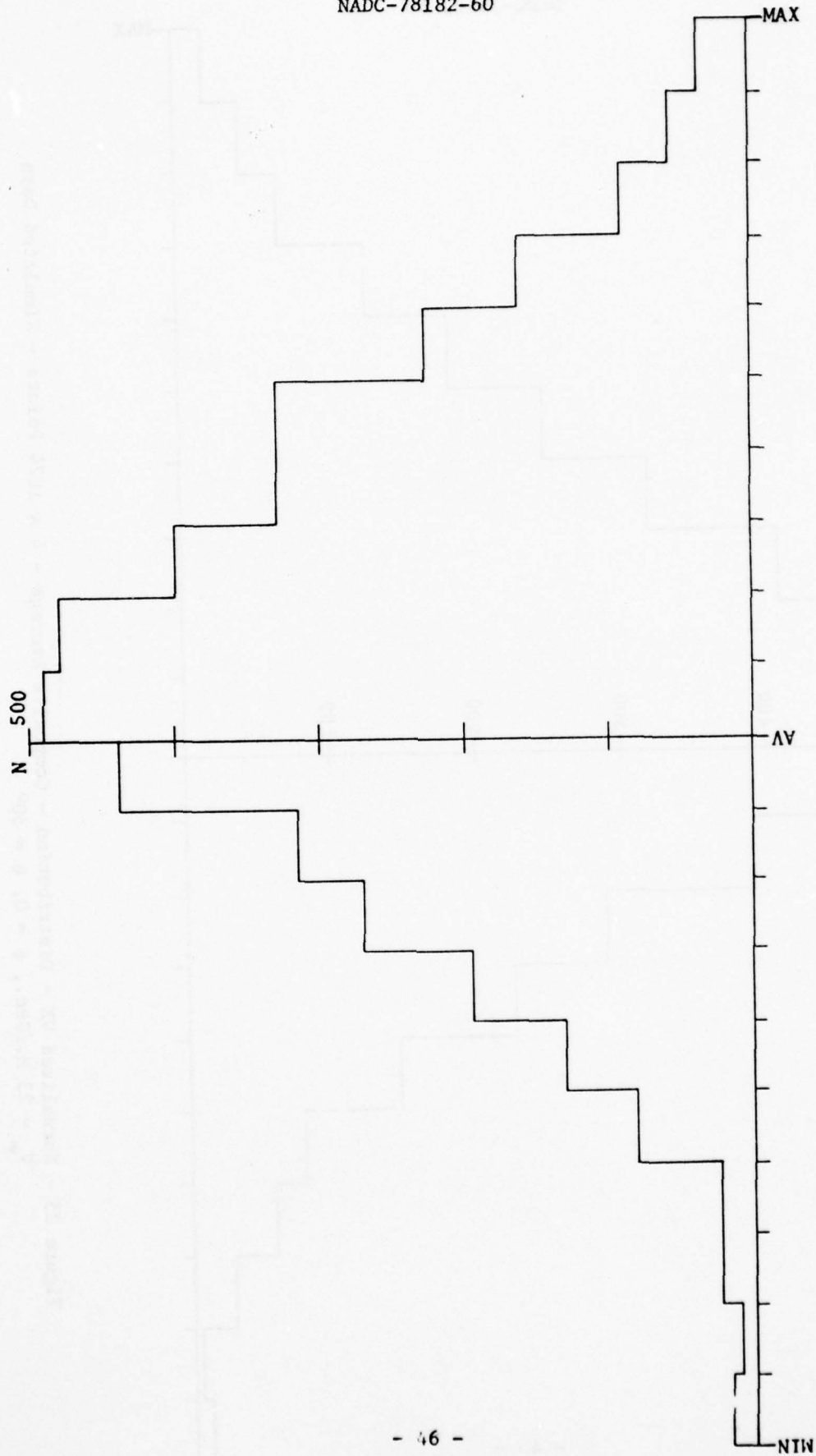


Figure 26 - Normalized VY - Distribution - Composite Average - 4 x 1024 Points - Simulated Data  
 $V_{\infty} = 23 \text{ M./Sec.}, \phi = 0, \psi = 50^{\circ}$

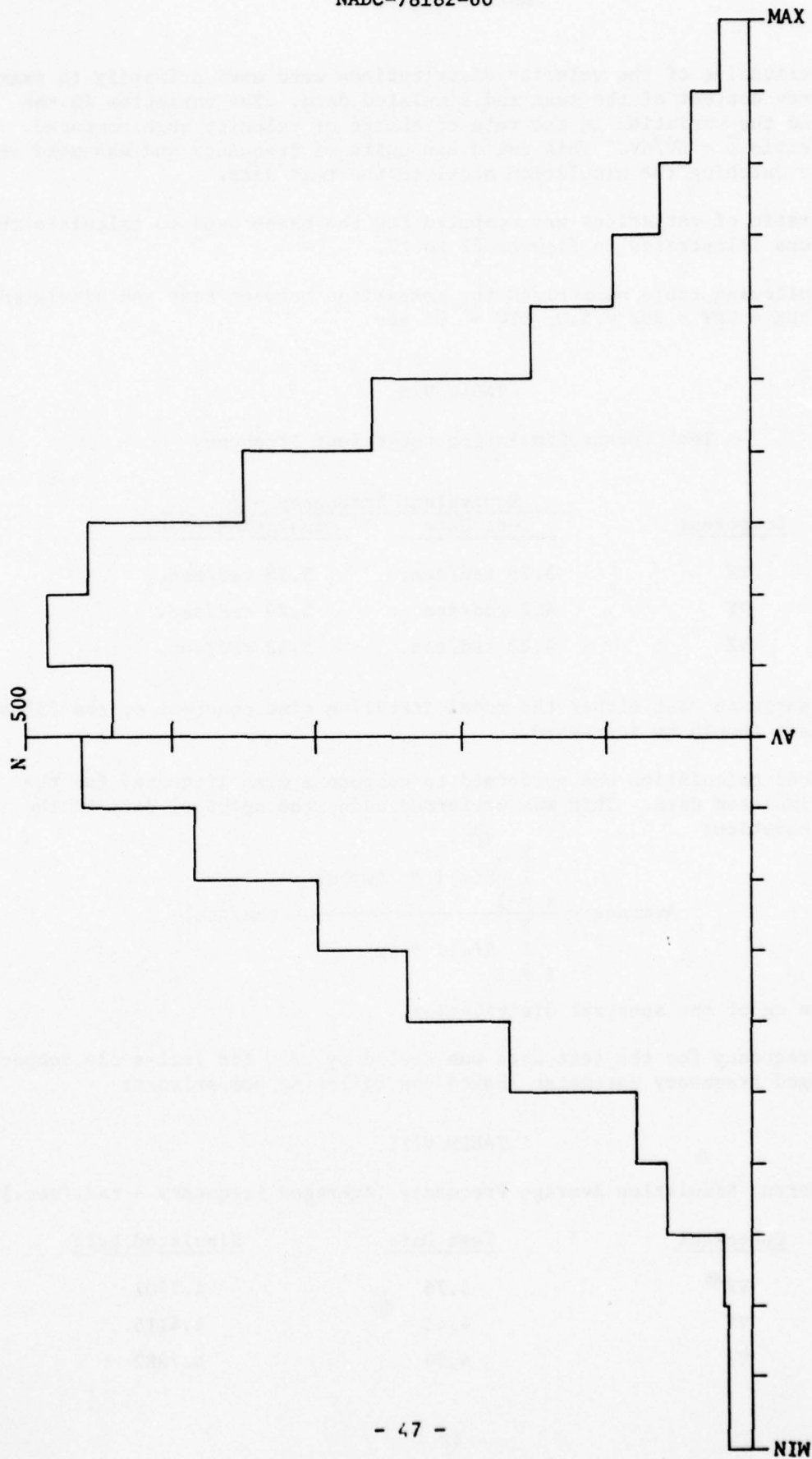


Figure 27 - Normalized VZ - Distribution - Composite Average - 4 x 1024 Points - Simulated Data  
 $V_{\infty} = 23 \text{ M./Sec.}, \phi = 0, \psi = 50^{\circ}$

The derivative of the velocity distributions were used primarily to examine the frequency content of the test and simulated data. The variation in the velocity and the variation in the rate of change of velocity were computed. Then, the ratio  $\bar{\omega} = \delta\dot{V}/\delta V$ . This ratio has units of frequency and was used as a basis for matching the simulation model to the test data.

This ratio of variations was computed for the cases used to calculate the distributions illustrated in figures 22 to 27.

The following table summarizes the comparison between test and simulated data with  $RNX = RNY = RNZ = 5.0$ ,  $DTW = .05$  sec.

TABLE VII

## Test Versus Simulation Equivalent Frequency

Component	Equivalent Frequency - $\bar{\omega}$	
	Test Data	Simulation Model
VX	3.78 rad/sec.	5.38 rad/sec.
VY	4.2 rad/sec.	5.29 rad/sec.
VZ	4.23 rad/sec.	5.52 rad/sec.

This suggests that either the model iteration time constant or the filter time constant should be increased.

A second calculation was performed to compute a mean frequency for the test and simulated data. This was performed using the spectral data in the following equation:

$$\text{Average} = \frac{\sum_{i=1}^N S(\omega)_i * \Delta\omega * \omega_i}{\sum_{i=1}^N S(\omega)_i * \Delta\omega} - \text{rad/sec.}$$

This is the cg of the spectral distribution.

The frequency for the test data was scaled by 1/50 for full-scale comparison. This averaged frequency parameter showed the following comparisons:

TABLE VIII

## Test Versus Simulation Average Frequency (Averaged Frequency - rad./sec.)

Component	Test Data	Simulated Data
VX	3.76	4.7707
VY	4.44	4.4115
VZ	4.54	4.7282

The fact that the equivalent frequency of all three components of the simulated turbulence is nearly identical in spite of differences in the filter constants suggests that the random number calling interval dominates the spectral distribution of the simulated turbulence. Therefore, the program scale factors RNX, RNY, and RNZ were adjusted from initial values of 5.0 to RNX = 7.12, RNY = 6.3, and RNZ = 6.52 based on the ratios of the equivalent frequency parameter. For these parameters, the equivalent and average frequencies compare as follows:

TABLE IX

## Test Versus Adjusted Simulation Frequency

Component	Test		Simulation	
	$\omega$	$\omega_{Av}$	$\omega$	$\omega_{Av}$
VX	3.78	3.76	4.51	3.64
VY	4.2	4.44	4.63	3.68
VZ	4.23	4.54	4.65	3.79

Given the accuracy of the analysis and the limited sample size examined, this appears to represent a near optimum match. Figure 28 illustrates the resulting spectra for a single simulation run.

## CORRELATION ANALYSIS

Certain test data points were selected for correlation analysis. The autocorrelation and cross-correlation functions were computed to determine if the gusts were purely random or if any time or space correlation existed. The equation used was

$$R_{XY}(N) = \frac{\sum_{i=N}^M (VX_i - \bar{VX}) \cdot (VY_{i-N} - \bar{VY})}{(M - N)}$$

$$\sqrt{\left( \frac{\sum_{i=N}^M (VX - \bar{VX})(VX - \bar{VX})}{M} \right) \cdot \left( \frac{\sum_{i=1}^M (VY - \bar{VY})(VY - \bar{VY})}{M} \right)}$$

As expected, the autocorrelation functions were found to have unit values for zero time shift, but were close to zero for all non-zero time shift values. This means that no significant periodicity exists in the measured data. Most of the crosscorrelation functions were found to be essentially zero for all time shift values. The condition examined was  $X = 0$ ,  $Y = 0$ ,  $\psi = 50^\circ$ ,  $\phi = 0^\circ$ ,  $H = 4.2, 7.6$  M. There was no space correlation between velocities at  $H = 4.2$  M. and  $H = 7.6$  M. above deck.

The only significant crosscorrelation uncovered was between the X and Y components at  $H = 4.2$  M. (14 ft.) This can be interpreted as a vorticity in the wind velocity about the Z axis at this point. This corresponds to an aircraft



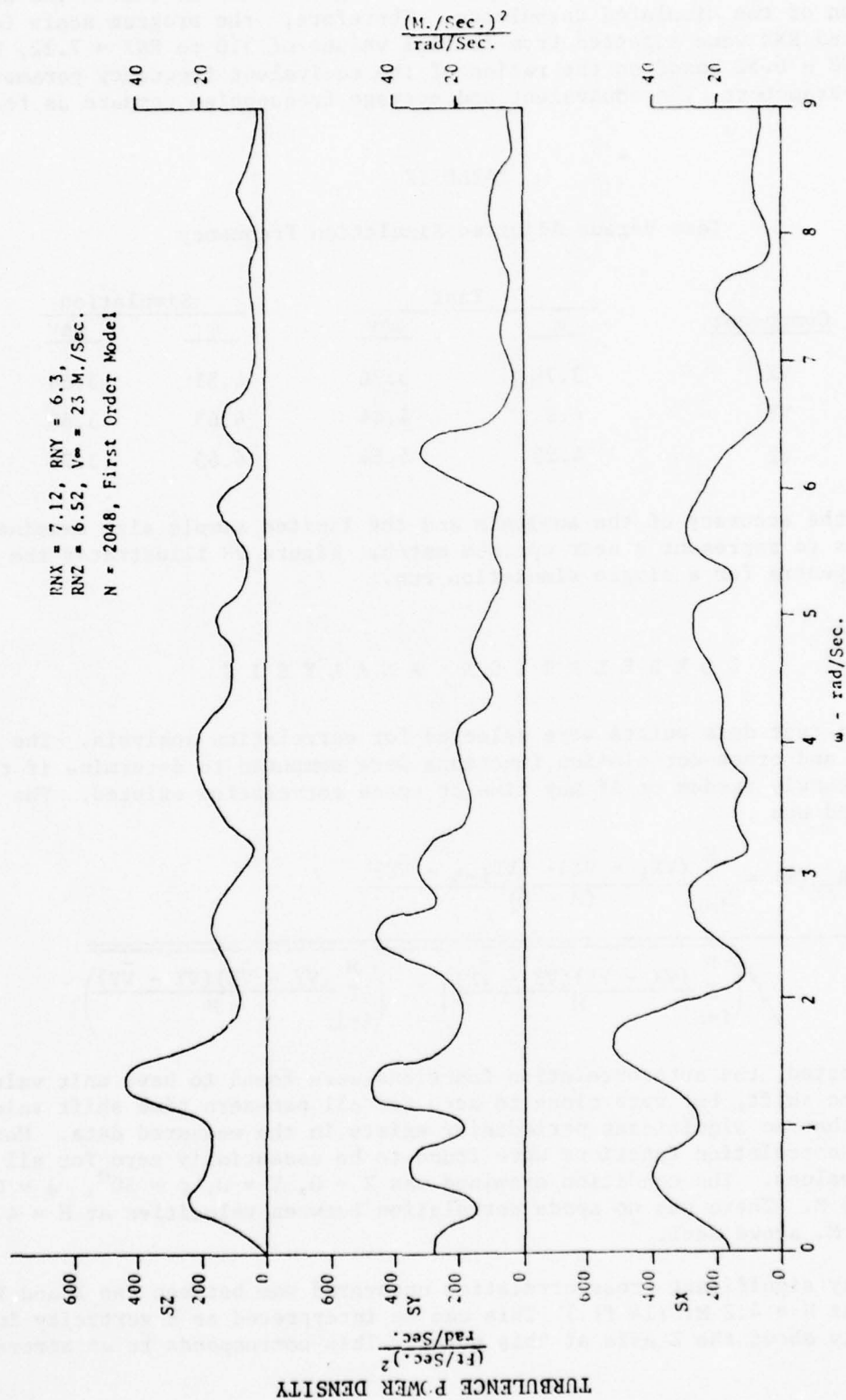


Figure 28 - Simulated Spectra With Adjusted Time Constants,  
X, Y, Z Components

TABLE X

Correlation Summary of Test Data  $V_{\infty} = 23 \text{ M./S.}$ ,  $\psi = 50^{\circ}$ ,  $\phi = 0$ Point 1:  $X = 0$ ,  $Y = 0$ ,  $Z = 4.2 \text{ M.}$ Point 2:  $X = 0$ ,  $Y = 0$ ,  $Z = 7.6 \text{ M.}$  $\Delta T = 0.0061 \text{ second model scale}$  $= 0.31 \text{ second full scale}$ 

Components		$\Delta T$ -Shift 0	1	2
$X_1$	$X_1$	1.0	0.288	-0.057
$Y_1$	$Y_1$	1.0	-0.08	-0.1
$Z_1$	$Z_1$	1.0	0.064	-0.014
$X_1$	$Y_1$	-0.544	-0.154	0.094
$Y_1$	$Z_1$	-0.05	-0.05	0.08
$X_1$	$Z_1$	-0.1	0.04	0.018
$X_2$	$X_2$	1.0	0.24	-0.01
$Y_2$	$Y_2$	1.0	-0.08	-0.002
$Z_2$	$Z_2$	0.998	-0.058	-0.206
$X_2$	$Y_2$	-0.303	-0.129	0.0409
$Y_2$	$Z_2$	0.0974	-0.081	-0.095
$X_1$	$Z_2$	-0.1	-0.001	0.08
$X_1$	$X_2$	0.237	0.16	-0.074
$Y_1$	$Y_2$	0.284	0.0107	-0.074
$Z_1$	$Z_2$	0.143	0.0446	0.0455
$X_1$	$Y_2$	-0.15	-0.076	-0.076
$Y_1$	$Z_2$	0.075	-0.174	-0.0216
$X_1$	$Z_2$	-0.096	0.121	0.171

yaw rate. It is not clear whether this has a significant effect on aircraft motion so that provision for including this effect should be added to the model. The effect does not appear strong enough to justify additional complexity in the model.

# S E N S I T I V I T Y   A N A L Y S I S   O F   T H E   E F F E C T S O F   T H E   A S S U M E D   F O R M   O F   T H E T U R B U L E N C E   S P E C T R U M

Evaluation of the test data and the various model algorithms do not lead to an exact and definite conclusion regarding the values of the model parameters.

A question arises as to whether the exact turbulence spectrum must be duplicated by the model in order to yield a useful analytical tool. In an attempt to answer this question, the closed-loop pitch response to horizontal gusts was computed using the original second-order model format. RMS pitch response was computed for a range of spectral gust frequency model parameters. A closed-loop pitch transfer function was calculated for a representative VSTOL (AV8A) at a 62 M./S. (120 knot) transition condition. The pitch loop was closed with a simple gain pitch SAS and pilot model incorporating pitch attitude and pitch rate feedback through a delay.

The closed-loop pitch to horizontal gust transfer function was calculated and the RMS gust response was then determined using the equation:

$$\delta\theta^2 = \frac{1}{2\pi} \int_{-\infty}^{\infty} \left| \frac{N_{ug}}{D'} \right|^2 \phi_{ugust}(j\omega) \cdot d\omega$$

where  $\frac{N_{ug}}{D'}$  is the closed-loop transfer function

and  $\phi_{ugust}$  is the gust power spectrum.

The gust power spectrum is developed by squaring the magnitude of the gust transfer function as follows

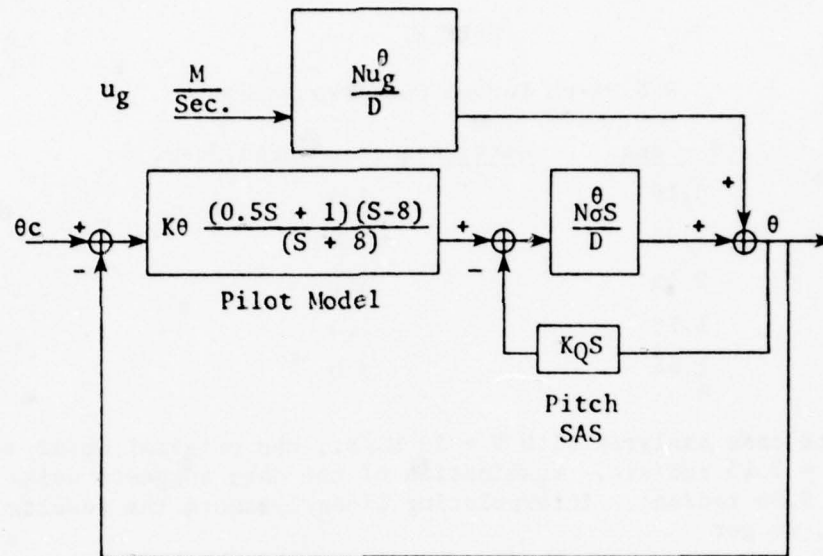
$$\frac{\text{Gust Velocity}}{\text{Random Input}}(S) = \frac{\delta \cdot 2 \cdot \sqrt{\zeta\omega^3}}{S^2 + 2\zeta\omega + \omega^2}$$

$$\phi_{gust}(S) = \frac{\delta^2 4 \zeta\omega^3}{(S^2 + 2\zeta\omega S + \omega^2)(S^2 - 2\zeta\omega S + \omega^2)}$$

The system block diagram is illustrated by figure 29.

The closed-loop gust transfer function then becomes

$$\frac{\theta}{ug}(S) = \frac{(3.28)(S + 8)(-0.002832S^2 + 0.0005604S + 0.0003527)}{(S^5 + 7.046S^4 + 17.9199S^3 + 27.827S^2 + 16.692S + 2.8202)}$$



$$\theta \text{ NoS} = -8.057 S^2 - 5.218 S - .823 \text{ Rad./rad.}$$

$$D = S^4 + 0.7382 S^3 - 0.9896 S^2 - 0.2859 S + 0.006864$$

$$\theta \text{ Nu}_g = 3.28 \times (-0.002832 S^2 + 0.0005604 S + 0.0003527) \frac{\text{Rad}}{\text{M./Sec.}}$$

$$K_\theta = 0.42 \text{ rad/rad.}$$

$$K_Q = -0.49 \text{ rad/rad/sec.}$$

Figure 29 - Closed-Loop Gust Response Transfer Function



RMS gust responses were calculated for the following parameters

$$\sigma_{ug} = 7.1 \text{ M./S. (23.3 ft/sec.)}, \quad \zeta = 0.4, \quad \omega = 1.4, 2, 3, 5, \text{ and } 7 \text{ rad/sec.}$$

The results follow:

TABLE XI

RMS Pitch Versus Gust Frequency

$\sigma\theta$ - deg.	Gust Frequency - rad./sec.
3.16	1.4
2.95	2.0
2.43	3.0
1.76	5.0
1.44	7.0

For the data case analyzed with  $V = 23 \text{ M./S.}$ , the original model uses  $\omega_x = 1.9 \times V/59 = 2.45 \text{ rad/sec.}$  Examination of the data suggests using  $\omega_x = 3 \times V/18 = 3.86 \text{ rad/sec.}$  Interpolating linearly among the results from the sample case, we get

$\sigma\theta$ - deg.	$\omega$ - rad./sec.
2.72	2.45
2.14	3.86

This corresponds to a 21-percent difference in sigma values for a 64-percent variation in frequency.

Thus, the frequency of the gust model does significantly affect the aircraft response for constant RMS gusts. However, a gust model which predicts gust response to within 10 percent would probably be a satisfactory tool. Thus, the assumed filter algorithm is not extremely critical. The sensitivity shown by the sample indicate that it would be sufficient to define the frequency parameter to within 25 percent of its true value. In contrast, the aircraft response varies directly with RMS gust amplitude. Thus, it is most important to accurately match the gust RMS amplitude.

#### TIME HISTORY COMPARISON

One final comparison of the simulated and measured turbulence was made by plotting the velocity time histories of the three velocity components. The case selected was

$$\begin{aligned} X &= 0 & V_{\infty} &= 23 \text{ M./S.} \\ Y &= 0 & \psi &= 50^\circ \\ Z &= 4.2 \text{ M.} & \phi &= 0 \end{aligned}$$

The experimental data was recorded at a time interval of 0.0061 second. This value was scaled up by a factor of 50 to yield a plot scale interval of 0.31 second. Simulated data points were calculated at a 0.05-second time interval. Because of the measurement interval, the bandwidth of the experimental data was limited to 10.13 rad./sec. Thus, higher frequency oscillations might have been present, but they could not be detected.

The simulated and test velocity sequences were compared on the basis of maximum, minimum, mean, and variance values as well as a qualitative comparison of the shapes of the plotted sequences. Figures 30 to 32 illustrate the relationships for the three velocity components. The mean and variance values compare well for all three components. The maximum and minimum values seem consistent in all cases with the magnitudes of the mean and variances.

A qualitative comparison of the number of local maxima and minima in a 10-second period show that the frequency content of the simulated and measured velocities compare satisfactorily.

## R E S U L T S   A N D   C O N C L U S I O N S

The CVA turbulence model contained herein remains basically unchanged from the version described in reference (c) as a result of analysis performed for this study. It is suitable for simulation of aft approaches and forward takeoffs of conventional and VSTOL aircraft.

The FF 1052 turbulence model is designed to permit VSTOL takeoff and landings from any angle. Wind conditions are currently limited to relative wind angles of 0, 30, and 50 degrees at total velocities of 10, 18, and 23 M./S. (20, 35, and 45 knots).

After considerable iteration, the FF1052 turbulence model structure was fixed with these features:

1. Exponential and linear extrapolation of tabulated mean and variance velocity values beyond the region of measured data.
2. First-order exponential filtering of random number inputs using inverse time constants that decrease linearly with range downstream.
3. The random number subroutine used to generate the three gust velocities are called less frequently than the basic simulation loop time, and the resultant random number sequences are linearly interpolated.
4. The random number update interval is selected to match test data spectral distributions.
5. The filter time constants vary inversely with freestream steady velocity.
6. The frequency content of the three velocity components display different characteristics with the horizontal component having a lower frequency spectrum than the Y and Z components.

NADC-78182-60

M./Sec.

Simulation Test Sample

V	40.7	39.3 Ft/Sec.
$\sigma$	24.3	23.3 Ft/Sec.
VMAX	92.6	93.9 Ft/Sec.
VMIN	-30.4	-22.4 Ft/Sec.

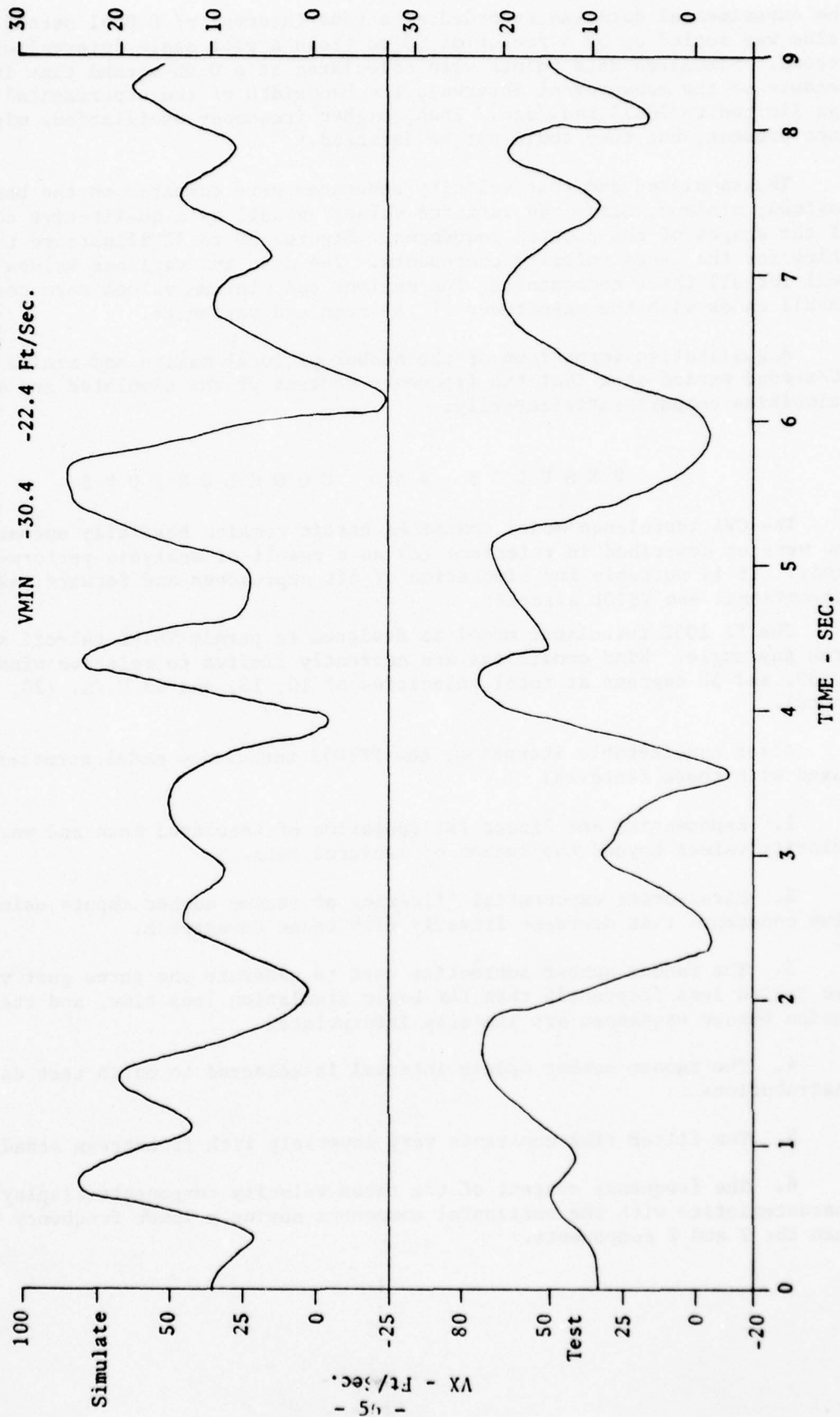


Figure 30 - X - Component Simulated and Measured Turbulence

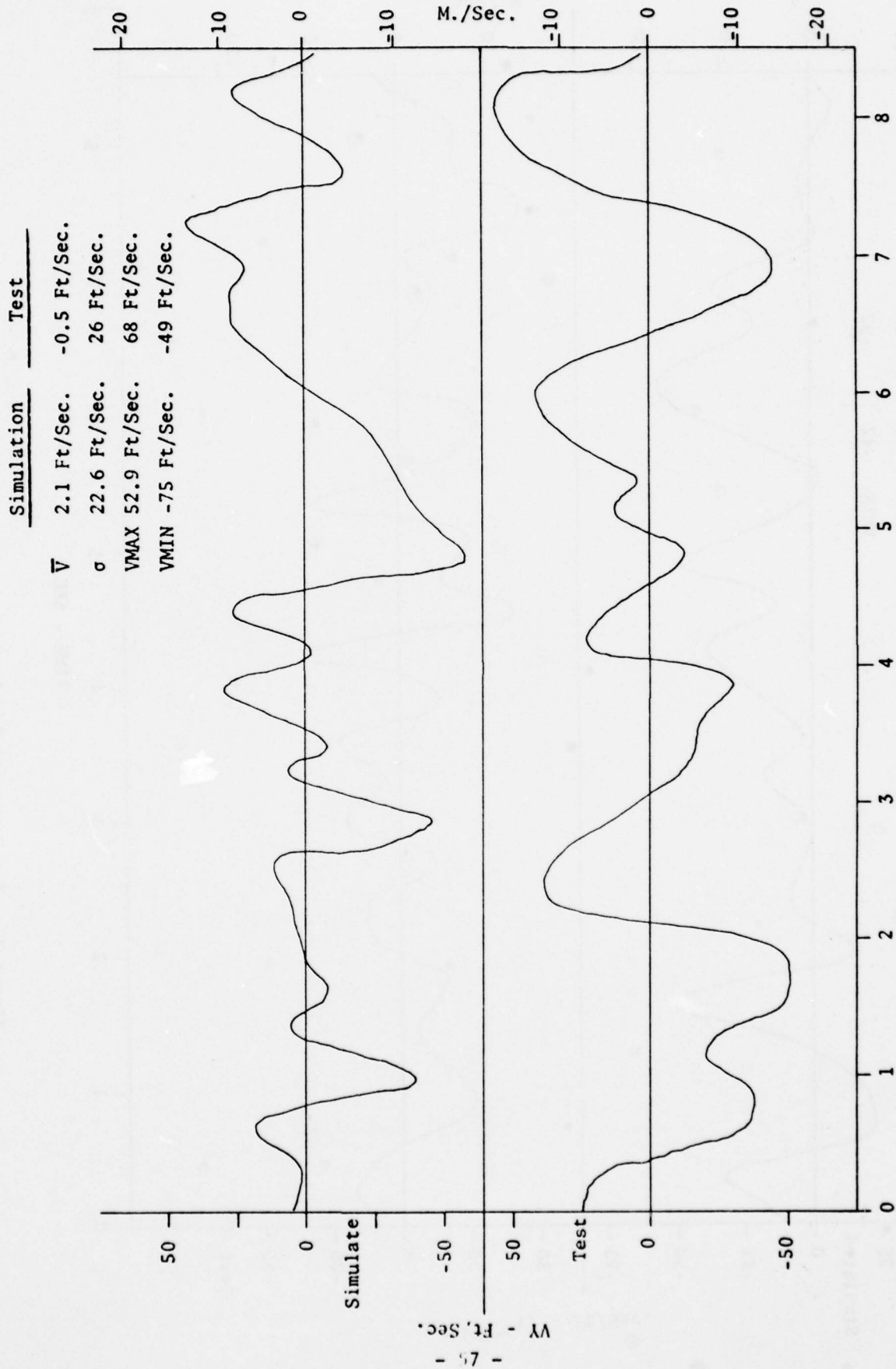


Figure 31 - Y - Component Simulated and Measured Turbulence



	Simulation	Test
$\bar{V}$	-11.7	-10.45
$\sigma$	20.01	20.48
VMAX	65	92
VMIN	-42	-52

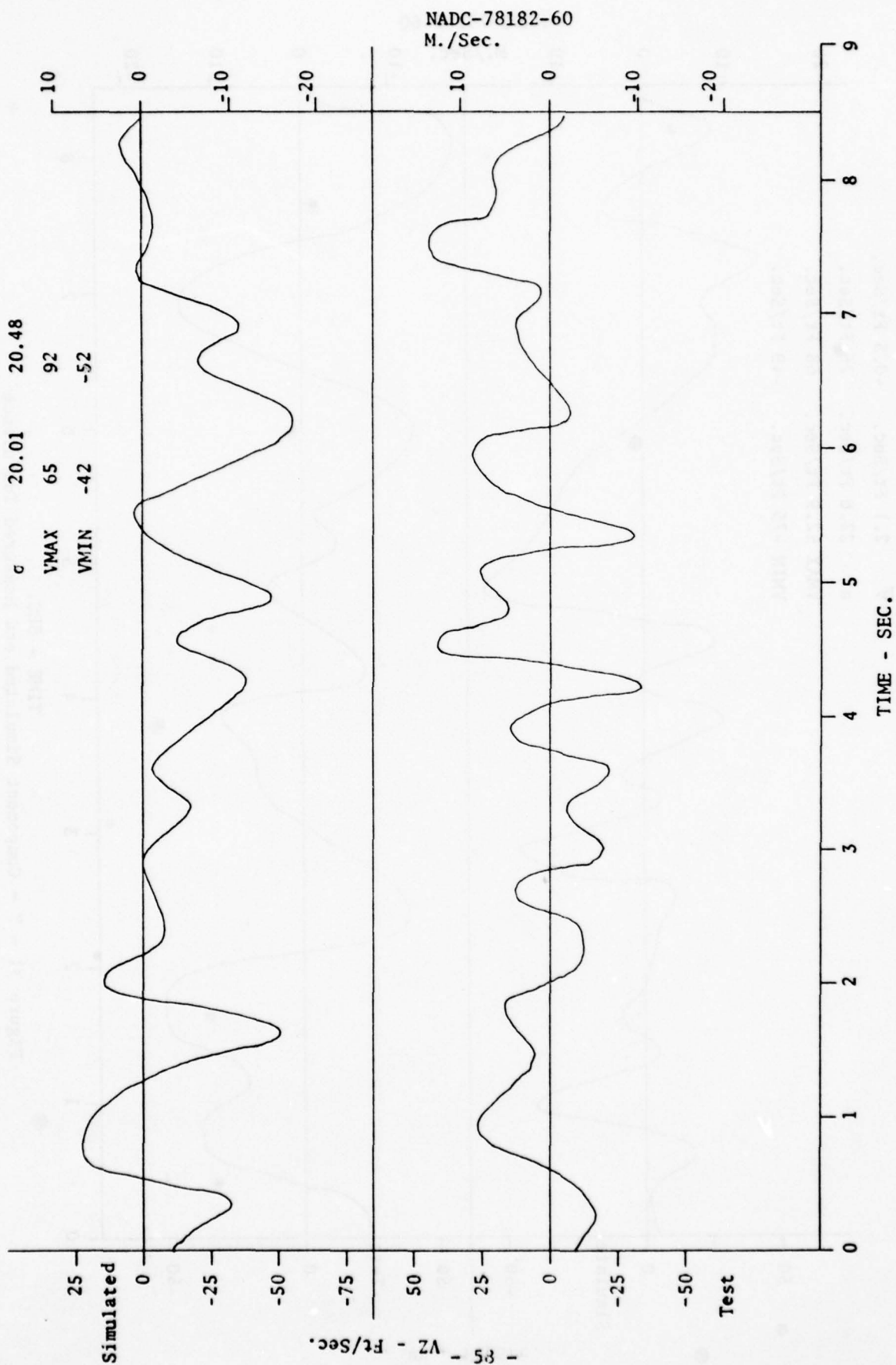


Figure 32 - Z - Component Simulated and Measured Turbulence

7. Although some cross-correlation between velocity components was observed in the measured data, it does not appear significant enough to include in the simulation model.

8. For 45-knot wind and the aircraft located over the deck, the filter frequency parameters were selected with the following values:

<u>Component</u>	<u>Frequency - rad./sec.</u>
X	8.17
Y	10.41
Z	10.00

9. These frequencies decrease linearly to  $X = 58$  M. (190 ft.) where the filter frequencies become

<u>Component</u>	<u>Frequency - rad./sec.</u>
X	1.58
Y	3.0
Z	2.88

10. The test simulation was set up to update wind velocity intervals at 0.05 second intervals. The random number sequences were updated at the following multiple interval size:

<u>Component</u>	<u>Update Interval - Sec.</u>
X	$0.05 \times 7.12 = 0.356$
Y	$0.05 \times 6.3 = 0.315$
Z	$0.05 \times 6.52 = 0.326$

11. Examination of the experimental data shows that the turbulence velocities reasonably approximated a Gaussian distribution. However, the distributions show some flattening and less peaking around the mean than do ideal theoretical distributions.

12. Analysis indicates that it is more important to exactly match the mean and variance of the turbulence velocities than to exactly match the spectral shape.

#### R E C O M M E N D A T I O N S

Because of differences in digital computers and particularly in random number generator subroutines, prospective users of these computer subroutines should follow the following precautions:

1. Run the model repeatedly for at least 100 seconds of simulation time at a fixed location in space.
2. Compare the mean and variance of the simulated data with that of the input tables corresponding to the selected point.
3. Compute the Fourier transform of the simulated turbulence and compare these with the spectral plots contained in this report.
4. Adjust the filter gains, time constants, and number update ratios RNX, RNY, RNZ if necessary.
5. The FF 1052 model should be tested on a moving base piloted simulation to get pilot confirmation of its validity.

## LIST OF SYMBOLS

CVA	Attack Aircraft Carrier
PSIS	Ship Heading - Rad.
PSIREL	Wind Over Deck Relative Angle - Rad.
Rxy	Cross Correlation Function
S	Laplace Operator - 1/Sec.
Sx, y, z	Power Spectral Density
STO	Short Take Off
u	Longitudinal Wind Velocity - M./Sec.
ug	Longitudinal Gust Velocity - M./Sec.
V	Lateral Wind Velocity - M./Sec.
VG	Lateral Gust Velocity - M./Sec.
v <sub>0</sub>	Trim Aircraft Velocity - M./Sec.
VEWBIC	East Component of Natural Wind - M./Sec.
VNWBIC	North Component of Natural Wind - M./Sec.
VW	Total Wind Over Deck - M./Sec.
VS	Ship Speed - M./Sec.
VX	X Component of Wind Velocity - M./Sec.
VY	Y Component of Wind Velocity - M./Sec.
VZ	Z Component of Wind Velocity - M./Sec.
V <sub>∞</sub>	Free Stream Wind Velocity - M./Sec.
W	Lateral Wind Velocity - M./Sec.
X	Aircraft Position Aft of Ship - M.
Y	Aircraft Position Left or Right of Ship Centerline - M.
Z	Aircraft Altitude Above Touchdown Point - M.
α	Aircraft Angle of Attack - Deg.
$\frac{\Delta u}{VS}$	Normalized Horizontal Velocity Increment
$\frac{\Delta w}{VS}$	Normalized Down Wash Velocity Increment
θ	Aircraft Pitch Attitude - Deg.
σ	Root - Mean Squared Value
τ	Gust Time Constant - Sec.
φ	Ship Roll Angle - Deg.



$\Phi \frac{\Delta u}{V_0}$	Horizontal Gust Power Spectrum - (ft/sec.) <sup>2</sup> /(rad/sec.)
$\Phi \frac{\Delta v}{V_0}$	Lateral Gust Power Spectrum - (ft/sec.) <sup>2</sup> /(rad/sec.)
$\Phi \frac{\Delta w}{V_0}$	Vertical Gust Power Spectrum - (ft/sec.) <sup>2</sup> /(rad/sec.)
$\psi$	Ship Heading Angle - Deg.

#### REFERENCES

- a. A Computerized VSTOL/Small Platform Landing Dynamics Investigation Model, Ronald L. Nave, Report No. NADC-77024-30, Naval Air Development Center, Sept 1977.
- b. Analysis and Comparison of Carrier Air Wakes, David H. Weir, Report No. TR-NO. 158-1, Systems Technology Inc., April 1966.
- c. A Simulator Comparison of an Integrated, Direct-Lift-Control Automatic Carrier Landing System With a Conventional Carrier Landing System, Robert L. Fortenbaugh, Report No. NADC-72210 - VT, Naval Air Development Center, 3 April 1973.
- d. Investigation to Study the Aerodynamic Ship Wake Turbulence Generated by a FF 1052 Frigate, Theodore S. Garnett, Jr., Contract No. N00019-75-C-0493 Boeing Vertol Company, December 1976.
- e. A Math Model for the Air Wake of a DE-1052 Class Ship, R. L. Fortenbaugh, Report No. 2-53300/7R-3397, Vought Corporation, 13 May 1977.
- f. MIL-F-8785 (ASG), Military Specification, Flying Qualities of Piloted Airplanes.
- g. Introduction to the Statistical Dynamics of Automatic Control Systems, V. V. Solodovnikov, Dover Publishing.
- h. MIL SPEC AR-40A, Automatic Carrier Landing System Airborne Subsystem, General Requirements for.
- i. A Wind Tunnel Air Wake Survey of a 1/144 Scale Model Aircraft Carrier With Deck and Island Modifications, Martin L. Cook, Report No. 1805, Naval Ship Research and Development Center, March 1967.

A P P E N D I X   A

Listing of CVA Turbulence Model

## CWINDC

## SUBROUTINE WINDC

COMMON/XFLUAT/A(500)/FIXFD/IA(200)

COMMON/CHT/9(200)/IC5F/IR(50)

COMMON/GAINI/GAI(100)

EQUIVALENCE(T11,A(16)),(T21,A(17)),(T31,A(18))

1,(T12,A(19)),(T22,A(20)),(T32,A(21))

2,(T13,A(22)),(T23,A(23)),(T33,A(24))

EQUIVALENCE(VNTURH,A(419)),(VETUR9,A(420)),(VDTURH,A(421))

EQUIVALENCE(A(61),UTURH)

EQUIVALENCE(A(62),VTURH)

EQUIVALENCE(A(63),WTURH)

EQUIVALENCE(A(70),VKW)

EQUIVALENCE(A(164),DT)

EQUIVALENCE(A(239),VEGIC)

EQUIVALENCE(XCG,A(174)),(YCG,A(175)),(STMETR,A(114)),(CTHETR,

1 A(115))

EQUIVALENCE(ALT,A(83))

EQUIVALENCE(A(303),TIME)

EQUIVALENCE(IA(1),IMODE)

EQUIVALENCE(IONCE,IR(16))

EQUIVALENCE(VS,A(30))

EQUIVALENCE(PH1P,B(112))

EQUIVALENCE(OMEGH,R(111))

EQUIVALENCE(UGST,R(153)),(VGST,B(154)),(WGST,B(155))

EQUIVALENCE(XFRZ,B(156)),(SWRSW,B(157)),(SUBSW,B(154))

EQUIVALENCE(TH(16),IPTICH)

EQUIVALENCE(PITCHM,B(110))

EQUIVALENCE(NCHK,IR(22))

EQUIVALENCE(R(95),X25), (R(94),X15)

EQUIVALENCE(ILHURH,IR(25))

EQUIVALENCE(THFRZ,IR(24)),(IWIND,IR(20)),(ILTURH,IR(21))

EQUIVALENCE(GA(30),GR(1))

EQUIVALENCE(HIS,B(100))

EQUIVALENCE(IDIST,IA(50))

EQUIVALENCE(FRTN,H(194)),(FRTD,B(195)),(FRTD,B(196)),(VMN,B(197))

EQUIVALENCE(VME,B(198)),(VMD,R(199)),(TOTURH,R(200))

DIMENSION PD(7),GR(7)

DIMENSION ROY(7),ROYI(7),IRDST(7),IRDSTI(7,10)

DIMENSION PDXT(7)

DATA SWBSW/1.,SUBSW/1./

DATA TIM370./

DATA(GR(1),I=1,7)/6.,6.,125.,125.,25.,3.,3./

DATA RIA7/1/

DATA PI/3.1415927

DATA FC/5./

DATA (IRDST(1), I=1,7)/1,3,5,7,9,11,13/

DATA IUR7/0.,IVMT/0.,IWB7/0/

DATA ZRI7/0017,ZR2/1.57,YRI7/0017,YR2/1.57

DATA XFRZ/1500./

DATA ((IRCSI(I,J), I=1,7),J=1,10)/1,3,5,7,9,11,13,13,13,5,7,9,11,

1 11,13,1,3,5,7,9,9,11,13,1,3,5,7,9,11,13,1,3, 5,5,7,9,11,

1 13,1,3,3, 5,7,9,11,13,1,15,17,19,21,23,25,27,27,15,17,19,21,

3 23,25,25,27,15,17,19,21,23/

1F(1015CT)7,7,30

SUBROUTINE MINIC CDC 66 FTN V3.0-2380 OPT=1 7-704/11. 16.03.42. PAGE 2

7 IF (IMODE) 2,3,4

2 CONTINUE

URIS=0.

WPLS=0.

WRSS=0.

WRSS=0.

PITCHM1=PITCHM/57.3

DT2=DT

VO=VELOC\*1.689

IF (VO.LT.60) VO=60.

RK10=SQRT(3.14159\*500.)\*.003

RK11=SQRT(5900.\*3.14159)\*3.\*VO/400000.

S110=VO/1000.

S210=3.\*VO/400.

Z01=EXP(S110\*DT)

Z02=EXP(S210\*DT)

Z11=-1./((S110-S210)\*RK10\*(1.-Z01))

Z12=-1./((S110-S210)\*RK10\*(1.-Z02))

Z13=-1./((S210-S110)\*RK11\*(1.-Z01)/S110)

Z14=-1./((S210-S110)\*RK11\*(1.-Z02)/S210)

Z011=EXP(-VO/100.\*DT2)

Z111=SQRT(71.63\*3.14159)/100.\*(1.-Z0111)

Z0112=EXP(-VO/100.\*DT2)

Z1112=SQRT(200.\*3.14159)/100.\*(1.-Z0112)

IX=2\*\*24-3

DO 10 I=1,7

RDX(I)=0.

ROY(I)=0.

IF (IONCE.GT.0) IMDST(1)=IMDSI(1,IONCE)

00010

CONTINUE

PN1=.044\*SQRT(PI)

NC=2.\*FC\*PI

IF (VELOC.NE.VEOLCP) IZX=1

VEOLCP=VEOLC

3 CONTINUE

WRSS=0.

UPSS=0.

UP25=0.

PDSP=0.

PD4=0.

PD3=0.

UG=0.

WG=0.

WR25=0.

UR255=0.

YR54=0.

ZR54=0.

UGSA=0.

WGS4=0.

WGS4=0.

UP21A=0.

WR21A=0.

WR255=0.

UGS=0.

VG1=0.



CDC 6600 FTN V3.0-P380 OPT=1 78/04/11. 16.03.42.

## SUBROUTINE WINDC

```

115  VG2=0.
    VG3=0.
    VG4=0.
    VGS=0.
    MGS=0.
    UGSS=0.
    VGSS=0.
    MGS=0.
    ZRS=0.
    YRS=0.
    ZRSS=0.
    YRSS=0.
    FACZ=EXP((-ABS(YCG)/100.))
    ALT1=HIS+50.-XCG*.1
    FACZ=1.
    IF (ALT.GT.ALT1) FACZ=EXP((ALT1-ALT)/50.)
    FACZ=FACZ*FACZ
    XD=XCG
    UTURN=-VS*SWRSS*FACW*TAB1(XD,0.,0.,68.1)
    WTURN=-VS*SWRSS*FACW*TAB1(XD,0.,0.,69.1)
    VTURB=C.
    TIM3=0.
    ZR=0.
    YR=0.
    RETURN
135  CONTINUE
    IF (IND.EQ.0) RETURN
    IF (CHK.GT.0) RETURN
    FACZ=EXP((-ABS(YCG)/100.))
    ALT1=HIS+50.-XCG*.1
    FACZ=1.
    IF (ALT.GT.ALT1) FACZ=EXP((ALT1-ALT)/50.)
    FACZ=FACZ*FACZ
    XD=XCG
    UHSS1=-VS*TAB1(XD,0.,0.,68.1)
    UHSS=UHSS1*SWRSS*FACW
    IF (ILAURB) 21,21,20
    WHSS1=-VS*TAB1(XD,0.,0.,69.1)
    WHSS=WHSS1*SWRSS*FACW
    GO TO 22
00021 WHSS1=-VS*TAB1(XD,0.,0.,70.1)
    WHSS=WHSS1*SWRSS*FACW
00020 WHSS1=-VS*TAB1(XD,0.,0.,70.1)
    WHSS=WHSS1*SWRSS*FACW
00022 CONTINUE
    VSD=1./(.H5*VS)
    CTERM=COS(4*EGP*(1.+(VRW-VS)*VSD)*TIME+XD*VSD*PHIP-1.57))*JPITCH
    UH1K=2.22+.0309*XD
    IF (UH1K.LT.0) UH1K=0.
    UR1=PITCHM1*VS*UH1K*CTERM*FACW
    IF (XCG.LT.-2236.) UB1=0.
    IF (XCG.GT.X25) UH1=0.
    WH1K=4.98+.0014*XD
    IF (WH1K.LE.0) WH1K=0.
    WB1=PITCHM1*VS*WB1K*CTERM*FACW
    IF (XCG.LT.-2536.) WH1=0.

```

## SUBROUTINE WINDC

```
IF(XCG.GT.X25) WB1=0.
```

```
SINWCT=SIN(WC*TIME)
```

```
DO 1 I=1,7
```

```
CALL RAND(IRDS(I),IX,I,1,U)
```

```
RDX(I)=U
```

```
RDY(I)=RDX(I)*RDYI(I)
```

```
RDYI(I)=RDYI(I)*RDA*RDY(I)*DT
```

```
RD(I)=RDYI(I)*SINWCT
```

```
CONTINUE
```

```
1 SUB2=TAB1(XD,0,0,0,71,1)
```

```
TUB2=TAB1(XD,0,0,0,72,1)
```

```
DTOT=DT/TUB2
```

```
UR2=UR2P*(1.-DTOT)*VS+SUB2*1.41*SQRT(TUB2)*DTOT*RD(1)*GR(1)
```

```
UR2P=UR2
```

```
180 DTOTW=DT/3.33
```

```
WH2=WH2P*(1.-DTOTW)*.035*VS*2.58*DTOTW*RD(2)*GR(2)
```

```
IF(XD.LT.-2540.1) WB2=0.
```

```
IF(XD.GT.X15) WH2=0.
```

```
WH2P=WH2
```

```
185 VYBR=WB2
```

```
VXBR=UBSS*UA1*UH2
```

```
VDR=WBSS*AB1*WD2
```

```
VNRR=VXBR*CTHETM-VYBR*STHETR
```

```
VEAR=VYBR*CTHETR-VXBR*STHETR
```

```
190 UHT=T11*VNRR+T12*VEAR+T13*VDBR
```

```
VBT=T21*VNRR+T22*VEAR+T23*VDBR
```

```
UHT=T31*VNRR+T32*VEAR+T33*VDBR
```

```
IF(UHT.EQ.1) UBT=0.
```

```
IF(UHT.EQ.1) VBT=0.
```

```
IF(UHT.EQ.1) WBT=0.
```

```
WG=Z0111*WG*Z111*RD3
```

```
195 RD3=RD(3)*GR(3)
```

```
UG=Z0112*UG*Z112*RD4
```

```
RD4=RD(4)*GR(4)
```

```
200 VGL=Z01*VGL*Z11*RD5P
```

```
VG2=Z02*VG2*Z12*RD5P
```

```
VG3=Z03*VG3*Z13*RD5P
```

```
VG4=Z04*VG4*Z14*RD5P
```

```
RD5P=RD(5)*GR(5)
```

```
VG=VGL*VG2*VG3*VG4
```

```
IF(ULTURB.EQ.1) GO TO 5
```

```
UG=0.0
```

```
VG=0.
```

```
WG=0.
```

```
210 CONTINUE
```

```
5 VTURB=URT*UG
```

```
VTURB=VBT*VG
```

```
WTURB=WBT*WG
```

```
215 ZP=RN1*RD(6)*GR(6)*17R1*ABS(XD)*2R2)
```

```
YR=RN1*RD(7)*GR(7)*17R1*ABS(XD)*YR2)
```

```
UH1S=UH1S*UA1
```

```
WH1S=WH1S*WB1
```

```
UH2S=UH2S*UH2
```

```
WH2S=WH2S*WB2
```

```
UB1SS=UB1SS*DT*UG1**2
```

## SUBROUTINE WINDC

```

225      WRISS=WRISS+DT*WB1**2
      UR2SS=UR2SS+DT*UR2**2
      WR2SS=WR2SS+DT*WR2**2
      UGS=UGS+UG
      VGS=VGS+VG
      WGS=WGS+WG
      UGSS=UGSS+DT*UG**2
      VGSS=VGSS+DT*VG**2
      WGS=UGSS+DT*WG**2
      ZRS=ZRS+ZK
      YRS=YRS+YR
      ZPSS=ZPSS+DT*ZR**2
      YPSS=YRSS+DT*YR**2
      IF (TIME) 30,30,25
      CONTINUE
      PAV=TIME/DT
      UB1A=UB1A/PAV
      WRI1=WRI1/PAV
      YRSA=YRSA/PAV
      ZRSA=ZRSA/PAV
      UGSA=UGS/PAV
      VGS4=VGS/PAV
      WGS4=WGS/PAV
      UR2TA=UR2S/PAV
      WR2TA=WR2S/PAV
      UR2ST=UR2SS/TIME
      WR2ST=WR2SS/TIME
      UGST=UGSS/TIME
      VGST=VGSS/TIME
      WGST=WGSS/TIME
      ZPST=ZPSS/TIME
      YPST=YRSS/TIME
      UR1ST=UR1SS/TIME
      WR1ST=WRISS/TIME
      CONTINUE
235      00025 IF (DISCT) 37,37,33
      CONTINUE
      FRT=AMAX1(FRTN,FRTD)
      PHASE=FRT*(TIME-TOTURB)
      IF (PHASE-6.28) 34,34,36
      34 IF (TIME-TOTURB) 36,36,35
      35 VNTURH=.5*VMD*(1.-COS(FRTN*(TIME-TOTURB)))
      VETURH=.5*VME*(1.-COS(FRTD*(TIME-TOTURB)))
      TOTURB=.5*VMD*(1.-COS(FRTD*(TIME-TOTURB)))
      GO TO 37
      36 VNTURB=0.
      VETURH=0.
      VOTURH=0.
      37 CONTINUE
      RETURN
      END

```

## SUBROUTINE WINDC

## SYMBOLIC REFERENCE MAP

ENTRY POINTS	DEF LINE	REFERENCES	137	138	270
1	2	135	137	138	270
WINDC					
VARIABLES	SN	TYPE	RELOCATION		
0 A			ARRAY	XFLOAT	
122 ALT	REAL				
1143 ALTI	REAL				
0 B	REAL				
115 CTEOM	REAL				
152 CTHETR	REAL				
247 DT	REAL				
1155 OTOT	REAL				
1170 OTOTW	REAL				
1055 DT2	REAL				
1145 FACW	REAL				
1142 FACY	REAL				
114 FACZ	REAL				
761 FC	REAL				
1216 FRT	REAL				
303 FRTN	REAL				
302 FRTN	REAL				
301 FRTN	REAL				
0 GA	REAL				
35 GP	REAL				
143 HIS	REAL				
1076 I	INTEGER				
0 IA	INTEGER				
0 IB	INTEGER				
27 IFRZ	INTEGER				
51 IDISCT	INTEGER				
30 ILHURR	INTEGER				
24 ILTURR	INTEGER				
0 IMODF	INTEGER				
17 IONCE	INTEGER				
21 IPITCH	INTEGER				
1234 IPOST	INTEGER				
1245 IPOST	INTEGER				
752 IUBT	INTEGER				
753 IUBT	INTEGER				
754 IUBT	INTEGER				
23 IWINO	INTEGER				
1075 IXX	INTEGER				
1112 IXX	INTEGER				
25 NCHK	INTEGER				
156 OMEGP	REAL				



NADC-78182-60

[illegible]

CUC 6600 FTM V3.0-0-PJ80 OPT=1 7/14/04/11. 16.03.42.

## SUBROUTINE WINDC

VARIABLES	SN	TYPE	RELOCATION	REFS	178	DEFINED	179	218	219	222
1167 UB2P	REAL			REFS	218	244	DEFINED	93		
1168 UB2S	REAL			REFS	222	246	DEFINED	100		
1169 UB2SS	REAL			DEFINED	246					
1210 UB2ST	REAL			DEFINED	106	244				
1121 UB2TA	REAL			REFS	198	211	224	227	DEFINED	97
1111 UG	REAL			207						198
1124 UGS	REAL			REFS	224	241	DEFINED	109	224	
1117 UGSA	REAL			DEFINED	103	241				
1133 UGSS	REAL			REFS	227	248	DEFINED	116	227	
230 UGST	REAL		CBF	REFS	25	DEFINED	248			
74 UTURB	REAL		XFLOAT	REFS	10	DEFINED	129	211		
1201 VBT	REAL			REFS	212	DEFINED	191	194		
1175 VDBR	REAL			REFS	190	191	192	DEFINED	187	
844 VDTURH	REAL		XFLOAT	REFS	9	DEFINED	254	268		
1177 VEMP	REAL			REFS	190	191	192	DEFINED	189	
355 VEMIC	REAL		XFLOAT	REFS	15	64	88	89		
1101 VETICP	REAL			REFS	89	DEFINED	89			
643 VETURB	REAL		XFLOAT	REFS	9	DEFINED	263	267		
1203 VG	REAL			REFS	212	225	228	DEFINED	205	208
1111 VGS	REAL			REFS	225	242	DEFINED	114	225	
1207 VGS4	REAL			DEFINED	242					
1134 VGS5	REAL			REFS	228	249	DEFINED	117	228	
231 VGST	REAL		CBF	REFS	25	DEFINED	249			
1125 VG1	REAL			REFS	200	205	DEFINED	110	200	
1126 VG2	REAL			REFS	201	205	DEFINED	111	201	
1127 VG3	REAL			REFS	202	205	DEFINED	112	202	
1130 VG4	REAL			REFS	203	205	DEFINED	113	203	
325 VMD	REAL		CBF	REFS	37	264				
325 VME	REAL		CBF	REFS	37	263				
325 VMN	REAL		CBF	REFS	36	262				
1176 VMNR	REAL			REFS	190	191				
62 VNTUPB	REAL		XFLOAT	REFS	9	DEFINED	192	DEFINED	188	
1056 V0	REAL			REFS	65	67	68	69	76	78
105 VRM	REAL		XFLOAT	DEFINED	64	65				
35 V5	REAL		CBF	REFS	13	156				
				REFS	22	129				
				156	159	164				
1153 VSD	REAL			REFS	20150	DEFINED	155			
75 VTURB	REAL		XFLOAT	REFS	11	DEFINED	131	212		
1174 VXHR	REAL			REFS	188	189	DEFINED	186		
1173 VYBR	REAL			REFS	188	189	DEFINED	185		
1103 WSS	REAL			REFS	187	DEFINED	91	150	153	
1152 WSS1	REAL			REFS	150	153	DEFINED	149	152	
1202 WRT	REAL			REFS	213	DEFINED	192	195		
1160 WRI	REAL			REFS	187	217	221	DEFINED	164	165
1206 WRI1	REAL			DEFINED	238					166
1157 WRIK	REAL			REFS	163	164	DEFINED	162	163	
1051 WRIS	REAL			REFS	221	254	DEFINED	59	217	
1052 WR1SS	REAL			REFS	254			60	221	
1215 WR1ST	REAL			DEFINED	184	185				
1171 WR2	REAL			REFS	181	182		219	223	
1172 WR2P	REAL			DEFINED	181	DEFINED				

## SUBROUTINE WINDC

VARIABLES	SN	TYPE	RELOCATION	REFS	219	245	247	219	99	219	98	196
111J W2S	REAL			REFS	223	247	247	223	108	223		
112J W2SS	REAL			DEFINED	247							
121J W2ST	REAL			DEFINED	107	245						
1122 W2TA	REAL			REFS	167	245		87				
1100 WC	REAL			REFS	196	213	226	226	229	DEFINED	98	196
1112 WG	REAL			209								
1132 WGS	REAL			REFS	226	243	243	226	115	226		
1120 WGS	REAL			DEFINED	104	105	243					
1135 WGS	REAL			REFS	229	250	250	229	118	229		
232 WGST	REAL		CBF	REFS	25	DEFINED	250					
76 WTURB	REAL		XFLOAT	REFS	12	DEFINED	130	213	213			
255 XCG	REAL		XFLOAT	REFS	16	124	128	140	140	144	160	161
114b XD	REAL			165	166							
				REFS	129	130	146	149	149	152	156	157
				162	175	176	182	183	183	214	215	
				DEFINED	128	144	145					
23J XFRZ	REAL		CBF	REFS	26	145	DEFINED	50				
135 X1S	REAL		CBF	REFS	30	183						
13b X2S	REAL		CBF	REFS	30	161	166					
25b YCG	REAL		XFLOAT	REFS	16	123	139					
1150 YH	REAL			REFS	231	233	DEFINED	134	215			
1137 YRS	REAL			REFS	231	239	DEFINED	120	231			
1115 YRSA	REAL			DEFINED	101	239						
1141 YRSS	REAL			REFS	233	252	DEFINED	122	233			
1213 YRST	REAL			DEFINED	252							
767 YP1	REAL			REFS	215	DEFINED	49	49				
770 YR2	REAL			REFS	215	DEFINED	49					
1065 Z11	REAL			REFS	200	DEFINED	72					
1072 Z1111	REAL			REFS	196	DEFINED	77					
1074 Z1112	REAL			REFS	198	DEFINED	79					
1065 Z12	REAL			REFS	201	DEFINED	73					
1067 Z13	REAL			REFS	202	DEFINED	74					
1070 Z14	REAL			REFS	203	DEFINED	75					
1063 Z01	REAL			REFS	72	74	200	202	202	DEFINED	70	
1071 Z0111	REAL			REFS	77	196	DEFINED	76	76			
1073 Z0112	REAL			REFS	79	198	DEFINED	78				
1065 Z02	REAL			REFS	73	75	201	203	203	DEFINED	71	
147 ZR	REAL			REFS	230	232	DEFINED	133	214			
1136 ZRS	REAL			REFS	230	240	DEFINED	119	230			
1116 ZRSA	REAL			DEFINED	102	240						
1140 ZRSS	REAL			REFS	232	251	DEFINED	121	232			
1212 ZRST	REAL			DEFINED	251							
765 ZR1	REAL			REFS	214	DEFINED	49	49				
765 ZR2	REAL			REFS	214	DEFINED	49					

EXTERNALS	TYPE	ARGS	REFERENCES
COS	REAL	1 LIBRARY	156
EXP	REAL	1 LIBRARY	70
RAND		5	169
SIN	REAL	1 LIBRARY	167
SORT	REAL	1 LIBRARY	66
TAH1	REAL	5	129
			262
			71
			263
			76
			264
			78
			123
			126
			139
			142
			178
			175
			176

## A P P E N D I X B

## Definition of Variables Used in CVA Program

A	Common Array
alt	Aircraft Altitude Above Sea Level - Ft.
alt <sub>1</sub>	Altitude Boundary on Turbulence - Ft.
B	Common Storage Array
CTERM	Periodic Amplitude of Sinusoidal Airwake Terms
DT	Time Increment - Sec.
DTOT	Nondimensionalized Time Increment of u Burble Component
DTOTW	Nondimensionalized Time Constant of W Burble Component
DT2	Time Increment - Second
FacW	Extrapolation Factor of Airwake Velocity
FacY	Extrapolation Function in Y Direction
FacZ	Extrapolation Function in Z Direction
FC	Shift Frequency - Cycle/Sec.
FRT	Maximum Gust Frequency - Rad./Sec.
FRTD	Frequency of Vertical Discrete Gust - Rad./Sec.
FRTE	Frequency of East Discrete Gust - Rad./Sec.
FRTN	Frequency of North Discrete Gust - Rad./Sec.
GA	Common Storage Array
GR	Array Containing Turbulence Gains
HIS	Steady Deck Height Above Sea Level - Ft.
I	Integer Counter
Ia	Integer Common Array
IB	Integer Common Array
IBFRZ	Constant Range Flag
IDISCT	Discrete Turbulence Flag
ILBURB	Downwash Selection Switch
ILTURB	Free Air Turbulence Switch
IMode	Operating Mode Switch
Ionce	Turbulence Initialization Option Switch
IPitch	Ship Pitch Flag
IRDSI	Start Up Array



IRDST	Start Up Array
IuBT	Switch for u Burble Component
IVBT	Switch for V Burble Component
IWBT	Switch for W Burble Component
Iwind	Turbulence Selection Switch
IX	Random Number Startup Parameter
OMEGP	Ship Pitch Frequency - Rad/Sec.
Phase	Discrete Turbulence Phase - Rad.
PHIP	Ship Pitch Phase - Rad.
PI	3.14159
PITCHM	Ship Pitch Magnitude - Deg.
PITCHMI	Ship Pitch Magnitude - Rad.
RAV	Averaging Parameter
RD	Filtered Output of Random Number Generator
RDA	Time Constant of Random Number Filter - 1/Sec.
RDX	Raw Output of Random Number Generator
RDY	Intermediate Random Number Value
RDYI	Intermediate Random Number Value
RD3	Intermediate Turbulence Variable
RD4	Intermediate Turbulence Variable
RD5P	Intermediate Turbulence Variable
RK10	Turbulence Filter Gain
RN1	Radar Noise Gain
SIN WCT	Frequency Shifting Function
STHETR	Sine of Ship Heading Angle
SuBSW	Steady u Burble Scale Factor
SuB2	Random u Burble RMS Magnitude
SwBSW	Steady w Burble Scale Factor
S110	Filter Parameter
S210	Filter Parameter
TDTURB	Discrete Turbulence Switch Time - Sec.
TIME	Simulation Running Time - Sec.
TuB2	Random u Burble Time Constant - Sec.
T11 - T33	Euler Angle Conversion Matrix Relating Aircraft Body Axes and Inertial Axes
u	Output of Random Number Generator

uBSS	Steady u Component of Burble - Ft./Sec.
UBSS1	Intermediate Turbulence Variable
UBT	u-Body Axis Burble Component - Ft./Sec.
uB1	X-Ship Axis Periodic Burble - Ft./Sec.
uB1A	Intermediate Variable
uB1K	Intermediate Variable
uB1S	Statistical Summary Variable
uB1SS	Statistical Summary Variable
uB1ST	Statistical Summary Variable
uB2	Ship X Axis Random Burble Component - Ft./Sec.
uB2P	Intermediate Variable
uB2S	Statistical Summary Variable
uB2SS	Statistical Summary Variable
uB2ST	Statistical Summary Variable
uB2TA	Statistical Summary Variable
uG	Aircraft X-Axis Free Air Turbulence Component - Ft./Sec.
uGS	Statistical Summary Variable
uGSA	Statistical Summary Variable
uGSS	Statistical Summary Variable
uGST	Statistical Summary Variable
uTURB	Total Aircraft X-Axis Turbulence - Ft./Sec.
VBT	Lateral Burble Velocity - Ft./Sec.
VDBR	Vertical Burble Component - Ft./Sec.
VDTURB	Vertical Turbulence Velocity - Ft./Sec.
VEBR	East Component of Burble - Ft./Sec.
VEQIC	Aircraft Trim Velocity - Knots
VEQICP	Previous Trim Velocity - Knots
VETURB	East Component of Turbulence - Ft./Sec.
VG	Aircraft Y-Axis Component of Free Air Turbulence - Ft./Sec.
VGS	Statistical Summary Variable
VGSA	Statistical Summary Variable
VGSS	Statistical Summary Variable
VGST	Statistical Summary Variable
VG1	Intermediate Variable
VG2	Intermediate Variable
VG3	Intermediate Variable

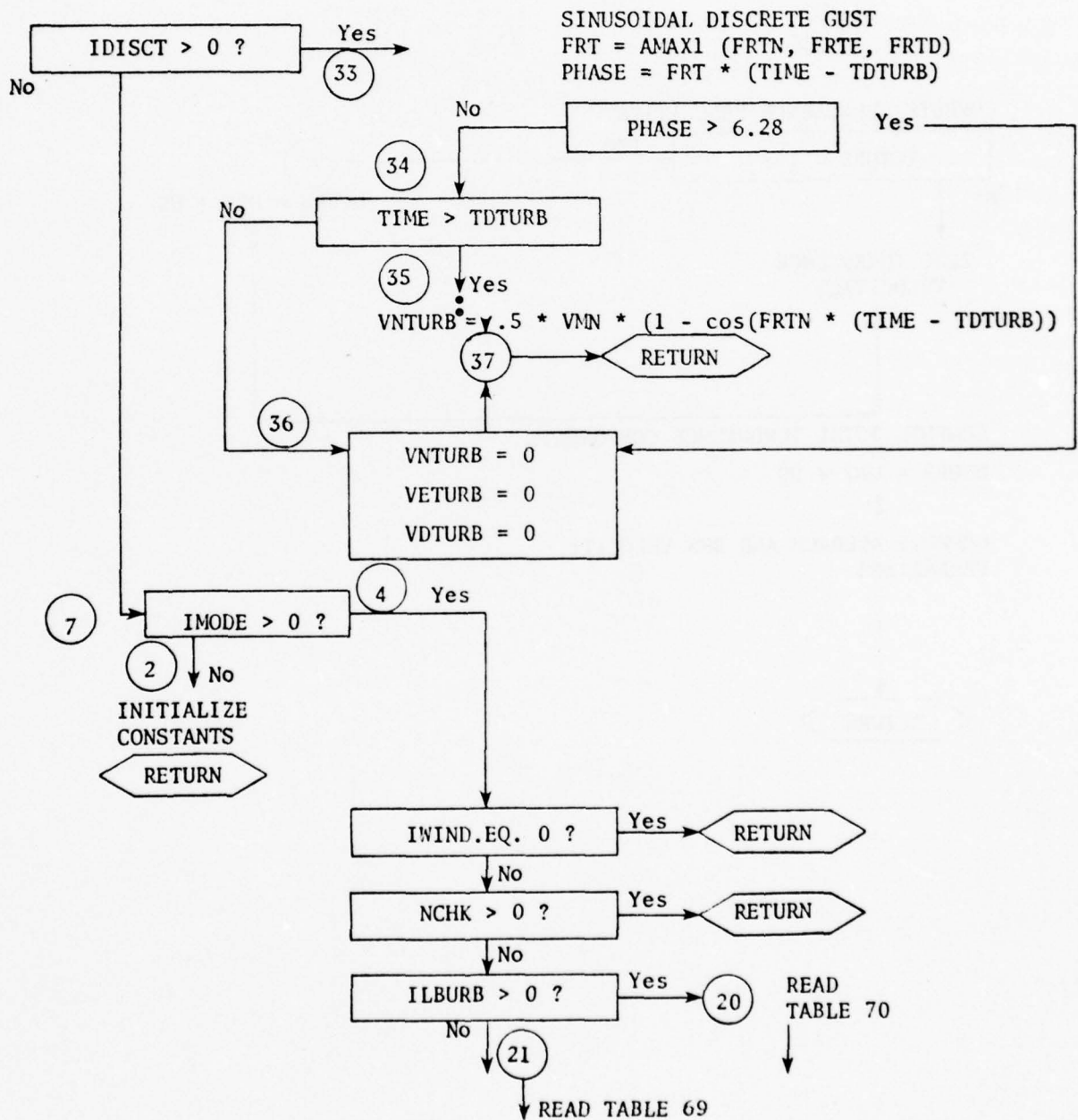
VG4	Intermediate Variable
VMD	Vertical Discrete Gust Magnitude - Ft./Sec.
VME	East Discrete Gust Magnitude - Ft./Sec.
VMN	North Discrete Gust Magnitude - Ft./Sec.
VNBR	North Burble Component - Ft./Sec.
VNTURB	North Turbulence Component - Ft./Sec.
VO	Trim Velocity - Ft./Sec.
VRW	Aircraft Airspeed - Ft./Sec.
VS	Relative Wind Over Deck Speed - Ft./Sec.
VSD	Burble Propagation Speed - Ft./Sec.
VTURB	Aircraft Y Axis Component of Total Turbulence - Ft./Sec.
VXBR	Ship X Axis Component of Burble - Ft./Sec.
VYBR	Ship Y Axis Component of Burble - Ft./Sec.
WBSS	Steady Downwash Velocity - Ft./Sec.
WBSS1	Intermediate Variable
WBT	Aircraft Z Axis Component of Burble - Ft./Sec.
WB1	Periodic Component of Ship Downwash - Ft./Sec.
WB1A	Statistical Summary Variable - Ft./Sec.
WB1K	Intermediate Variable
WB1S	Statistical Summary Variable
WB1SS	Statistical Summary Variable
WB1ST	Statistical Summary Variable
WB2	Vertical Random Burble Component - Ft./Sec.
WB2P	Intermediate Variable
WB2S	Statistical Summary Variable
WB2SS	Statistical Summary Variable
WB2ST	Statistical Summary Variable
WB2TA	Statistical Summary Variable
WC	Frequency Shift Parameter - Rad./Sec.
WG	Aircraft Z-Axis Free Air Turbulence
WGS	Statistical Summary Variable
WGSA	Statistical Summary Variable
WGSS	Statistical Summary Variable
WGST	Statistical Summary Variable
WTURB	Aircraft Z-Axis Turbulence Velocity - Ft./Sec.
XCG	Aircraft X Position Relative to Ship cg - Ft.

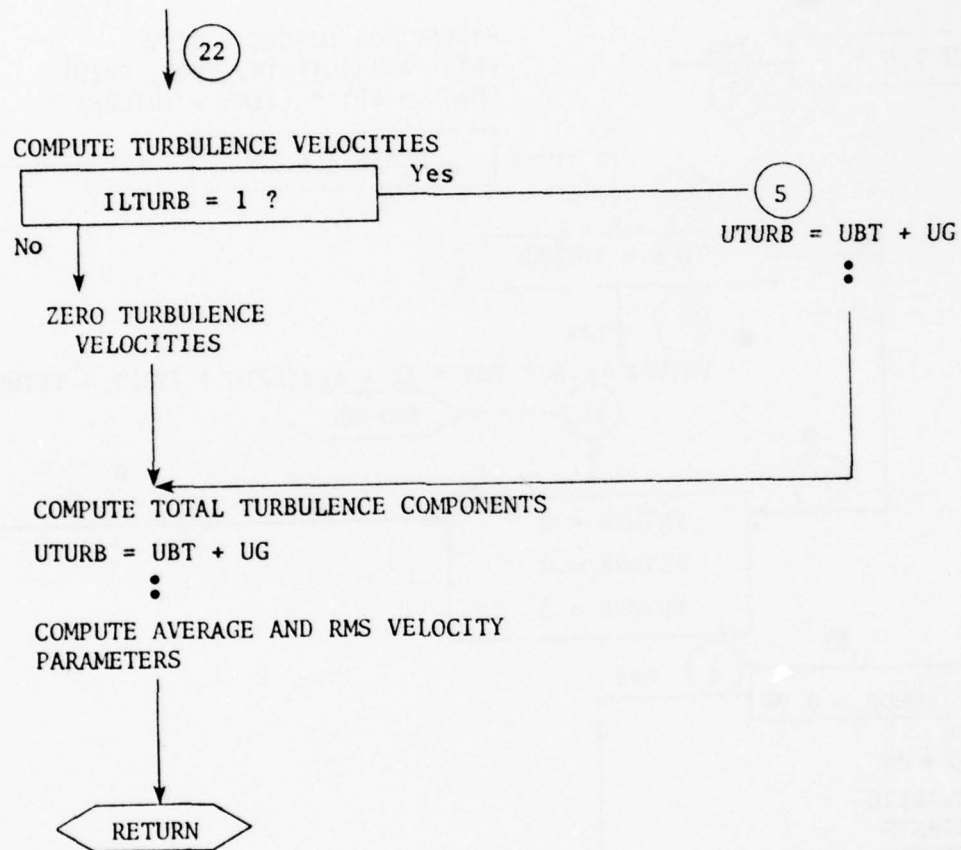
XD	X-Position Variable Used in Table Look Up - Ft.
XFRZ	Fixed Position Used in Table Look Up - Ft.
X1S	Forward Turbulence Limit - Ft.
X2S	Forward Turbulence Limit - Ft.
YCG	Aircraft Lateral Position Relative to Ship - Ft.
YR	Lateral Radar Error - Ft.
YRS	Statistical Summary Variable
YRSA	Statistical Summary Variable
YRSS	Statistical Summary Variable
YRST	Statistical Summary Variable
YR1	Scale Factor on Radar Noise Function
YR2	Scale Factor on Radar Noise Function
ZI1	Turbulence Filter Parameters
ZI111	Turbulence Filter Parameters
ZI112	Turbulence Filter Parameters
ZI2	Turbulence Filter Parameters
ZI3	Turbulence Filter Parameters
ZI4	Turbulence Filter Parameters
Z01	Turbulence Filter Parameters
Z0111	Turbulence Filter Parameters
Z0112	Turbulence Filter Parameters
Z02	Turbulence Filter Parameters
ZR	Vertical Radar Noise - Ft.
ZRS	Statistical Summary Parameter
ZRSA	Statistical Summary Parameter
ZRSS	Statistical Summary Parameter
ZRST	Statistical Summary Parameter
ZR1	Radar Noise Parameter
ZR2	Radar Noise Parameter



## APPENDIX C

Flow Chart for CVA Model





NADC-78182-60

A P P E N D I X   D

Listing of FF 1052 Turbulence Subroutine

n = 2



79/01/15. 09.01.01

FTN 4.5+424

SUBROUTINE WINDC 74/74 CPT=1

```

50  V=SQRT(VEX**2+VNY**2)
    PSI=ATAN2(VEX,VNY)-PI
    CPSI=COS(PSI)
    SPSI=SIN(PSI)
    PSIPCL=PSI-PSISK
    CPSIPCL=COS(PSIPCL)
    SPSIPCL=SIN(PSIPCL)
    C      COMPUTE TURBULENCE EXTRAPOLATION BOUNDARIES
    VMAX=-RLTDCPSIPCL*BFAM/2.*CPSIPCL
    VMIN=-BFAM/2.*CPSIPCL*(PLS-RLTDCPSIPCL
    VMIN=VMIN
    XMIN=-RLTDCPSIPCL*BFAM/2.*SARS(SPSIPCL)
    XMAX2=(PLS-RLTDCPSIPCL*BFAM/2.*SARS(SPSIPCL)
    IF(VMIN.GT.-14.75) VMIN=-14.75
    IF(VMAX.LT.170.) VMAX=170.
    IF(SPSIPCL) 50,40,50
    IF(SLOPE=(XMIN-XMIN2)/(YMAX-YMIN))
    CONTINUE
    VML=VM/76.
    VHI=VH/59.
    2    CONTINUE
    100  IF(TIME-TCOUNT)101,100,100
        TCOUNT=TCOUNT+DTX
        VTO=VTOIN
        VTI=VTOIN
        VTO=VTOIN
        VTI=VTOIN
        XMIN=XMIN2+XDCOSW
        YMIN=YMIN2+YDCOSW
        C      GUST MODEL EXTRAPOLATIONS FUNCTIONS
        C      XTAR,YTAR,ZTAR ARE INPUT TO TABLES
        XTAR=XTAR
        YTAR=YTAR
        ZTAR=ZTAR
        FX1=1.
        FY1=1.
        FZ1=1.
        IF(ZTAR.LT.0) ZTAR=0.
        IF(ZTAR.GT.31.31) ZTAR=31.31
        FX1=EXP((44.95-ZTAR)/BFAM)
        FY1=EXP((44.95-ZTAR)/BFAM)
        FZ1=EXP((44.95-ZTAR)/BFAM)
        30  CONTINUE
        IF(ZTAR.GT.44.95) ZTAR=44.95
        IF(YTAR.YMAX) 3,5,4
        FY1=EXP((YMAX-YTAR)/BFAM)
        GO TO 5
        3  IF(YTAR-YMIN) 4,5,5
        6  FY1=EXP((YTAR-YMIN)/BFAM)
        5  CONTINUE
        IF(SPSIPCL) 7,4,7
        XMIN=XMIN1
        GO TO 13
        7  IF(YMIN-YMAX) 9,10,10
        10  XMIN=XMIN1
        GO TO 13
        4  IF(YTAR-YMIN) 11,12,12
        11  XMIN=XMIN2
        GO TO 13

```

THIS PAGE IS BEST QUALITY PRACTICALLY  
FROM COPY FURNISHED TO DOD

74/01/15. 08.01.01

FIN 0.5424

ROUTINE N1.DC 74/74 OPT=1

```

115 12 VMIN=MIN2-SLOPE1*(V4*IND-VMIN)
13 13 CONTINUE
14 14 IF (X14-XTA) 14.14,16
15 15 EX1=EXP((X14-XTA)/RETA)
16 16 GO TO 17
17 17 CONTINUE
18 18 IF (X14-240.) 17.17,18
19 19 CONTINUE
20 20 EX1=1-(X14-250.)*SLOPEX
21 21 IF (X14-250.) EX1=0.
22 22 CONTINUE
23 23 IF (X14-250.) X14=0.
24 24 IF (X14-250.) X14=250.
25 25 IF (X14-250.) X14=18.75
26 26 IF (X14-250.) X14=170.
27 27 IF (X14-250.) X14=170.
28 28 IF (X14-250.) X14=170.
29 29 IF (X14-250.) X14=170.
30 30 IF (X14-250.) X14=170.
31 31 IF (X14-250.) X14=170.
32 32 IF (X14-250.) X14=170.
33 33 IF (X14-250.) X14=170.
34 34 IF (X14-250.) X14=170.
35 35 IF (X14-250.) X14=170.
36 36 IF (X14-250.) X14=170.
37 37 IF (X14-250.) X14=170.
38 38 IF (X14-250.) X14=170.
39 39 IF (X14-250.) X14=170.
40 40 IF (X14-250.) X14=170.
41 41 IF (X14-250.) X14=170.
42 42 IF (X14-250.) X14=170.
43 43 IF (X14-250.) X14=170.
44 44 IF (X14-250.) X14=170.
45 45 IF (X14-250.) X14=170.
46 46 IF (X14-250.) X14=170.
47 47 IF (X14-250.) X14=170.
48 48 IF (X14-250.) X14=170.
49 49 IF (X14-250.) X14=170.
50 50 IF (X14-250.) X14=170.
51 51 IF (X14-250.) X14=170.
52 52 IF (X14-250.) X14=170.
53 53 IF (X14-250.) X14=170.
54 54 IF (X14-250.) X14=170.
55 55 IF (X14-250.) X14=170.
56 56 IF (X14-250.) X14=170.
57 57 IF (X14-250.) X14=170.
58 58 IF (X14-250.) X14=170.
59 59 IF (X14-250.) X14=170.
60 60 IF (X14-250.) X14=170.
61 61 IF (X14-250.) X14=170.
62 62 IF (X14-250.) X14=170.
63 63 IF (X14-250.) X14=170.
64 64 IF (X14-250.) X14=170.
65 65 IF (X14-250.) X14=170.
66 66 IF (X14-250.) X14=170.
67 67 IF (X14-250.) X14=170.
68 68 IF (X14-250.) X14=170.
69 69 IF (X14-250.) X14=170.
70 70 IF (X14-250.) X14=170.
71 71 IF (X14-250.) X14=170.
72 72 IF (X14-250.) X14=170.
73 73 IF (X14-250.) X14=170.
74 74 IF (X14-250.) X14=170.
75 75 IF (X14-250.) X14=170.
76 76 IF (X14-250.) X14=170.
77 77 IF (X14-250.) X14=170.
78 78 IF (X14-250.) X14=170.
79 79 IF (X14-250.) X14=170.
80 80 IF (X14-250.) X14=170.
81 81 IF (X14-250.) X14=170.
82 82 IF (X14-250.) X14=170.
83 83 IF (X14-250.) X14=170.
84 84 IF (X14-250.) X14=170.
85 85 IF (X14-250.) X14=170.
86 86 IF (X14-250.) X14=170.
87 87 IF (X14-250.) X14=170.
88 88 IF (X14-250.) X14=170.
89 89 IF (X14-250.) X14=170.
90 90 IF (X14-250.) X14=170.
91 91 IF (X14-250.) X14=170.
92 92 IF (X14-250.) X14=170.
93 93 IF (X14-250.) X14=170.
94 94 IF (X14-250.) X14=170.
95 95 IF (X14-250.) X14=170.
96 96 IF (X14-250.) X14=170.
97 97 IF (X14-250.) X14=170.
98 98 IF (X14-250.) X14=170.
99 99 IF (X14-250.) X14=170.
100 100 IF (X14-250.) X14=170.

```

THIS PAGE IS BEST QUALITY PRACTICABLE  
FROM COPY FURNISHED TO DDC







THIS PAGE IS BEST QUALITY PRACTICABLE  
FROM COPY FURNISHED TO DDC

79/01/15. 03.01.01

FT 4.54425

74/74 OPT=1

ROUTINE WINDC

RELOCATION

VARIABLES SN TYPE

VARIABLES	SN	TYPE	RELOCATION	FT 4.54425	79/01/15. 03.01.01	PAGE
504 WLS	64	REAL		71	DEFINED	
505 ALTO	56	REAL		54	70	13
702 PRDRE	144	REAL		184	190	DEFINED
574 MAX	50	REAL		DEFINED	16	145
575 RNY	51	REAL		DEFINED	16	
576 RNY	52	REAL		DEFINED	16	
757 SIGRX	140	REAL		DEFINED	142	
760 SIGVY	140	REAL		DEFINED	143	
761 SIGVZ	140	REAL		DEFINED	144	
761 SIGX	142	REAL		213	DEFINED	136
762 SIGY	143	REAL		213	DEFINED	137
763 SIGZ	144	REAL		213	DEFINED	138
577 SLOPEX	123	REAL		DEFINED	17	
574 SLOPEL	115	REAL		213	DEFINED	75
715 SPSTDEL	66	REAL		64	70	DEFINED
707 SPSTSR	55	REAL		DEFINED	54	64
715 SPSTX	85	REAL		66	199	DEFINED
701 TCOMPT	80	REAL		61	200	DEFINED
573 TCOMPTX	150	REAL		153	154	DEFINED
574 TCOMPTY	155	REAL		150	154	DEFINED
575 TCOMPTZ	150	REAL		153	154	DEFINED
1004 TFC	210	REAL		211	212	DEFINED
450 TIME	11	REAL	XFLOAT	60	150	159
733 VMTN	104	REAL		204	212	201
734 VMTN	84	REAL		204	212	201
644 VMTN	20210	REAL	XFLOAT	DEFINED	54	
115 VMT	4	REAL	XFLOAT	DEFINED	22	
727 VMTN	4	REAL	XFLOAT	205	211	200
725 VMTN	4	REAL	XFLOAT	DEFINED	52	
643 VMTN	20211	REAL	XFLOAT	DEFINED	21	56
114 VMT	4	REAL	XFLOAT	58	59	
43 VMT-IC	4	REAL	C-F	56		
731 VMTN	4	REAL		204	210	199
730 VMTN	4	REAL		204	210	
642 VMTN	20210	REAL	XFLOAT	DEFINED	43	
113 VMT	4	REAL	XFLOAT	DEFINED	20	57
42 VMT-IC	4	REAL	C-F	56	59	
35 VS	4	REAL	C-F	57		
711 VS	4	REAL		56	57	
725 VS	77	REAL		78	139	54
754 VXBAP	154	REAL		147	164	77
655 VXT	145	REAL		REFINED	134	
270 VXT	141	REAL		150	DEFINED	27
1001 VXTN	144	REAL		DEFINED	30	188
746 VXS	144	REAL		200	DEFINED	191
755 VXS	134	REAL		213	DEFINED	195
655 VYT	146	REAL		DEFINED	140	132
671 VYT	142	REAL		146	DEFINED	140
1002 VYT	144	REAL		DEFINED	31	189
747 VYS	144	REAL		200	DEFINED	192
755 VYS	140	REAL		213	DEFINED	196
657 VZT	147	REAL		DEFINED	141	133
672 VZT	143	REAL		147	DEFINED	141
1003 VZT	140	REAL		DEFINED	32	190
750 VZS	141	REAL		213	DEFINED	193
214 XS	7	REAL	C-F	45	134	134

## RELOCATION

VARIABLES	SV	TYPE
744 XWIND	REAL	
745 XWIND1	REAL	
746 XWIND2	REAL	
747 XWIND3	REAL	
748 XWIND4	REAL	
749 XWIND5	REAL	
750 XWIND6	REAL	
751 XWIND7	REAL	
752 XWIND8	REAL	
753 XWIND9	REAL	
754 XWIND10	REAL	
755 XWIND11	REAL	
756 XWIND12	REAL	
757 XWIND13	REAL	
758 XWIND14	REAL	
759 XWIND15	REAL	
760 XWIND16	REAL	
761 XWIND17	REAL	
762 XWIND18	REAL	
763 XWIND19	REAL	
764 XWIND20	REAL	
765 XWIND21	REAL	
766 XWIND22	REAL	
767 XWIND23	REAL	
768 XWIND24	REAL	
769 XWIND25	REAL	
770 XWIND26	REAL	
771 XWIND27	REAL	
772 XWIND28	REAL	
773 XWIND29	REAL	
774 XWIND30	REAL	
775 XWIND31	REAL	
776 XWIND32	REAL	
777 XWIND33	REAL	
778 XWIND34	REAL	
779 XWIND35	REAL	
780 XWIND36	REAL	
781 XWIND37	REAL	
782 XWIND38	REAL	
783 XWIND39	REAL	
784 XWIND40	REAL	
785 XWIND41	REAL	
786 XWIND42	REAL	
787 XWIND43	REAL	
788 XWIND44	REAL	
789 XWIND45	REAL	
790 XWIND46	REAL	
791 XWIND47	REAL	
792 XWIND48	REAL	
793 XWIND49	REAL	
794 XWIND50	REAL	
795 XWIND51	REAL	
796 XWIND52	REAL	
797 XWIND53	REAL	
798 XWIND54	REAL	
799 XWIND55	REAL	
800 XWIND56	REAL	
801 XWIND57	REAL	
802 XWIND58	REAL	
803 XWIND59	REAL	
804 XWIND60	REAL	
805 XWIND61	REAL	
806 XWIND62	REAL	
807 XWIND63	REAL	
808 XWIND64	REAL	
809 XWIND65	REAL	
810 XWIND66	REAL	
811 XWIND67	REAL	
812 XWIND68	REAL	
813 XWIND69	REAL	
814 XWIND70	REAL	
815 XWIND71	REAL	
816 XWIND72	REAL	
817 XWIND73	REAL	
818 XWIND74	REAL	
819 XWIND75	REAL	
820 XWIND76	REAL	
821 XWIND77	REAL	
822 XWIND78	REAL	
823 XWIND79	REAL	
824 XWIND80	REAL	
825 XWIND81	REAL	
826 XWIND82	REAL	
827 XWIND83	REAL	
828 XWIND84	REAL	
829 XWIND85	REAL	
830 XWIND86	REAL	
831 XWIND87	REAL	
832 XWIND88	REAL	
833 XWIND89	REAL	
834 XWIND90	REAL	
835 XWIND91	REAL	
836 XWIND92	REAL	
837 XWIND93	REAL	
838 XWIND94	REAL	
839 XWIND95	REAL	
840 XWIND96	REAL	
841 XWIND97	REAL	
842 XWIND98	REAL	
843 XWIND99	REAL	
844 XWIND100	REAL	

C=1

213

71

115

113

115

113

115

113

115

113

115

113

115

113

115

113

115

113

115

113

115

113

115

113

115

113

115

113

115

113

115

113

115

113

115

113

115

113

115

113

115

113

115

113

115

113

115

113

115

113

115

113

115

113

115

113

115

113

115

113

115

113

115

113

115

113

115

113

115

113

115

113

115

113

115

113

115

113

115

113

115

113

115

113

115

113

115

113

115

113

115

113

115

113

115

113

115

113

115

113

115

113

115

113

115

113

115

113

115

113

115

113

115

113

115

113

115

113

115

113

115

113

115

113

115

113

115

113

115

113

115

113

115

113

115

113

115

113

115

113

115

113

115

113

115

113

115

113

115

113

115

113

115

113

115

113

115

113

115

113

115

113

115

113

115

113

115

113

115

113

115

113

115

113

115

113

115

113

115

113

115

113

115

113

115

113

115

113

115

113

115

113

115

113

115

113

115

113

115

113

115

113

115

113

115

113

115

113

115

113

115

113

115

113

115

113

115

113

115

113

115

113

115

113

115

113

115

113

115

113

115

113

115

113

115

113

115

113

115

113

115

113

115

113

115

113

115

113

115

113

115

113

115

113

115

113

115

113

115

113

115

113

115

74/74 0-1-1

ROUTINE KIPDC

STATEMENT LEVELS REF LINE REFERENCES

STATEMENT	LEVELS	REF LINE	REFERENCES
0 30	INACTIVE	07	95
155 31		98	2095
117 44		76	74
0 50	INACTIVE	75	2074
0 100	INACTIVE	41	2020
4-5 101		202	50
0 102	INACTIVE	204	203
454 103		207	203
017 104		215	213
0 200	INACTIVE	151	20150
302 202		154	150
0 300	INACTIVE	156	20154
315 302		159	155
0 400	INACTIVE	161	20140
302 402		164	160
0 500	INACTIVE	170	20160
302 501		173	169
0 502	INACTIVE	174	173
351 503		177	20173
354 504		179	172

176

COMMON BLOCKS LENGTH MEMBERS - BIAS NAME (LENGTH)

COMMON BLOCKS	LENGTH	MEMBERS	BIAS NAME (LENGTH)
XELCAT	500	0 4	(500)
FIXED	200	0 14	(200)
C-F	200	0 4	(200)
IC-F	50	0 14	(50)

EQUIV CLASSES LENGTH MEMBERS - BIAS NAME (LENGTH)

EQUIV CLASSES	LENGTH	MEMBERS	BIAS NAME (LENGTH)
IA	200	75 VOW	(1)
4	200	42 ALT	(1)
		419 VETURB	(1)
		400 PSIA	(1)
		0 I-UFF	(1)
		24 VS	(1)
		03 PSIS	(1)
		141 Y2	(1)
IA	50	15 I-ORCE	(1)

77 VOW (1)  
302 TIME (1)  
420 VOTURB (1)

35 VFWBIC (1)  
140 XE (1)

STATISTICS  
PROGRAM LENGTH 10043 517  
COMMON LENGTH 16664 450

THIS PAGE IS BEST QUALITY PRACTICABLE  
FROM COPY FURNISHED TO DDC

ה - 10



44.54	0	780506111	37.	90.	VX72- VSS=45 KNOT PSIS=50 DEG 7=14.58	125.	250.	1
-14.75	7	7	72.79	56.34	57.45	125.	250.	2
0.	78.49	75.16	56.57	53.25	51.35	125.	250.	3
14.75	74.76	56.22	41.50	40.71	43.60	125.	250.	4
54.	55.52	44.19	71.63	61.04	58.71	125.	250.	5
104.	17.65	35.79	47.93	46.83	54.44	125.	250.	6
170.	14.48	77.63	58.18	67.5	74.64	125.	250.	7
14.58	0.	780506111	37.	90.	VX72- VSS=45 KNOT PSIS=50 DEG 7=14.58	125.	250.	1
-14.75	-4.55	-11.73	73	-2.45	3.45	125.	250.	2
0.	5.16	-7.2	-0.7	-2.3	2.44	125.	250.	3
14.75	-15.63	-15.71	-4.41	4	8.3	125.	250.	4
54.	-1.15	-4.26	1.33	3.27	-1.54	125.	250.	5
104.	5.02	12.74	7.56	3.54	-9.16	125.	250.	6
170.	-8.26	-5.34	3.10	6.38	9.02	125.	250.	7
25.	0.	780506111	37.	90.	VX72- VSS=45 KNOT PSIS=50 DEG 7=25	125.	250.	1
-14.75	-7.9	-3.53	-7.1	1.23	5.9	125.	250.	2
0.	-5.2	-1.3	-9.3	-0.7	6.93	125.	250.	3
14.75	1.4	-7.26	-3.	4.42	5.7	125.	250.	4
54.	-6.7	3.1	9.11	9.	1.11	125.	250.	5
104.	15.64	13.55	8.07	5.33	-5.54	125.	250.	6
170.	-13.04	-4.45	6.75	4.61	8.47	125.	250.	7
44.54	0.	780506111	37.	90.	VX72- VSS=45 KNOT PSIS=50 DEG 7=25	125.	250.	1
-14.75	1.6	2.42	6.04	5.	14.44	125.	250.	2
0.	-5.24	2.19	4.77	3.67	4.54	125.	250.	3
14.75	6.19	11.74	3.59	2.45	7.81	125.	250.	4
54.	4.24	4.32	9.8	10.13	7.5	125.	250.	5
104.	5.35	10.58	14.84	8.25	6.24	125.	250.	6
170.	-14.78	-12.27	-4.33	-2.09	5.414	125.	250.	7
14.54	0.	780506111	37.	90.	VX72- VSS=45 KNOT PSIS=50 DEG 7=14.58	125.	250.	1
-14.75	-24.54	-1.09	-0.4	-2.22	-7.7	125.	250.	2
0.	-10.45	1.2	-5.47	-5.13	2.14	125.	250.	3
14.75	-4.45	-5.27	-6.56	-4.14	5.41	125.	250.	4
54.	-23	-5.15	-6.4	-3.22	7.14	125.	250.	5
104.	-12.45	-2.1	2.42	6.74	12.7	125.	250.	6
170.	-14.13	-24.31	-23.13	-7.45	-14.45	125.	250.	7
25.	0.	780506111	37.	90.	VX72- VSS=45 KNOT PSIS=50 DEG 7=25	125.	250.	1
-14.75	-21.37	-13.51	-3.26	-7.64	-2.59	125.	250.	2
0.	-22.44	-7.15	-5.21	-3.5	5.17	125.	250.	3
14.75	-5.45	-6.19	-4.54	-3.03	5.14	125.	250.	4
54.	-3.77	-4.55	-4.91	-5.4	5.51	125.	250.	5
104.	-13.57	-1.05	5.56	9.54	14.29	125.	250.	6
170.	-22.506	-24.5	-22.404	-2.301	-12.75	125.	250.	7
44.54	0.	780506111	37.	90.	VX72- VSS=45 KNOT PSIS=50 DEG 7=14.58	125.	250.	1
-14.75	-17.25	-14.44	-15.28	-2.43	7.1	125.	250.	2
0.	-23.42	-14.45	-4.45	-3.74	7.1	125.	250.	3
14.75	-14.37	-4.4	3.24	4.07	11.51	125.	250.	4
54.	-14.34	-6.74	5.	1.12	19.49	125.	250.	5
104.	-4.7	-2.54	2.66	6.6	10.42	125.	250.	6
170.	-11.44	-17.22	-14.24	-17.92	-11.454	125.	250.	7
14.54	0.	780506111	37.	90.	VX72- VSS=45 KNOT PSIS=50 DEG 7=14.58	125.	250.	1
-14.75	7.45	14.22	14.45	14.94	17.07	125.	250.	2
0.	24.31	20.14	14.56	13.2	16.14	125.	250.	3
14.75	12.44	14.31	12.43	12.43	16.17	125.	250.	4
54.	12.43	14.7	14.42	15.45	16.4	125.	250.	5
104.	17.95	12.34	12.34	14.51	12.45	125.	250.	6
170.	17.71	14.04	14.44	14.51	14.51	125.	250.	7

THIS PAGE IS BEST QUALITY PRACTICABLE  
FROM COPY FURNISHED TO DDC

25.	37.	50.	125.	250.	1
-16.75	2.86	11.70	19.77	15.24	20.54
0.	15.91	20.76	16.35	12.51	14.57
15.75	20.61	16.79	17.	16.67	16.45
54.	17.5	19.49	15.66	17.57	16.76
104.	19.21	15.25	15.12	14.95	13.51
170.	14.09	13.66	13.657	12.53	5.72
44.53	37.	50.	125.	250.	1
-16.75	1.05	3.72	12.02	15.17	16.4
0.	2.56	13.73	15.33	17.11	14.11
14.75	4.22	20.34	25.52	19.55	14.93
54.	2.06	4.75	15.93	17.07	16.14
104.	15.16	16.43	14.13	13.59	13.23
170.	14.24	14.01	15.18	14.05	2.772
14.75	37.	50.	125.	250.	1
-16.75	7.1	20.47	22.41	14.59	17.49
0.	26.1	20.57	17.02	15.01	15.73
14.75	11.53	15.44	14.03	15.45	15.4
54.	14.06	17.44	15.66	17.73	17.44
104.	14.55	11.01	10.60	15.64	15.77
170.	15.705	17.604	17.19	17.33	9.503
25.	37.	50.	125.	250.	1
-15.75	4.7	13.77	21.29	20.51	14.33
0.	20.41	25.7	16.81	14.08	16.57
14.75	21.24	23.84	13.56	14.51	16.44
54.	17.02	17.05	14.64	15.08	14.31
104.	14.5	13.95	14.47	17.16	17.68
170.	22.24	14.89	12.242	17.52	7.04
44.53	37.	50.	125.	250.	1
-14.75	1.19	4.24	14.92	17.14	17.54
0.	2.63	14.53	21.24	20.55	16.31
14.75	3.3	21.63	27.21	24.25	14.54
54.	2.50	5.82	12.01	20.52	16.61
104.	15.77	14.74	14.95	14.45	15.37
170.	15.34	16.32	14.52	17.23	5.464
14.75	37.	50.	125.	250.	1
-16.75	3.11	17.01	17.64	17.4	15.67
0.	20.44	14.33	16.38	15.74	14.31
14.75	12.41	14.11	13.04	14.33	13.47
54.	15.76	14.34	14.29	16.47	14.62
104.	14.05	13.52	11.15	11.5	14.63
170.	14.02	14.37	14.47	13.53	7.234
25.	37.	50.	125.	250.	1
-14.75	5.04	12.43	16.53	14.44	14.7
0.	14.46	16.58	17.42	15.4	14.12
14.75	19.5	17.39	17.43	15.04	14.11
54.	14.74	14.47	20.11	16.29	14.56
104.	17.15	14.66	13.52	13.46	14.64
170.	14.018	14.54	14.72	13.37	7.114
44.53	37.	50.	125.	250.	1
-15.75	1.42	3.46	13.32	13.34	15.34
0.	4.41	16.07	20.04	20.21	14.6
14.75	3.44	20.17	24.03	21.62	14.24
54.	2.21	5.3	17.04	17.49	14.31
104.	14.34	10.43	17.43	14.77	12.77

THIS PAGE IS BEST QUALITY PRACTICABLE  
FROM COPY FURNISHED TO DDC

## A P P E N D I X E

## Variable Definitions for FF 1052 Program

A	Common Array
ALT	Altitude of Aircraft cg Above Sea Level - Ft.
B	Common Array
Beam	Ship Beam - Ft.
CPSIREL	Cosine of Relative Wind Angle
CPSISR	Cosine of Ship Heading Angle
CPSIW	Cosine of Absolute Wind Direction
DT	Integration Frame Time - Sec.
DTW	Integration Frame Time of Turbulence Subroutine - Sec.
DTX	Update Time Increment of X-Random Number Generator - Sec.
DTY	Update Time Increment of Y Component Random Number Generator
DTZ	Update Increment of Z Component Random Number Generator
EXPX	X Component Difference Equation Parameter
EXPY	Y Component Difference Equation Parameter
EXPZ	Z Component Difference Equation Parameter
FOMEGX	X Frequency Extrapolation Function
FOMEGY	Y Frequency Extrapolation Function
FX1	X Direction Extrapolation Function
FY1	Y Direction Extrapolation Function
FZ1	Z Direction Extrapolation Function
F1	Total Extrapolation Function
HTD	Height of Touchdown Point Above Sea Level - Ft.
IA	Integer Common Array
IB	Integer Common Array
IMODE	Simulation Mode Switch
IONCE	Random Number Startup Option Switch
IRDSTX	Initial Value of X - Random Number Sequence
IRDSTXI	Current Value of X - Random Number Sequence
IRDSTY	Initial Value of Y - Random Number Sequence
IRDSTYI	Current Value of Y - Random Number Sequence
IRDSTZ	Initial Value of Z - Random Number Sequence

IRDSTZI	Current Value of Z - Random Number Sequence
IWIND	Turbulence on/off Flag
IX	Machine Dependent Random Number Generator Parameter
OMEGX	X - Component Filter Constant
OMEGY	Y - Component Filter Constant
OMEGZ	Z - Component Filter Constant
PI	3.14159
PSIREL	Angle of Relative Wind With Respect to Ship - Rad.
PSIS	Ship Heading - Deg.
PSISR	Ship Heading - Rad.
PSIW	Absolute Wind Direction - Rad.
RANDX	Interpolated Value of X - Component Random Number Generator
RANDXN	Current Output of X - Random Number Generator
RANDXO	Previous Output of Y - Component Random Number Generator
RANDY	Interpolated Value of Y Component Random Number Generator
RANDYN	Current Output of Y Random Number Generator
RANDYO	Previous Output of Y Random Number Generator
RANDZ	Interpolated Value of Z Component Random Number Generator
RANDZN	Current Output of Z Random Number Generator
RANDZO	Previous Output of Z Random Number Generator
RLS	Ship Length - Ft.
RLTD	Distance From Bow to Touchdown Point - Ft.
RMODE	Mode Parameter
RNX	X Component Time Increment Ratio
RNY	Y Component Time Increment Ratio
RNZ	Z Component Time Increment Ratio
SIGVX	X Velocity Variance - Ft./Sec.
SIGVY	Y Velocity Variance - Ft./Sec.
SIGVZ	Z Velocity Variance - Ft./Sec.
SIGX	Tabulated X Component Variance - Ft./Sec.
SIGY	Tabulated Y Component Variance - Ft./Sec.
SIGZ	Tabulated Z Component Variance - Ft./Sec.
SLOPEX	X Extrapolation Parameter
SLOPE1	X Boundary Definition Parameter
SPSIREL	Sine of Relative Heading Angle
SPSISR	Sine of Ship Heading

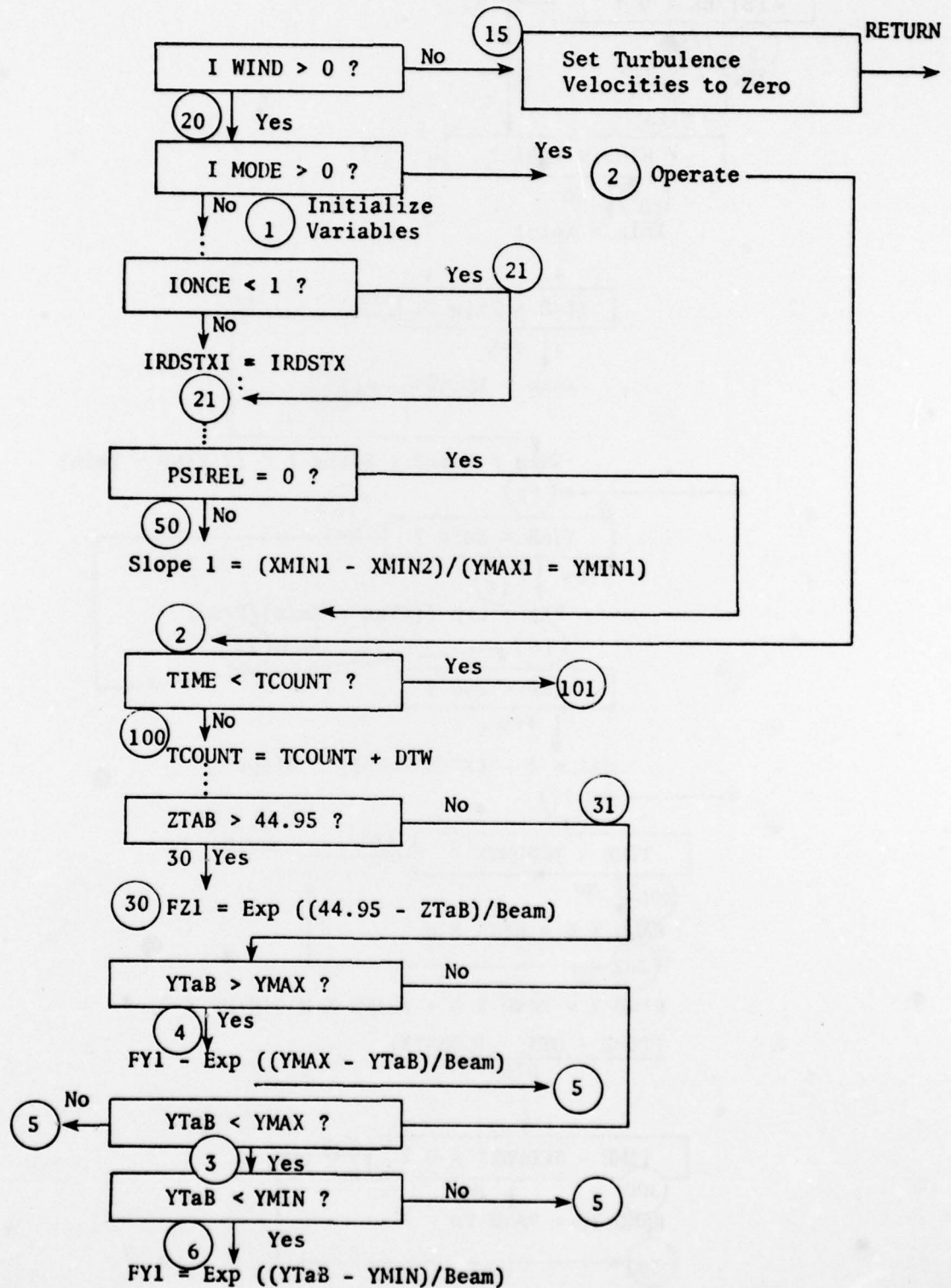


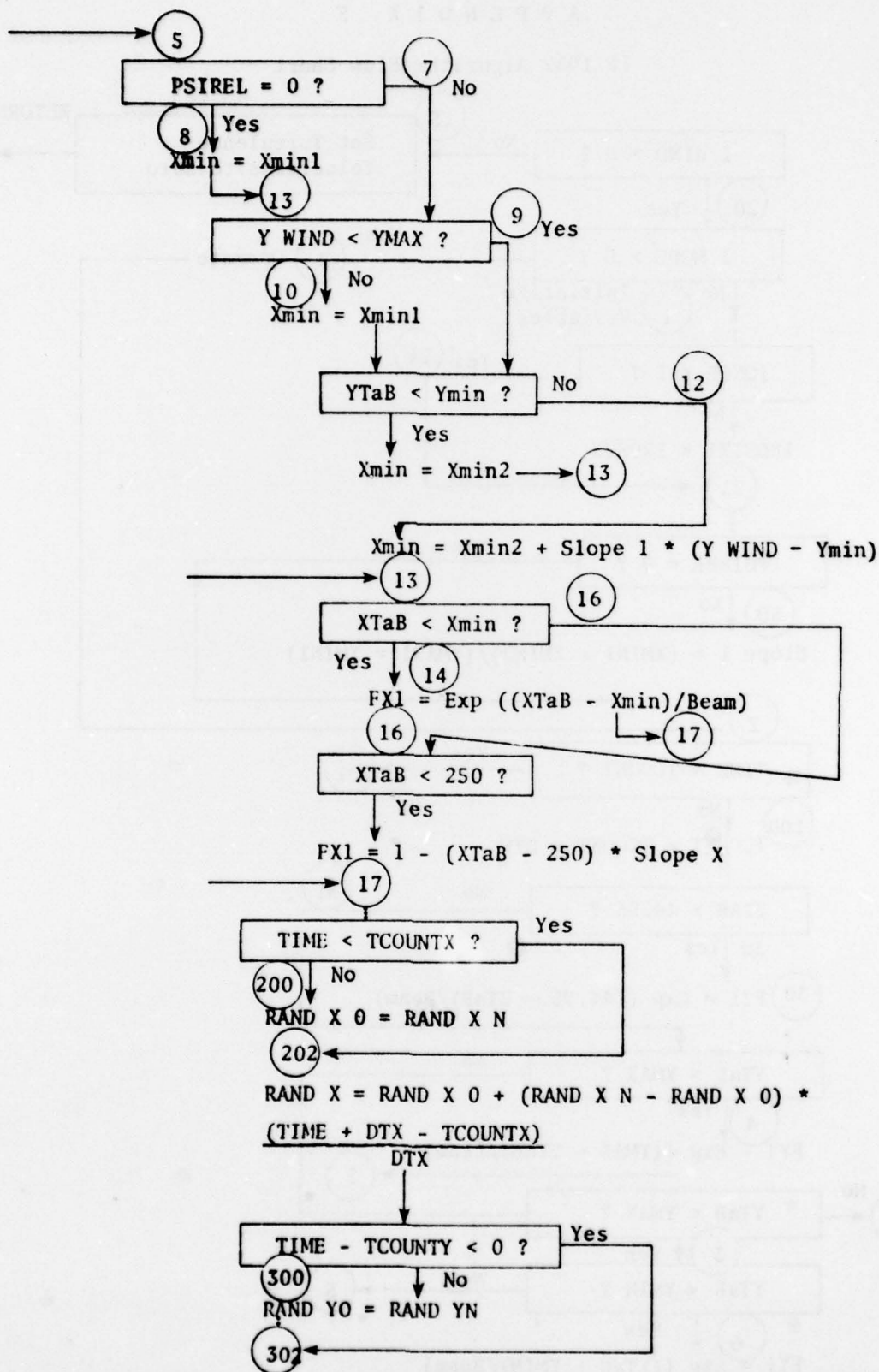
SPSIW	Sine of Wind Heading
TCOUNT	Update Time Counter - Sec.
TCOUNTX	X Update Time - Sec.
TCOUNTY	Y Update Time - Sec.
TCOUNTZ	Z Update Time - Sec.
TFAC	Turbulence Update Paramater
TIME	Simulation Time - Sec.
VDTN	Current Value of Vertical Turbulence Component - Ft./Sec.
VDTO	Previous Value of Vertical Turbulence Component - Ft./Sec.
VDTURB	Interpolated Value of Vertical Turbulence - Ft./Sec.
VDW	Total Vertical Wind Including Free Air Wind - Ft./Sec.
VETN	Current Value of Computed East Turbulence Component - Ft./Sec.
VETO	Previous Value of Vertical Turbulence Component - Ft./Sec.
VETURB	Interpolated Value of East Turbulence - Ft./Sec.
VEW	Total East Wind - Ft./Sec.
VEWBIC	Initial East Wind Component - Ft./Sec.
VNTN	Current North Turbulence Update - Ft./Sec.
VNTO	Previous North Turbulence Update - Ft./Sec.
VNTURB	Interpolated North Turbulence Component - Ft./Sec.
VNW	North Wind Component - Ft./Sec.
VNWBIC	Initial North Wind Component - Ft./Sec.
VS	Ship Speed - Ft./Sec.
VW	Total Steady Wind - Ft./Sec.
VW1	Velocity Ratio
VXBar	Mean X Turbulence Velocity - Ft./Sec.
VXT	Random X Component of Turbulence - Ft./Sec.
VXTP	Previous Value of VXT - Ft./Sec.
VXTURB	Total X Component of Turbulence - Ft./Sec.
VXWS	Tabulated Mean X Velocity Component - Ft./Sec.
VYBar	Mean Y Turbulence Velocity - Ft./Sec.
VYT	Random Y Component of Turbulence - Ft./Sec.
VYTP	Previous Value of VYT - Ft./Sec.
VYTURB	Total Y Component of Turbulence - Ft./Sec.
VYWS	Tabulated Mean Y Velocity Component - Ft./Sec.
VZBar	Z Component Mean Turbulence Velocity - Ft./Sec.
VZT	Z Component of Random Turbulence - Ft./Sec.
VZTP	Previous Value of VZT - Ft./Sec.

VZTURB	Total Z Component of Turbulence - Ft./Sec.
VZWS	Tabulated Mean Z Turbulence Velocity - Ft./Sec.
XE	North - South Distance From Aircraft cg to Touchdown Pt. - Ft.
XMIN	Forward Limit on Turbulence Region - Ft.
XMIN1	Intermediate Value of XMIN - Ft.
XMIN2	Intermediate Value of XMIN - Ft.
XTaB	X Table Lookup Parameter - Ft.
XWIND	Aircraft Position Measured Parallel to Relative Wind - Ft.
YE	Aircraft East - West Position Relative to Touchdown Point - Ft.
YMAX	Right Limit on Turbulence - Ft.
YMAX1	Intermediate Value of YMAX - Ft.
YMIN	Left Limit on Turbulence - Ft.
YMIN1	Intermediate Value of YMIN - Ft.
YTaB	Y Table Lookup Parameter
YWIND	Aircraft Position Relative to Touchdown Point Measured Transverse to Wind Direction - Ft.
ZTaB	Z Table Lookup Parameter - Ft.

## APPENDIX F

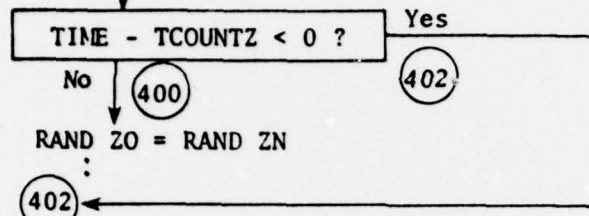
## FF 1052 Algorithm Flow Chart



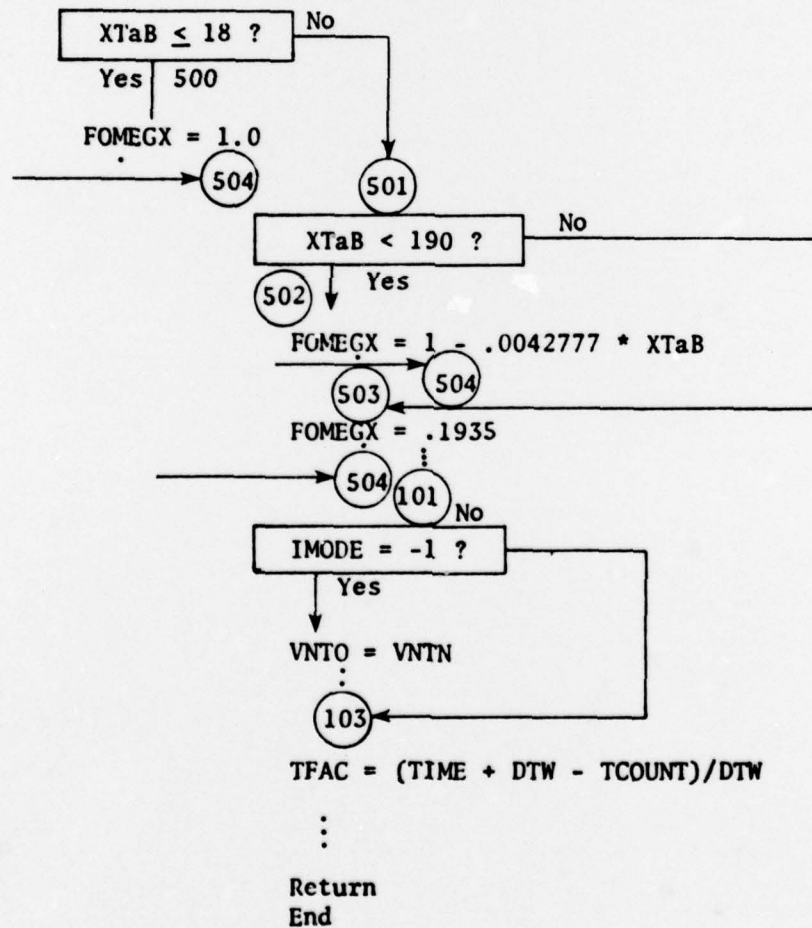




$RAND\ Y = RAND\ YO + (RAND\ YN - RAND\ YO) * (TIME + DTY - TCOUNT)/DTY$



$RAND\ ZN = RAND\ ZO + (RAND\ ZN - RAND\ ZO) * (TIME + DTZ - TCOUNTZ)/DTZ$



# D I S T R I B U T I O N   L I S T (Continued)

	No. of Copies
Boeing AeroSpace Corp., Mail Stop 41-11, P.O. Box 98124, Seattle, Wash 98124 ..... (1 for Mr. Donald West)	1
Naval Ship Research & Development Center, Bethesda, MD 20084, Code 1613 ..... (1 for Mr. Charles Bernitt)	1
Naval Air Engineering Ctr., Lakehurst, NJ 08733, Code 91315 ..... (1 for Mr. Robert Black)	1
Delft University of Technology, Dept. of Aeronautical Engineering, Delft - The Netherlands ..... (1 for G.A.J. vande Moesdijk)	1
Superintendent, Naval Postgraduate School, Monterey, CA 93940 ..... (Attn: Dr. L. Schmidt)	1

# D I S T R I B U T I O N   L I S T

REPORT NO. NADC-78182-60

AIRTASK NO. WF-41-400-000

P.E. No. 62241N

	No. of Copies
NAVAIR (AIR-950D.....	8
(2 for retention)	
(3 for AIR-320D)	
(3 for AIR-530112)	
DDC .....	12
NAVAIRTESTCEN, Patuxent River, Md. 20970 .....	1
(1 for Mr. Anthony Rosetti)	
NASA Ames Research Center, Moffet Field, CA 94035 .....	1
(1 for Mr. Walter McNeill)	
Boeing Vertol Company, P.O. Box 16858, Phila., PA 19142 .....	1
(1 for Mr. Theodore Garnett, Jr.)	
McDonnell Aircraft Company, St. Louis, MO 63166 .....	1
(1 for Mr. Douglas Miller, Harrier Project)	
Vought Corporation, P.O. Box 5907, Dallas, TX 75222 .....	2
(1 for Mr. Robert Fortenbaugh)	
(1 for Dr. Julian Wolkowitch)	
Systems Control Incorporated, 1801 Page Mill Road, Palo Alto, CA 94304 .....	1
(1 for Mr. Jeffrey Bohn)	
Rockwell International, Columbus, OH 43216 .....	1
General Dynamics Corporation, Ft. Worth, TX 76101, P. O. Box 748 .....	1
Northrup Corporation, Hawthorne, CA 90250 .....	1
Grumman Aerospace Corp., Beth Page, L.I., NY 11714 .....	2
(1 for Mr. S. Kalemaris)	
(1 for Mr. P. Martorella)	
Royal Aeronautical Establishment, Bedford, England .....	2
(1 for Mr. A. Woodfield)	
(1 for Mr. B. N. Tomlinson)	
Systems Technology, Inc., 13766 Hawthorne Blvd., Hawthorne, CA 90250 .....	1
Bell Helicopter Company, Fort Worth, TX 76101 .....	1
(1 for Mr. Peter O'Reilly)	
NAVEDTRA SUPP CENLANT, Bldg 286, Naval Station, Norfolk, VA 23511 .....	1
(1 for Mr. Brian Sonberg)	
Lockheed California, Company 75-84/63/A-1, Burbank, CA 91520 .....	1
(1 for Mr. Arthur Schuetz)	
National Research Council Canada, Ottawa, Canada .....	1
(1 for Dr. Maxwell Sinclair)	

CONTINUED ON INSIDE OF COVER